Zoological Journal of the Linnean Society, 2020, **189**, 1249–1312. With 26 figures.

Patterns of morphological diversification in giant *Berberomeloe* blister beetles (Coleoptera: Meloidae) reveal an unexpected taxonomic diversity concordant with mtDNA phylogenetic structure

ALBERTO SÁNCHEZ-VIALAS[1], MARIO GARCÍA-PARÍS[1], JOSÉ L. RUIZ[2] and ERNESTO RECUERO[1,*]

[1]*Museo Nacional de Ciencias Naturales (MNCN-CSIC), Madrid, Spain*
[2]*Instituto de Estudios Ceutíes, Ceuta, Spain*

Received 8 May 2019; revised 21 September 2019; accepted for publication 15 November 2019

Delimiting species boundaries is a complex challenge usually hindered by overlooked morphological diversification or misinterpretation of geographically structured phenotypic variability. Independent molecular data are extremely useful to characterize and understand such morphological diversity. Morphological and molecular variability of the non-phoretic and apterous, widely distributed, giant blister beetles of the genus *Berberomeloe*, were investigated within and between lineages across most of the distributional range of the genus. We used two mtDNA gene fragments to characterize genetic variability and to produce a time-calibrated phylogeny of the genus. Our results reveal several mitochondrial lineages, allopatrically, parapatrically and sympatrically distributed. Most clades are not distinguishable between each other based on morphometrics. However, no morphometric overlap is observed between two closely related clades, one of them occurring in sympatry with a distantly congeneric species (*B. insignis*), suggesting that sympatry could trigger morphological diversification. Although most species share a morphometric space, they can be morphologically identified by a combination of easily observed characteristic qualitative features. Based on the concordance between mtDNA clades and morphological units, we describe six new species of *Berberomeloe* (***B. castuo* sp. nov., *B. comunero* sp. nov., *B. indalo* sp. nov, *B. yebli* sp. nov., *B. payoyo* sp. nov.** and ***B. tenebrosus* sp. nov.**), revalidate two taxa (***B. maculifrons* comb. nov.** and ***B. laevigatus* comb. nov.**) and redefine *B. majalis*.

ADDITIONAL KEYWORDS: biogeography – Iberian Peninsula – morphological evolution – new species – non-cryptic diversity – North Africa – phylogeography – speciation – species complex – sympatry.

INTRODUCTION

Allopatric diversification is the most common mode of speciation, particularly in organisms with limited dispersal capabilities. Allopatric speciation is mostly a consequence of time and isolation, usually driven by the emergence of extrinsic barriers (geological, ecological, etc.), setting the perfect conditions for morphological and niche conservatism (Wiens, 2004; Moritz *et al.*, 2017). However, morphological diversification or conservatism, are not necessarily associated with speciation and are usually the result of different evolutionary processes (Pfennig & Murphy, 2000). For instance, some studies support the hypothesis of competitive exclusion among closely related and ecologically similar cryptic or poorly differentiated morphological taxa as the factor that limits their local coexistence (Vodă *et al.*, 2015; Darwell & Cook, 2017). In this case, ecological sorting or character displacement processes that could sort out different morphological phenotypes are probably enhanced by secondary sympatry among closely related species (Brown & Wilson, 1956; Darwell & Cook, 2017; Moritz *et al.*, 2017).

---

*Corresponding author. E-mail: ernestorecuerogil@gmail.com

[Version of record, published online 23 January 2020; http://zoobank.org/ urn:lsid:zoobank.org:pub:BA81CEE6-9D1C-49A9-A9D1-FB0501198097]

© 2020 The Linnean Society of London,

Downloaded from https://academic.oup.com/zoolinnean/article-abstract/189/4/1249/5714599 by 81263633 user on 05 August 2020

Divergent phenotypes resulting from ecological sorting or character displacement in separate species are easily misunderstood for variable expression of phenotypic plasticity following local ecological selection within a single evolutionary unit, especially if the characters in question vary over large geographic areas (Martin & Pfenning, 2011). Discerning between these two hypotheses generally involves the use of independent markers, like mitochondrial DNA (mtDNA), able to identify genetic patterns of geographic differentiation not necessarily related with nuclear-based trait polymorphisms (Stuart & Losos, 2013; Salvador de Jesús-Bonilla *et al.*, 2018).

Over the past two decades a growing number of phylogeographic studies has frequently revealed the presence of unanticipated, deep genetic divergence and phylogenetic structure within species (Bickford *et al.*, 2007; Pfenninger & Schwenk, 2007; Baselga *et al.*, 2011; Porco *et al.*, 2012; Pérez-Ponce de León & Poulin, 2016). In many cases, observed results are consistent with the existence of species complexes. These species complexes might be represented by genetically differentiated cryptic species, but in other cases, the findings correspond to either overlooked morphological diversification (Rodríguez-Flores *et al.*, 2018) or to misinterpretation of geographically structured phenotypic variability, assumed to be locally determined by recent demographic processes or by ecological pressures instead of representing independent evolutionary units (Brown *et al.*, 2007; Posso-Terranova & Andrés, 2018). Phylogeography has become a useful approach to identify potential species boundaries, providing independent information to better characterize and discriminate between inter- and intraspecific differentiation, especially in taxa with either reduced, or high but heterogeneous, phenotypic variability (Posso-Terranova & Andrés, 2018). Consequently, even in well-studied regions and taxa (e.g. conspicuous groups like terrestrial vertebrates), the discovery of an extensive hidden or ignored fraction of biodiversity represents an increasingly common phenomenon (Oliver *et al.*, 2009; Recuero *et al.*, 2012; Murphy *et al.*, 2016; García-Porta *et al.*, 2017; Rosado *et al.*, 2017).

The genus *Berberomeloe* Bologna, 1989 (Coleoptera: Meloidae: Lyttini), includes two of the largest beetle species of the western Mediterranean basin (Bologna & Pinto, 2001, 2002; Bologna, 2008), showing conspicuous inter- and intraspecific phenotypic variability in multiple traits (Bologna, 1989; García-París, 1998; Ruiz & García-París, 2013), and also microsympatric populations in some regions (García-París, 1998; García-París *et al.*, 1999; García-París *et al.*, 2003). Bravo *et al.* (2017) demonstrated that colour variation in the abdominal terga (black with red transverse bars vs. only black, without red bars) is likely the result of recent processes, a consequence of relaxation of selection pressures on the phenotype of these highly toxic insects. Entirely black or red-barred specimens do not form reciprocally monophyletic clades. Additionally, limited dispersal abilities (both as adult, flightless and as larvae, non-phoretic) (Bologna, 1989, 1991) could have played a role on the strong phylogeographic structure detected within *Berberomeloe* (Percino-Daniel *et al.*, 2013; Bravo *et al.*, 2017), but whether this pattern of diversity corresponds with intraspecific diversification, or if it rather reflects the existence of independent evolutionary units, remains unknown.

Species of *Berberomeloe* are characterized by the presence of a long and voluminous abdomen, reduced elytra and absence of wings, and by its non-phoretic first instar larva, which is a parasitoid of Anthophoridae and Andrenidae bees, and perhaps also of Megachilidae (Apoidea: Hymenoptera) (Bologna, 1989, 1991; Bologna & Pinto, 2002). Currently, two species are recognized: *Berberomeloe majalis* (Linnaeus, 1758), widely distributed across the Iberian Peninsula (except the northern coast), and north-western Africa, from Morocco to western Tunisia (Bologna, 1991; García París *et al.*, 2003), and *Berberomeloe insignis* (Charpentier, 1818), endemic to south-eastern Spain, along the coastal provinces of Granada, Almería and Murcia (García-París, 1998; García-París *et al.*, 2003; García-París & Ruiz, 2008, 2011a; Ruiz & García-París, 2013). *Berberomeloe insignis* was included in the synonymy of *B. majalis* (Borchmann, 1917; Bologna, 1989, 1991) until the revision by García-París (1998), who resurrected this overlooked Iberian endemic based on imaginal morphological characters. Larval morphology also supports their status as an independent species (Settanni *et al.*, 2009). Both species can be found in sympatry in some areas in Almería and Murcia, but no trace of hybridization has been observed (García-París *et al.*, 1999, 2003).

In this work, we integrate a study of the morphological variation over an extensive sampling area across most of the distribution of *Berberomeloe*, and a phylogeographic analysis based on mitochondrial markers assumed to be completely independent from the nuclear-based morphological variation. We attempt (1) to characterize morphological patterns of diversity of qualitative and quantitative traits, (2) to determine if observed morphological patterns of diversity are geographically structured, concordantly or not with the mtDNA phylogeography here obtained, (3) to elucidate the biogeographic history and the effect of geographic barriers in the speciation processes and (4) to review the taxonomy of the genus *Berberomeloe*, making the necessary taxonomic decisions.

Downloaded from https://academic.oup.com/zoolinnean/article-abstract/189/4/1249/5714599 by 81263633 user on 05 August 2020

MATERIAL AND METHODS

MORPHOMETRIC ANALYSES AND QUALITATIVE CHANGE IN MORPHOLOGICAL TRAITS

To examine quantitative morphological variation, we selected seven morphological traits studied in 189 imaginal specimens of *Berberomeloe*. These specimens correspond to genotyped geographic areas in the Iberian Peninsula (148 specimens) and Morocco (41 specimens). All specimens were preserved in absolute ethanol and stored at –20 °C (Supporting Information, Table S1). Additionally, photographs of the types of *Meloe majalis* Linnaeus, 1758, held in the Linnean collection at the Linnean Society in London (catalogued as Linn 6662, Linn 6663), were examined to designate an appropriate lectotype to stabilize nomenclatural and taxonomic decisions.

Morphometric measurements used in the analyses were as follows: PDW, pronotum distal width (between both posterior apexes of pronotum); PPW, pronotum proximal width (between both fore apexes of pronotum); PL, pronotum length on sagittal plane; LM, longitude of metafemur; EL, longitude of elytra; TW2, width of the second tergal bar; TW3, width of the third tergal bar; HW, head width; AW, abdominal width (Fig. 1; Supporting Information, Table S1). All measurements were taken from pictures using a Leica MZ16A stereomicroscope with a Leica DFC550 camera and processed with software LAS v.4.3. Original trait measurements were size-corrected by taking the residuals from regression against head width. Discriminant function analyses (DFA) were carried out using the statistical software IBM SPSS v.19.0 (IBM SPSS, Armonk, NY). Specimens from lineages H, I and J were not included in the morphometric analyses because of limited sample size.

For qualitative trait revision, a total of 755 specimens of *Berberomeloe* have been studied, distributed as follows: 189 specimens used in the morphometric analysis (Supporting Information, Table S1), 137 type specimens (holotypes of nominal taxa previously described and holo- and paratypes of species described herein) and 429 additional specimens (preserved in ethanol or dry) held at several entomological collections (but mainly at the Museo Nacional de Ciencias Naturales, Madrid, Spain; see species accounts) (Supporting Information, Appendix S1): Linnean Society of London, UK (LSL); Museo Nacional de Ciencias Naturales, Madrid, Spain (MNCN-CSIC); Estación Experimental de Zonas Áridas, Almería, Spain (EEZA-CSIC); Hungarian Natural History Museum, Budapest, Hungary (HNHM); Museum of Natural History and Archaeology, Trondheim, Norway (MNHAT); Muséum National d'Histoire Naturelle, Paris, France (MNHN); Emirates Center for Wildlife Propagation, Missour, Morocco (ECWP) and J. L. Ruiz's collection, Ceuta, Spain (JLR).

Qualitative traits included: pronotum shape, head and pronotum puncturation (density, depth, size and distribution pattern of the punctures), shape of antennomeres (especially in the male), width of the transverse abdominal coloured bars, presence or absence of red blotches over the temples, male and female genitalia.

Morphological descriptions of new species include additional measurements: body length (frons to posterior border of elytra; abdomen is not included in this measurement, as its length can vary along the adult life of individuals and also can be altered in preserved specimens; total body length, including abdomen, is provided only for holotypes and largest specimens of each species, in both cases from preserved specimens), maximum body width (at the level of elytral posterior apexes), length of each antennomere, length and width of clypeus and labrum, length of metatibia and fourth tarsomere of metatarsus. Scanning electronic microscope was used to study some anatomical features, including male genitalia, metatarsi, labial palpi, maxillary palpi, galeae and laciniae of maxillae, mentum, antennomeres and setation of pronotum and head. Digital pictures were taken with a Canon 600D camera coupled with a Tamron 90 mm f2.8 macrolens and two external flashes (scale bars = 1 mm).

DNA EXTRACTION AND MTDNA SEQUENCING

A total of 191 specimens of *Berberomeloe* were sampled for tissue collection, across most of the distribution range of the genus (Iberian Peninsula and Morocco) (Table 1; Fig. 2). Tissue samples were extracted from the coxae or femora from specimens preserved in ethanol (96° to absolute) stored at –20 °C. Genomic DNA was extracted using the Qiagen DNeasy extraction kit (Qiagen, Valencia, California, USA).

Polymerase chain reaction (PCR) was used to amplify fragments of two mitochondrial regions: 657 base pairs (bp) of cytochrome oxidase I (*Cox1*) using the set of primers LCO 1490 (Folmer *et al.*, 1994) and COI-H (Machordom *et al.*, 2003) and 510 bp of 16S ribosomal RNA (*16S*) using the set of primers 16Sar and 16Sbr (Palumbi *et al.*, 1991). Polymerase chain reactions were performed in 25 µL, including 23 µL of the PCR mix, including 17.5 µL of H_2O, 2.5 µL of a reaction buffer with $MgCl_2$ (2 mM), 1 µL of dNTP (10 mM), 0.8 µL of $MgCl_2$ (50 mM), 0.5 µL of each primer (10 mM), 0.4 µL of Taq polymerase (Biotools, 5 U/mL) and 2 µL of specimen DNA. PCR conditions for *Cox1*: 5 min at 95 °C, 40 cycles with a denaturing temperature of 94 °C (45 s), annealing at 42 °C (45 s) and extension at 72 °C (1 min) with a final single extra extension step at 72 °C for 10 min; for *16S*: 5 min at 94 °C, 35 cycles with a denaturing temperature of

Downloaded from https://academic.oup.com/zoolinnean/article-abstract/189/4/1249/5714599 by 81263633 user on 05 August 2020

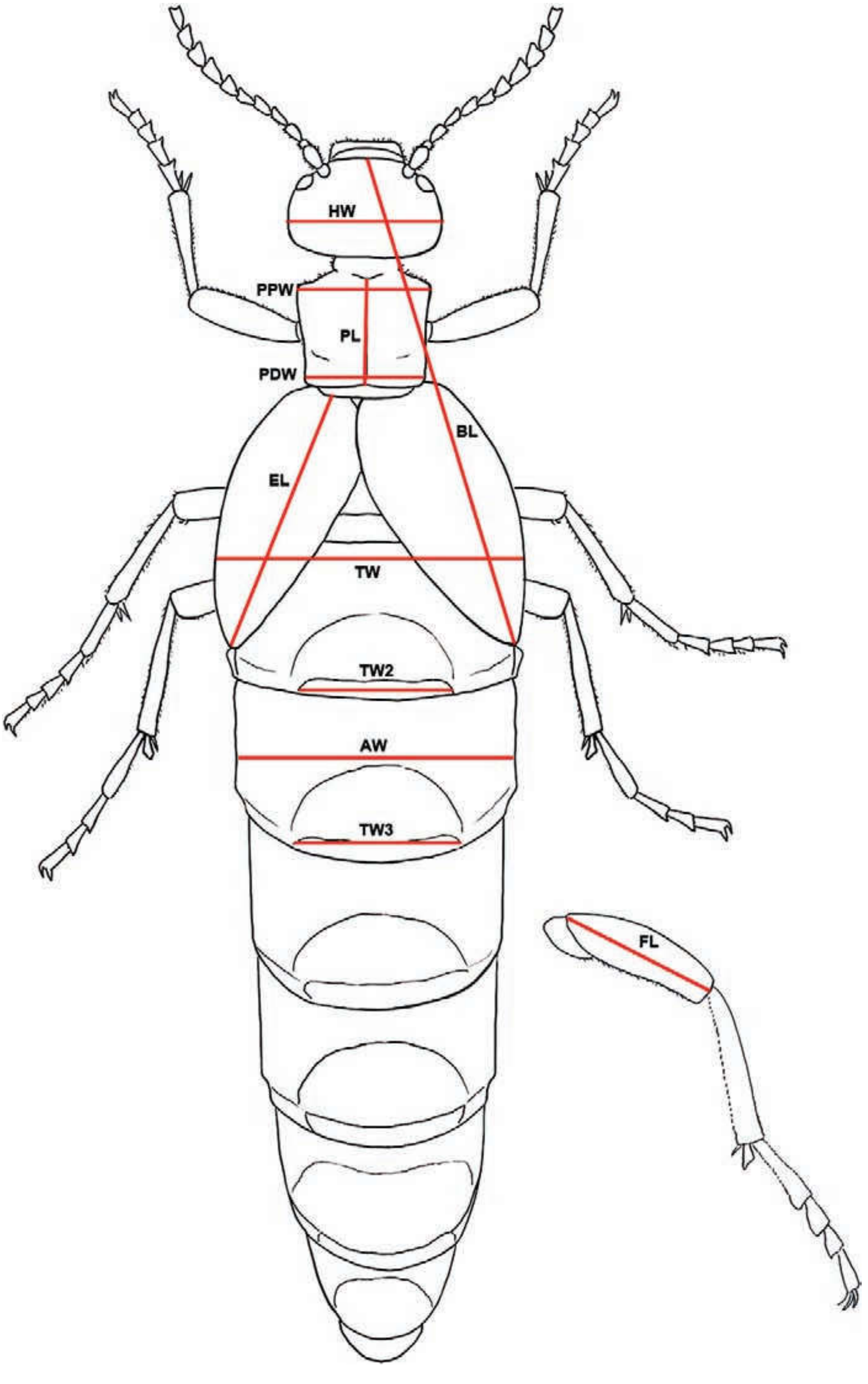

Figure 1. Morphometric measurements taken: (1) HW, head width; (2) PPW, pronotum proximal width; (3) PDW, pronotum distal width; (4) PL, pronotum length; (5) EL, elytra length; (6) BL, body length (only taken from the holotype of each newly described species); (7) BW body width (only taken from the holotype of each newly described species); (8) TW2, second tergal bar width; (9) TW3, third tergal bar width; (10) AW, abdominal width; (11) FL, femur length. P. Chamorro drawing.

94 °C (30 s), annealing at 42 °C (30 s) and extension at 72 °C (45 s) with a final single extra extension step at 72 °C for 5 min. PCR products were checked in 1% agarose gel and products with expected length were directly sequenced at Macrogen Inc. (Macrogen Europe, Amsterdam, The Netherlands).

Downloaded from https://academic.oup.com/zoolinnean/article-abstract/189/4/1249/5714599 by 81263633 user on 05 August 2020

Table 1. Species identities, collecting localities, voucher numbers and GenBank accession numbers for *Berberomeloe* samples analysed in this study

Taxon	Locality	Voucher number	Genbank # *Cox1*	Genbank # *16S*
Berberomeloe castuo	Portugal: Odemira	APP17003	MN252860	MN252741
Berberomeloe castuo	Portugal: Odemira	APP17004	MN252861	MN252742
Berberomeloe castuo	Spain: Ourense: West of Soño, Verín	ASV16020	MN252778	MN252609
Berberomeloe castuo	Spain: Castilblanco: Badajoz	ASV16021	MN252779	MN252610
Berberomeloe castuo	Spain: Avila: 1.5 km South of Ávila	ASV16022	MN252780	MN252611
Berberomeloe castuo	Spain: Cáceres: Jaraíz de la Vera	ASV16023	MN252781	MN252612
Berberomeloe castuo	Spain: Huelva: San Silvestre de Guzmán	ASV16026	MN252784	MN252615
Berberomeloe castuo	Spain: Huelva: 4 km SO Cabezas Rubias	ASV16027	MN252785	MN252616
Berberomeloe castuo	Portugal: Barrancos	ASV16034	MN252787	MN252618
Berberomeloe castuo	Spain: Badajoz: Calera de León, Monasterio de Tentudía	ASV16035	MN252788	---
Berberomeloe castuo	Spain: Ourense: Lampaza-Pedrosa	ASV16040	MN252789	MN252619
Berberomeloe castuo	Portugal: Boticas	ASV16045	MN252794	MN252624
Berberomeloe castuo	Spain: Huelva: Cabezas del Pasto	ASV16046	MN252795	MN252625
Berberomeloe castuo	Spain: Zamora: Fornillos de Aliste	ASV16048	MN252796	MN252626
Berberomeloe castuo	Spain: Ávila: 5 km West of La Cañada	ASV16049	MN252797	MN252627
Berberomeloe castuo	Portugal: Estremoz	ASV16066	MN252810	MN252640
Berberomeloe castuo	Portugal: Cabeça Carneiro	ASV16067	MN252811	MN252641
Berberomeloe castuo	Spain: Salamanca: Villagonzalo de Tormes	ASV16070	MN252814	MN252644
Berberomeloe castuo	Spain: Badajoz: Castilblanco	ASV16078	MN252862	MN252743
Berberomeloe castuo	Spain: Cáceres: Losar de la Vera	ASV16079	MN252863	MN252744
Berberomeloe castuo	Spain: León: Quintanilla de Flórez	BmMAB117ln	MN252824	MN252662
Berberomeloe castuo	Spain: Cáceres: 4 km of Arroyo De la luz	BmMAB121cc	MN252825	MN252666
Berberomeloe castuo	Spain: Cáceres: Santuario de la Virgen del Prado	BmMAB125cc	MN252827	MN252668
Berberomeloe castuo	Spain: Cáceres: 3 km South of Navas del Madroño	BmMAB131	MN252829	MN252674
Berberomeloe castuo	Spain: Toledo: Fuentes	BmMAB136to	MN252831	MN252679
Berberomeloe castuo	Spain: Cáceres: 25 km South of Aliseda	BmMAB141cc	MN252833	MN252683
Berberomeloe castuo	Spain: Cáceres: 1 km North of Navas del Madroño	BmMAB151cc	MN252836	MN252692
Berberomeloe castuo	Spain: Cáceres: 1 km North of Navas del Madroño	BmMAB152cc	MN252837	MN252693
Berberomeloe castuo	Spain: Cáceres: Torre de Don Miguel	BmMAB160cc	MN252840	MN252700
Berberomeloe castuo	Spain: Cáceres: M° Sta Gracia	BmMAB165cc	MN252842	MN252705
Berberomeloe castuo	Spain: Cáceres: M° Sta Gracia	BmMAB166cc	MN252843	MN252706
Berberomeloe castuo	Spain: Cáceres: 3 km South of Navas del Madroño	BmMAB174cc	KC853095	KC853074
Berberomeloe castuo	Spain: Cáceres: 3 km South of Navas del Madroño	BmMAB175cc	KC853096	KC853075
Berberomeloe comunero	Spain: Madrid: Miraflores de la Sierra	APP17002	MN252859	---
Berberomeloe comunero	Spain: Guadalajara: Villares de Jadraque	ASV16055	MN252801	MN252631
Berberomeloe comunero	Spain: Guadalajara: Torrebeleña	ASV16056	MN252802	MN252632
Berberomeloe comunero	Spain: Guadalajara: Marchamalo	ASV16057	MN252803	MN252633
Berberomeloe comunero	Spain: Guadalajara: Riofrío del Llano	ASV16058	MN252804	MN252634
Berberomeloe comunero	Spain: Guadalajara: Negredo	ASV16062	MN252807	MN252637
Berberomeloe comunero	Spain: Madrid: Valdilecha	ASV16069	MN252813	MN252643
Berberomeloe comunero	Spain: Madrid: Rivas de Jarama	BmMAB100md	KX495701	MN252650
Berberomeloe comunero	Spain: Valladolid: San Miguel del Arroyo	BmMAB106vd	KX495704	MN252656
Berberomeloe comunero	Spain: Guadalajara: Uceda	BmMAB109gu	KX495705	MN252657
Berberomeloe comunero	Spain: Burgos: Monasterio de Rodilla	BmMAB116bu	KC853094	KC853073

Downloaded from https://academic.oup.com/zoolinnean/article-abstract/189/4/1249/5714599 by 81263633 user on 05 August 2020

Table 1. Continued

Taxon	Locality	Voucher number	Genbank # *Cox1*	Genbank # *16S*
Berberomeloe comunero	Spain: Guadalajara: Uceda	BmMAB118gu	KX495709	MN252663
Berberomeloe comunero	Spain: Burgos: Monasterio de Rodilla	BmMAB123bu	KC853093	KC853072
Berberomeloe comunero	Spain: Valladolid: San Miguel del Arroyo	BmMAB128vd	KX495714	MN252671
Berberomeloe comunero	Spain: Segovia: Prádena	BmMAB129sg	KX495715	MN252672
Berberomeloe comunero	Spain: Madrid: 5 km Northeast of Molino de Aldehuela	BmMAB133md	KX495716	MN252676
Berberomeloe comunero	Spain: Guadalajara: Uceda	BmMAB134gu	KX495717	MN252677
Berberomeloe comunero	Spain: Guadalajara: Uceda	BmMAB135gu	KX495718	MN252678
Berberomeloe comunero	Spain: Segovia: Navafría	BmMAB143sg	KX495722	MN252685
Berberomeloe comunero	Spain: Valladolid: San Miguel del Arroyo	BmMAB144vd	KX495723	MN252686
Berberomeloe comunero	Spain: Madrid: 4 km South of Colmenar de Oreja	BmMAB146md	KC853100	KC853079
Berberomeloe comunero	Spain: Guadalajara: Uceda	BmMAB150gu	KX495726	MN252691
Berberomeloe comunero	Spain: Valladolid: San Miguel del Arroyo	BmMAB154vd	KX495728	MN252695
Berberomeloe comunero	Spain: Madrid: 3 km East of Villaconejos	BmMAB157md	KX495730	MN252698
Berberomeloe comunero	Spain: Madrid: 4 km South of Colmenar de Oreja	BmMAB159md	KC853101	KC853080
Berberomeloe comunero	Spain: Madrid: 5 km South of Villaconejos	BmMAB164md	KX495733	MN252704
Berberomeloe comunero	Spain: Guadalajara:Uceda	BmMAB167gu	KX495734	MN252707
Berberomeloe comunero	Spain: Madrid: 5 km North-east of Molino de la Aldehuela	BmMAB172md	KX495738	MN252711
Berberomeloe comunero	Spain: Madrid: Montejo de la Sierra	BmMAB183md	KX495744	MN252717
Berberomeloe comunero	Spain: Madrid: Alcalá de Henares	BmMAB186md	KX495745	MN252718
Berberomeloe comunero	Spain: Madrid: Canencia	BmMAB187md	KX495746	MN252719
Berberomeloe comunero	Spain: Madrid: Montejo de la Sierra	BmMAB188md	KX495747	MN252720
Berberomeloe comunero	Spain: Madrid: Montejo de la Sierra	BmMAB189md	KX495748	MN252721
Berberomeloe comunero	Spain: Madrid: Montejo de la Sierra	BmMAB190md	KX495749	MN252722
Berberomeloe comunero	Spain: Madrid: Alcalá de Henares	BmMAB198md	KX495751	MN252724
Berberomeloe comunero	Spain: Madrid: 1 km South-east of Villanueva de la Torre	BmMAB202md	KX495752	MN252728
Berberomeloe comunero	Spain: Madrid: 1 km North-east of Meco	BmMAB203md	KX495753	MN252729
Berberomeloe indalo	Spain: Almería: La Mela	ASV16074	MN252848	MN252731
Berberomeloe indalo	Spain: Almería: La Mela	ASV16091	MN252865	MN252746
Berberomeloe indalo	Spain: Almeria: Campohermoso	BmMAB162al	MN252841	MN252702
Berberomeloe indalo	Spain: Almería: El Puntal	BmMAB185al	KC853091	KC853070
Berberomeloe indalo	Spain: Almería: El Puntal	BmMAB197al	KC853092	KC853071
Berberomeloe indalo	Spain: Almería: El Puntal	BmMAB199al	MN252844	MN252725
Berberomeloe indalo	Spain: Almería: Peñas Negras-Los Perales	BmMAB200al	MN252845	MN252726
Berberomeloe indalo	Spain: Almería: Peñas Negras	BmMAB201al	MN252846	MN252727
Berberomeloe insignis	Spain: Almería: El Puntal	BiMAB181	KC853087	KC853066
Berberomeloe insignis	Spain: Almería: 4.5 km South of Zurgena	BiMAB182	KC853086	KC853065
Berberomeloe insignis	Spain: Almería: El Puntal	BiMAB184	KC853088	KC853067
Berberomeloe insignis	Spain: Almería: Peñas Negras-Los Perales	BiMAB192	MN252815	MN252645
Berberomeloe insignis	Spain: Almería: El Puntal	BiMAB193	MN252816	MN252646
Berberomeloe insignis	Spain: Almería: El Puntal	BiMAB194	MN252817	MN252647
Berberomeloe insignis	Spain: Almería: El Puntal	BiMAB195	MN252818	MN252648
Berberomeloe insignis	Spain: Almería: El Puntal	BiMAB196	MN252819	MN252649
Berberomeloe laevigatus	Spain: Zaragoza: 3 km N de Ariza	ASV16030	MN252786	MN252617
Berberomeloe laevigatus	Spain: Soria: Castil de Tierra	ASV16054	MN252800	MN252630
Berberomeloe laevigatus	Spain: Guadalajara: Tamajón	ASV16059	MN252805	MN252635
Berberomeloe laevigatus	Spain: Soria: Barcones	ASV16068	MN252812	MN252642
Berberomeloe maculifrons	Morocco: Seba Ayoun-Ain Taoujdate	ASV16000	MN252759	MN252590

Downloaded from https://academic.oup.com/zoolinnean/article-abstract/189/4/1249/5714599 by 81263633 user on 05 August 2020

Table 1. Continued

Taxon	Locality	Voucher number	Genbank # *Cox1*	Genbank # *16S*
Berberomeloe maculifrons	Morocco: Seba Ayoun-Ain Taoujdate	ASV16001	MN252760	MN252591
Berberomeloe maculifrons	Morocco: Seba Ayoun-Ain Taoujdate	ASV16002	MN252761	MN252592
Berberomeloe maculifrons	Morocco: paysaje d´Ito, Azrou	ASV16009	MN252767	MN252598
Berberomeloe maculifrons	Morocco: Azrou	ASV16012	MN252770	MN252601
Berberomeloe maculifrons	Morocco: Azrou	ASV16013	MN252771	MN252602
Berberomeloe maculifrons	Morocco: Ifrane	ASV16014	MN252772	MN252603
Berberomeloe maculifrons	Morocco: Ifrane	ASV16015	MN252773	MN252604
Berberomeloe maculifrons	Morocco: Nador-Aknoul	ASV16016	MN252774	MN252605
Berberomeloe maculifrons	Morocco: Nador-Aknoul	ASV16017	MN252775	MN252606
Berberomeloe maculifrons	Morocco: Saidia-Berkane	ASV16018	MN252776	MN252607
Berberomeloe maculifrons	Morocco: Ain Leuh-Afennourir	ASV16019	MN252777	MN252608
Berberomeloe maculifrons	Morocco: 18 km East of Targuist	ASV16041	MN252790	MN252620
Berberomeloe maculifrons	Morocco: Barrage Hassan II	ASV16042	MN252791	MN252621
Berberomeloe maculifrons	Morocco: Ras el Ma (Ras Kebdana)	ASV16043	MN252792	MN252622
Berberomeloe maculifrons	Morocco: Saidia-Berkane	ASV16044	MN252793	MN252623
Berberomeloe maculifrons	Morocco: Ain Leuh-Afennourir	ASV16077	MN252850	MN252733
Berberomeloe maculifrons	Morocco: Enjil	ASV16085	MN252852	MN252735
Berberomeloe maculifrons	Morocco: Enjil	ASV16086	MN252853	MN252736
Berberomeloe maculifrons	Morocco: Enjil	ASV16087	MN252854	MN252737
Berberomeloe maculifrons	Morocco: Debdú: Gaada de Debdú	ASV16088	MN252855	MN252738
Berberomeloe maculifrons	Morocco: Debdú: Gaada de Debdú	ASV16089	MN252856	MN252739
Berberomeloe maculifrons	Morocco: Ain Beni Mathar	ASV16090	MN252857	MN252740
Berberomeloe maculifrons	Morocco: Middle Atlas	BmMAB149ma	MN252835	MN252690
Berberomeloe maculifrons	Morocco: Oumallal, Oum er Rbia river	BmMAB176ma	KX495739	MN252712
Berberomeloe maculifrons	Morocco: Oumallal, Oum er Rbia river	BmMAB177ma	KX495740	MN252713
Berberomeloe maculifrons	Morocco: Oumallal, Oum er Rbia river	BmMAB178ma	KX495741	MN252714
Berberomeloe maculifrons	Morocco: Oumallal, Oum er Rbia river	BmMAB179ma	KX495742	MN252715
Berberomeloe maculifrons	Morocco: Oumallal, Oum er Rbia river	BmMAB180ma	KX495743	MN252716
Berberomeloe majalis	Spain: Castellón: Morella-Cinctorres	207cs	MN252752	MN252583
Berberomeloe majalis	Spain: Castellón: Morella-Cinctorres	208cs	MN252753	MN252584
Berberomeloe majalis	Spain: Castellón: Morella-Cinctorres	209cs	MN252754	MN252585
Berberomeloe majalis	Spain: Teruel: Cubla-Villaspesa	211te	MN252755	MN252586
Berberomeloe majalis	Spain: Teruel: 3.5 km South-east of Valdelinares	213te	MN252756	MN252587
Berberomeloe majalis	Spain: Teruel: Cabra de Mora	214te	MN252757	MN252588
Berberomeloe majalis	Spain: Teruel: Sollavientos	215te	MN252758	MN252589
Berberomeloe majalis	Spain: Castellón: Cinctorres	ASV16024	MN252782	MN252613
Berberomeloe majalis	Spain: Castellón: Cinctorres	ASV16025	MN252783	MN252614
Berberomeloe majalis	Spain: Toledo: Dosbarrios	ASV16052	MN252798	MN252628
Berberomeloe majalis	Spain: Teruel: 4 km Northwest of Valdelinares	ASV16053	MN252799	MN252629
Berberomeloe majalis	Spain: Guadalajara: Motos	ASV16060	MN252806	MN252636
Berberomeloe majalis	Spain: Teruel: Fortanete	ASV16063	MN252808	MN252638
Berberomeloe majalis	Spain: Albacete: Pedro Andrés	ASV16065	MN252809	MN252639
Berberomeloe majalis	Spain: Castellón: Sant Joan de Penyagolosa	ASV16084	MN252851	MN252734
Berberomeloe majalis	Spain: Ciudad Real: El Alamillo	ASV16092	MN252866	MN252747
Berberomeloe majalis	Spain: Ciudad Real: 2 km North of Carrión de Calatrava	BmMAB103cr	KX495702	MN252653
Berberomeloe majalis	Spain: Ciudad Real: 2 km North of Carrión de Calatrava	BmMAB105cr	KX495703	MN252655
Berberomeloe majalis	Spain: Cuenca: Fuentes	BmMAB110cu	KX495706	MN252658
Berberomeloe majalis	Spain: Valencia: Camporrobles	BmMAB112vl	KX495707	MN252659
Berberomeloe majalis	Spain: Jaén: 10 km North of Úbeda	BmMAB119jn	KX495710	MN252664
Berberomeloe majalis	Spain: Toledo: 2 km North of El Emperador	BmMAB120to	KX495711	MN252665

Downloaded from https://academic.oup.com/zoolinnean/article-abstract/189/4/1249/5714599 by 81263633 user on 05 August 2020

Table 1. Continued

Taxon	Locality	Voucher number	Genbank # *Cox1*	Genbank # *16S*
Berberomeloe majalis	Spain: Toledo: 2 km North-east of El Emperador	BmMAB122to	KC853102	KC853081
Berberomeloe majalis	Spain: Guadalajara: 5 km North-east of Illana	BmMAB126gu	KX495712	MN252669
Berberomeloe majalis	Spain: Jaén: 10 km North of Ubeda	BmMAB127jn	KX495713	MN252670
Berberomeloe majalis	Spain: Ciudad Real: Calzada de Calatrava	BmMAB137cr	MN252832	MN252680
Berberomeloe majalis	Spain: Ciudad Real: Argamasilla de Calatrava	BmMAB138cr	KX495719	MN252681
Berberomeloe majalis	Spain: Cuenca: Villajero de Fuentes	BmMAB139cu	KX495720	MN252682
Berberomeloe majalis	Spain: Albacete: El Bonillo	BmMAB140ab	KC853090	KC853069
Berberomeloe majalis	Spain: Guadalajara: 5 km West of Cogolludo	BmMAB142gu	KX495721	MN252684
Berberomeloe majalis	Spain: Ciudad Real: Argamasilla de Calatrava	BmMAB145cr	MN252834	MN252687
Berberomeloe majalis	Spain: Guadalajara: 5 km West of Cogolludo	BmMAB147gu	KX495724	MN252688
Berberomeloe majalis	Spain: Toledo: 6 km North of El Emperador	BmMAB148to	KX495725	MN252689
Berberomeloe majalis	Spain: Jaén: Orcera	BmMAB153jn	KX495727	MN252694
Berberomeloe majalis	Spain: Toledo: Valmojado	BmMAB155to	MN252838	MN252696
Berberomeloe majalis	Spain: Ciudad Real: 6 km South of Malagón	BmMAB156cr	KX495729	MN252697
Berberomeloe majalis	Spain: Jaén: 10 km North of Úbeda	BmMAB161jn	KX495731	MN252701
Berberomeloe majalis	Spain: Cuenca: Villar de Cañas	BmMAB163cu	KX495732	MN252703
Berberomeloe majalis	Spain: Guadalajara: 5 km North-east of Illana	BmMAB168gu	KX495735	MN252708
Berberomeloe majalis	Spain: Albacete: El Bonillo	BmMAB169ab	KC853089	KC853068
Berberomeloe majalis	Spain: Toledo: 2 km West of Urda	BmMAB170to	KX495736	MN252709
Berberomeloe majalis	Spain: Toledo: 2 km West of Urda	BmMAB171to	KX495737	MN252710
Berberomeloe majalis	Spain: Toledo: 2 km North-east of El Emperador	BmMAB173to	KC853103	KC853082
Berberomeloe majalis	Spain: Madrid: Brea de Tajo	BmMAB191md	KX495750	MN252723
Berberomeloe majalis	Spain: Ciudad Real: Piedrabuena	BmMAB500cr	KC853098	KC853077
Berberomeloe majalis	Spain: Ciudad Real: Piedrabuena	BmMAB501cr	KC853099	KC853078
Berberomeloe payoyo	Spain: Cádiz: Paterna de Rivera	APP17001	MN252858	---
Berberomeloe payoyo	Spain: Cádiz: 7 km South-west of Benalup de Sidonia	BmMAB101ca	MN252820	MN252651
Berberomeloe payoyo	Spain: Cádiz: 7 km South-west of Benalup de Sidonia	BmMAB102ca	MN252821	MN252652
Berberomeloe payoyo	Spain: Cádiz: 4 km North-east of San José del Valle	BmMAB104ca	MN252822	MN252654
Berberomeloe payoyo	Spain: Cádiz: 3 km South of Alcalá de los Gazules	BmMAB107ca	KC853097	KC853076
Berberomeloe payoyo	Spain: Cádiz: 4 km North-east of San José del Valle	BmMAB113ca	MN252823	MN252660
Berberomeloe payoyo	Spain: Granada: Santa Cruz del Comercio	BmMAB115gr	KX495708	MN252661
Berberomeloe payoyo	Spain: Cádiz: Benalup de Sidonia	BmMAB124ca	MN252826	MN252667
Berberomeloe payoyo	Spain: Cádiz: 3 km South of Alcalá de Gazules	BmMAB130ca	MN252828	MN252673
Berberomeloe payoyo	Spain: Cádiz: 7 km South-west of Benalup de Sidonia	BmMAB132ca	MN252830	MN252675
Berberomeloe payoyo	Spain: Cádiz: 7 km South-west of Benalup de Sidonia	BmMAB158ca	MN252839	MN252699
Berberomeloe tenebrosus	Spain: Almería: Puerto La Ragua	APP17005	MN252870	MN252751
Berberomeloe tenebrosus	Spain: Almería: Puerto La Ragua	APP17006	MN252871	---
Berberomeloe tenebrosus	Spain: Almería: Calar Alto	ASV16028	MN252867	MN252748
Berberomeloe tenebrosus	Spain: Almería: Calar Alto	ASV16036	MN252868	MN252749
Berberomeloe tenebrosus	Spain: Granada: El Veleta	ASV16071	MN252869	MN252750
Berberomeloe tenebrosus	Spain: Almería: Escúllar	ASV16080	MN252864	MN252745
Berberomeloe tenebrosus	Spain: Granada: Pradollano	ASV17075	MN252849	MN252732
Berberomeloe yebli	Morocco: Chefchaouen	ASV16004	MN252762	MN252593
Berberomeloe yebli	Morocco: Chefchaouen	ASV16005	MN252763	MN252594
Berberomeloe yebli	Morocco: Torreta-Tetouan	ASV16006	MN252764	MN252595

Downloaded from https://academic.oup.com/zoolinnean/article-abstract/189/4/1249/5714599 by 81263633 user on 05 August 2020

Table 1. Continued

Taxon	Locality	Voucher number	Genbank # *Cox1*	Genbank # *16S*
Berberomeloe yebli	Morocco: Bab Taza	ASV16007	MN252765	MN252596
Berberomeloe yebli	Morocco: Bab Taza	ASV16008	MN252766	MN252597
Berberomeloe yebli	Morocco: Moulay Abdeselam	ASV16010	MN252768	MN252599
Berberomeloe yebli	Morocco: Moulay Abdeselam	ASV16011	MN252769	MN252600
Berberomeloe yebli	Morocco: Moulay Abdeselam	ASV16073	MN252847	MN252730

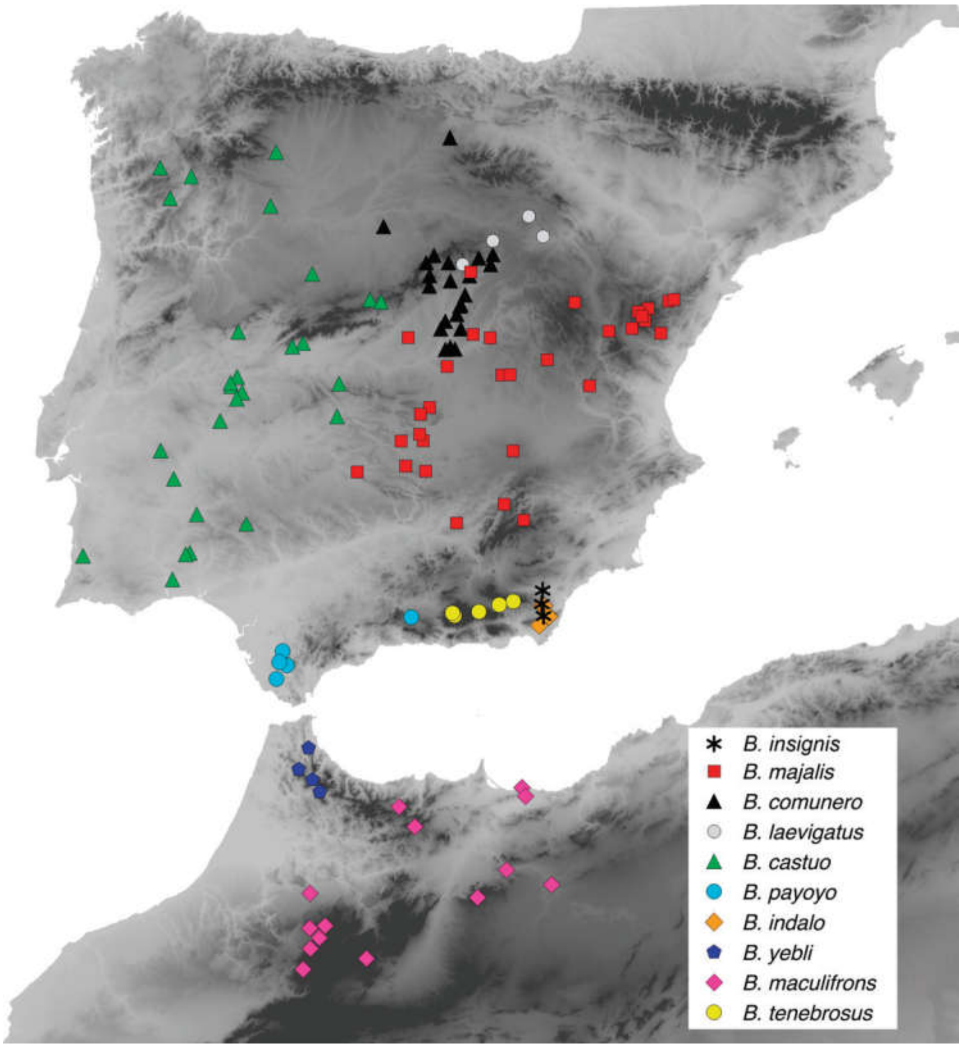

Figure 2. Map of the Iberian Peninsula and north-western Africa showing the sampling localities of sequenced specimens of *Berberomeloe*.

SEQUENCE ALIGNMENT, PHYLOGENETIC ANALYSES AND DIVERGENCE TIME ESTIMATION

The dataset consists of 191 newly generated *16S* sequences, while for *Cox1* it includes 109 unpublished sequences plus 67 previously published sequences (Percino-Daniel *et al.*, 2013; Bravo *et al.*, 2017). Sequences are deposited in GenBank (Table 1).

All sequences were compiled using SEQUENCER v.4.9 to assemble and to edit the sequence contigs and aligned with MAFFT (Katoh & Toh, 2008). DNA

Downloaded from https://academic.oup.com/zoolinnean/article-abstract/189/4/1249/5714599 by 81263633 user on 05 August 2020

sequences were visually checked in MESQUITE v.3.04 (Maddison & Maddison, 2016) to refine the final alignments. *Oenas fusicornis* Abeille de Perrin, 1880 (Meloidae: Lyttini) was used as outgroup.

Phylogenetic analyses were carried out under a Bayesian inference (BI) framework and performed using the combined mtDNA dataset of 191 specimens. Bayesian inference analyses were conducted with MrBayes v.3.2.3 (Ronquist *et al.*, 2012) with four partitions of the dataset. Analyses started with a randomly generated tree and were run four Metropolis coupled Monte Carlo Markov chains for 10 × 10^6 generations, sampled every 1000. We discarded 25% of the obtained trees as burn-in and generated a 50% consensus tree in MrBayes. We explored the substitution model space with the option lset nst=mixed rates=invgamma (Percino-Daniel *et al.*, 2013). Posterior clade probabilities were used to assess nodal support.

We estimated divergence times by using a coalescence analysis implemented in BEAST 1.8.2 (Drummond *et al.*, 2012). Analyses were run for 100 × 10^6 generations, sampled every 10 000, under a lognormal relaxed molecular clock with the substitution models calculated in JModelTest v.2 (Darriba *et al.*, 2012), which were HKI+G+I for *Cox1* and TN93+G+I for *16S*. Yule Process speciation was selected as tree prior (Gernhard, 2008). Estimates of time to the most recent common ancestor (TMRCA) were based on substitution rates proposed in Papadopoulou *et al.* (2010). For *Cox1* we used a log normal distribution in real space with initial value = 0.0178, Log (Mean) = 0.0178, Log (SD) = 0.2, and for *16S* we used a log normal distribution in real space with initial value = 0.0049, Log (Mean) = 0.0049, Log (SD) = 0.2. Trace plots and effective sample size (ESS) values were examined in TRACER v.1.5 to evaluate the convergence of the MCMC. The results, once the first 25% of trees was removed as burn-in, were summarized and annotated in a maximum clade credibility tree using TreeAnnotator (Drummond *et al.*, 2012).

TAXONOMY AND SPECIES DELIMITATION

To define the evolutionary units that represent taxonomic entities within *Berberomeloe*, we identified levels of geographic congruence between morphological diagnosable units and mitochondrial clades, adopting the evolutionary species concept (Wiley, 1978; Wiley & Mayden, 2000), which considers species as 'a single lineage of ancestral descendant populations of organisms that maintain its identity from other such lineages and which has its own evolutionary tendencies and historical fate'. This concept combines implications from the phylogenetic species concept, such as reciprocal monophyly, with subjective additional properties, like phenetic distinguishability and reproductive isolation among other relevant lines of evidence that can be used to assess the historical fate of the lineages (i.e. likelihood for losing monophyly once the lineages come together in a secondary contact zone).

Additionally, we compared our diagnosable evolutionary units with the results obtained from single-locus species delimitation methods. We implemented two different single-locus species delimitation methods: (1) the Generalized Mixed Yule Coalescent model (GMYC; Pons *et al.*, 2006; Fujisawa & Barraclough, 2013) using the GMYC we-server (available at: https://species.h-its.org/gmyc/) and (2) the Multi-rate Poison Tree Process model (mPTP; Kapli *et al.*, 2017), performed using the Exelixis Lab species delimitation web-server (available at http://www.exelixis-lab.org/). Default values were used for the priors in both analyses. GMYC was run with an ultrametric tree previously obtained from the BEAST analysis. For mPTP analyses, a non-ultrametric tree calculated from BI was used, but the matrix was previously collapsed by removing identical haplotypes using ALTER (Glez-Peña *et al.*, 2010).

RESULTS

MTDNA PHYLOGEOGRAPHY

Length of the mtDNA studied fragments comprise a total of 1167 bp, 657 bp of *Cox1* and 510 bp of *16S*, for 191 specimens of *Berberomeloe* (Table 1). The phylogenetic hypothesis based on BI (Fig. 3) shows a strong phylogenetic structure in *Berberomeloe*, with two highly supported clades (Bayesian posterior probability, PP = 1) representing the *B. majalis* and *B. insignis* species groups. A highly diversified *B. majalis* species group is formed by most lineages previously assigned to *B. majalis s.l.* (e.g. Bologna, 1989, 1991, 2008; García-París, 1998, García-París *et al.*, 2003, 2010), while a poorly diversified *B. insignis* species group is formed by only two lineages: *B. insignis* plus an additional lineage previously assigned to *B. majalis*. Therefore, our phylogenetic hypothesis suggests that *B. majalis*, as formerly recognized, is paraphyletic (Fig. 3).

Eight strongly supported, major mitochondrial lineages, distributed in three subclades, are recovered within the *B. majalis* species group (Fig. 3). One subclade includes lineages A and B (PP = 0.9) from central-eastern Spain. The second one includes lineages C, D, E, F and G (PP = 1) from North Africa and the southern and western Iberian Peninsula. The third one includes only lineage H, sampled from Aragón, Soria and northern Guadalajara (PP = 1).

Downloaded from https://academic.oup.com/zoolinnean/article-abstract/189/4/1249/5714599 by 81263633 user on 05 August 2020

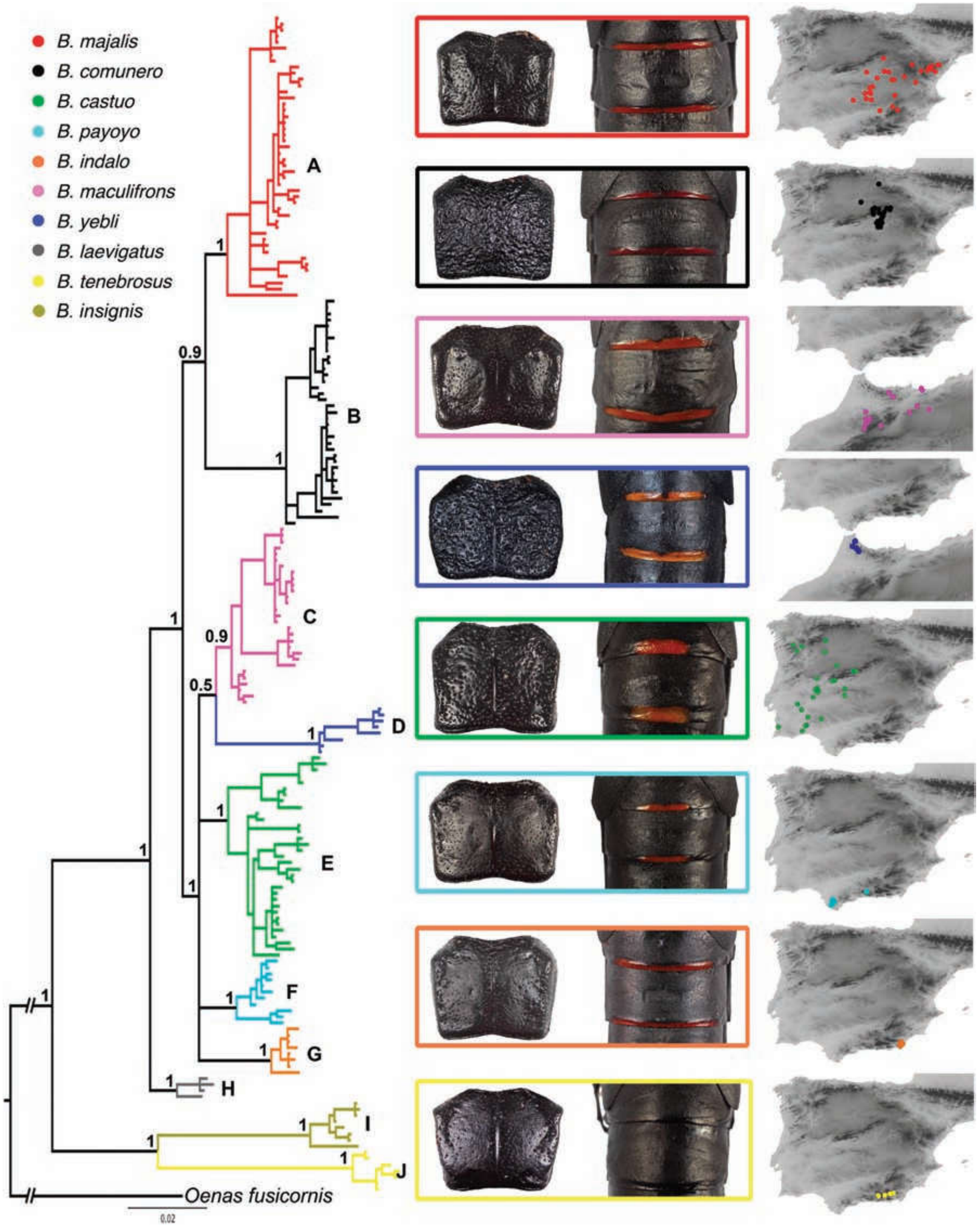

Figure 3. Bayesian phylogeny of the genus *Berberomeloe*. Colour-coded rectangles include dorsal side of pronotum and abdominal terga of: *B. majalis* (red), *B. comunero* (black), *B. maculifrons* (pink), *B. yebli* (dark blue), *B. castuo* (green), *B. payoyo* (light blue), *B. indalo* (orange), *B. laevigatus* (grey), *B. insignis* (khaki), *B. tenebrosus* (yellow). Each species, except *B. laevigatus* and *B. insignis*, are represented together with its distribution map.

Downloaded from https://academic.oup.com/zoolinnean/article-abstract/189/4/1249/5714599 by 81263633 user on 05 August 2020

Lineage A (PP = 0.98) is distributed along a wide area of central and eastern Spain (Figs 2, 3), across the provinces of Madrid, Guadalajara, Cuenca, Toledo, Ciudad Real, Jaén, Teruel, Albacete, Valencia and Castellón. Lineage B (PP = 1), narrowly parapatric with respect to lineage A, is present over central and northern Spain, in the provinces of Madrid, Segovia, Valladolid, Guadalajara and Burgos.

Lineages from the second subclade present allopatric or narrowly parapatric distributions, and their relationships are not fully resolved (Figs 2, 3). Lineage E (PP = 0.99) has the widest distribution among them, ranging over the entire western region of the Iberian Peninsula, including all Portugal and westernmost Spain, from Ourense to Huelva. Lineage F (PP = 0.99) occurs throughout the southernmost Spanish provinces: Cádiz, Málaga and western Granada. Lineage G (PP = 1) has been recorded exclusively from Almería province in south-eastern Spain, where it co-occurs with *B. insignis*. Two lineages occur in northern Africa: lineage C (PP = 0.98), sampled from the Middle Atlas in Morocco and lineage D (PP = 1) from the Rif Mountains and the Tingitana Peninsula.

The *B. insignis* species group includes lineage I, corresponding to *B. insignis*, endemic to south-eastern Spain (García-París, 1998; García-París *et al.*, 2003; García-París & Ruiz, 2011a), and lineage J (PP = 1), restricted to medium-high-elevation areas of the Sierra Nevada and Sierra de los Filabres in Almería and Granada provinces (Figs 2, 3). MrBayes (Fig. 3) and BEAST (Fig. 4) analyses provide similar topologies, except for the position of clade H: well supported as sister lineage to the rest of the *B. majalis* species group (MrBayes) or in an unresolved position within *B. majalis* species group (BEAST).

Times to the most recent common ancestor (TMRCAs) of *Berberomeloe* fall within the Miocene–Pliocene transition [5.18 Mya (95% HDP = 3.24–7.51)], while differentiation of the main lineages within *B. majalis* and *B. insignis* species groups started along the Pliocene–Pleistocene transition [3.07 Mya (2–4.31) and 3.67 Mya (2.03–5.75), respectively] (Fig. 4).

MORPHOLOGICAL DIVERSIFICATION

Our results show an overlap of morphometric spaces among lineages for the first two axes of the discriminant functions (DF1 and DF2; Fig. 5). However, the first discriminant function evidences a clear separation of two closely parapatric lineages included in the same subclade of the *B. majalis* species group: lineage F (distributed across Cádiz–Granada) and lineage G (restricted to Almería). Each of these lineages seems to occupy a different particular morphometric space with no trace of overlap between them.

In the classification based on discriminant functions, only 46.7% of the 139 specimens are correctly classified. Lineage G is the lineage with the highest correct classification score (86.7%), followed by lineage F (83.4%). The lowest percentages of lineage ascription correspond to lineage B (26.9%) and lineage A (21.4%), almost completely overlapping with each other. The first two discriminant functions (DF1 and DF2) explain 91.6% of total variation. Along DF1 axis (73.1% of total variation) the highest loadings were for the width of distal portion of pronotum (WDP) and for the width of the second coloured tergal bar (WCB). Along DF2 (18.4% of total variation), the distal portion of pronotum (WDP) and the width of the second (WCB) and third coloured tergal bar (WA) have the highest loading. Over DF1 axis, lineage G shows the higher loadings, whereas lineage F had the lowest loadings.

Several qualitative morphological traits show strong geographic concordance with mitochondrial clades. Informative traits are density, depth and size of pronotum and head punctures, pronotum shape, width of coloured tergal bars, presence or absence of conspicuous red blotches over the temples, shape of male antennomeres and male genitalia. The different states of these morphological traits are almost invariant across the geographic areas corresponding to each mtDNA lineage (see diagnosis for each species in the species accounts section). We have not detected intermediate patterns, even in potential secondary contact zones, but sampling in these areas is limited. A single specimen morphologically assignable to lineage E, presents a haplotype corresponding to the geographically close lineage A. We observe shallow intraclade variation in lineages A and E. Variation within lineage E occurs in the width of tergal bars, longer in the northern population group. Variation within lineage A is present in the depth of pronotum punctures, deeper in the population from Penyagolosa mountain in Castellón.

SPECIES DELIMITATION ANALYSES

Both species delimitation methods, mPTP and GMYC analyses, recover a high number of potential species according to our mtDNA data (Supporting Information, Fig. S1). Both methods offer similar results, but the GMYC model, with 12 suggested species, offers a more conservative result than the mPTP model, which suggests the existence of 15 species. They consistently recover all ten main mtDNA lineages as potential species. In the case of the GMYC model, it also splits a single, divergent sample from lineage A as a different species, as well as the two sublineages recovered in lineage E. When using the mPTP model, lineages A, F and I are split in two species, while lineage E is split in three.

Downloaded from https://academic.oup.com/zoolinnean/article-abstract/189/4/1249/5714599 by 81263633 user on 05 August 2020

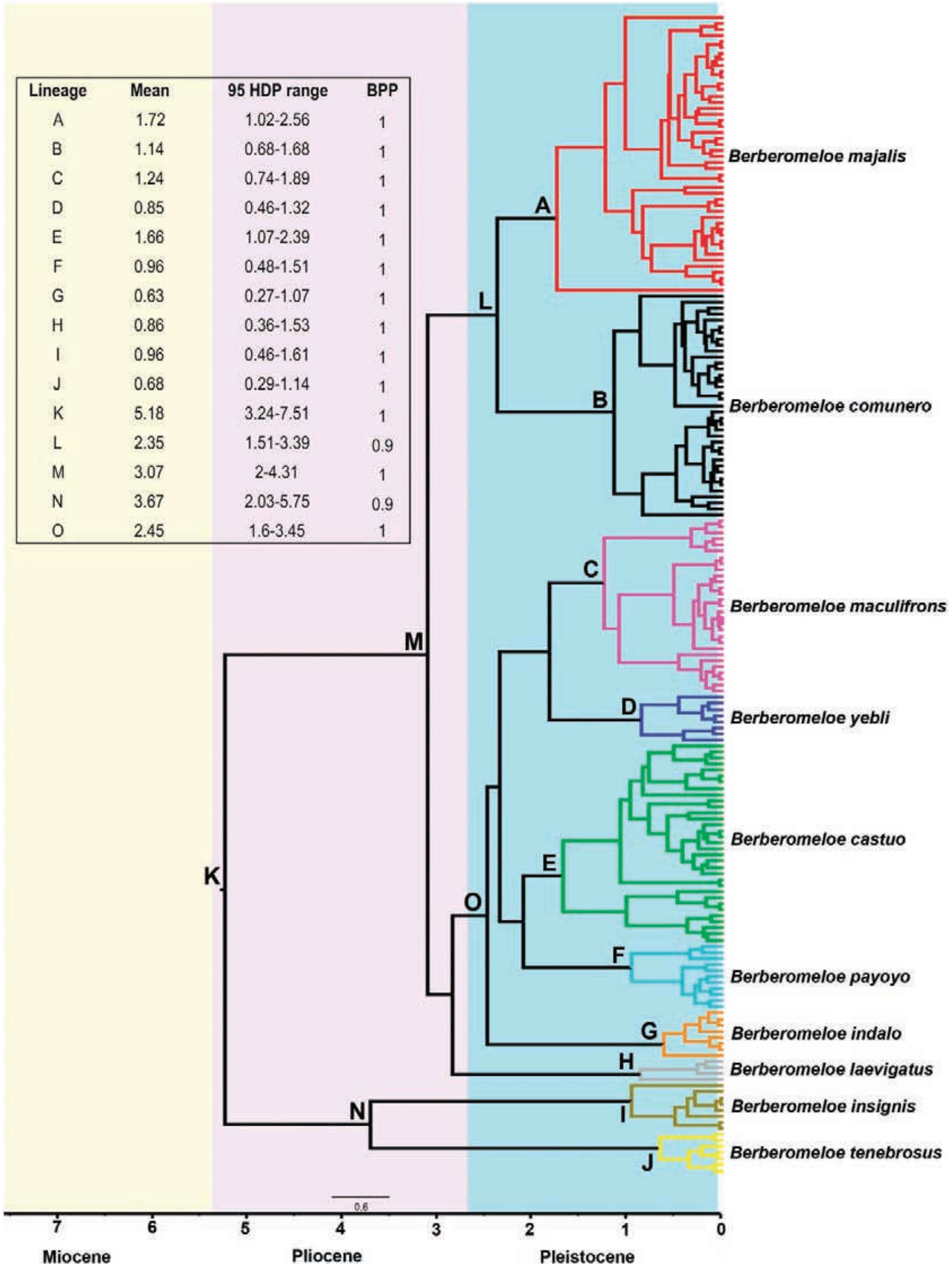

Lineage	Mean	95 HDP range	BPP
A	1.72	1.02-2.56	1
B	1.14	0.68-1.68	1
C	1.24	0.74-1.89	1
D	0.85	0.46-1.32	1
E	1.66	1.07-2.39	1
F	0.96	0.48-1.51	1
G	0.63	0.27-1.07	1
H	0.86	0.36-1.53	1
I	0.96	0.46-1.61	1
J	0.68	0.29-1.14	1
K	5.18	3.24-7.51	1
L	2.35	1.51-3.39	0.9
M	3.07	2-4.31	1
N	3.67	2.03-5.75	0.9
O	2.45	1.6-3.45	1

Figure 4. Bayesian chronogram of the genus *Berberomeloe*. Mean, highest posterior densities (95% HPD) and posterior probabilities of the main clades are shown.

Downloaded from https://academic.oup.com/zoolinnean/article-abstract/189/4/1249/5714599 by 81263633 user on 05 August 2020

TAXONOMIC OUTPUT

The presence of well-supported, reciprocally monophyletic, mitochondrial DNA clades, concordant with geographically structured morphological units, suggests that taxonomic diversity within *B. majalis s.l.* was largely underestimated. Additionally, the paraphyly of *B. majalis s.l.*, with lineage J sister to *B. insignis*, renders untenable the species 'idea'

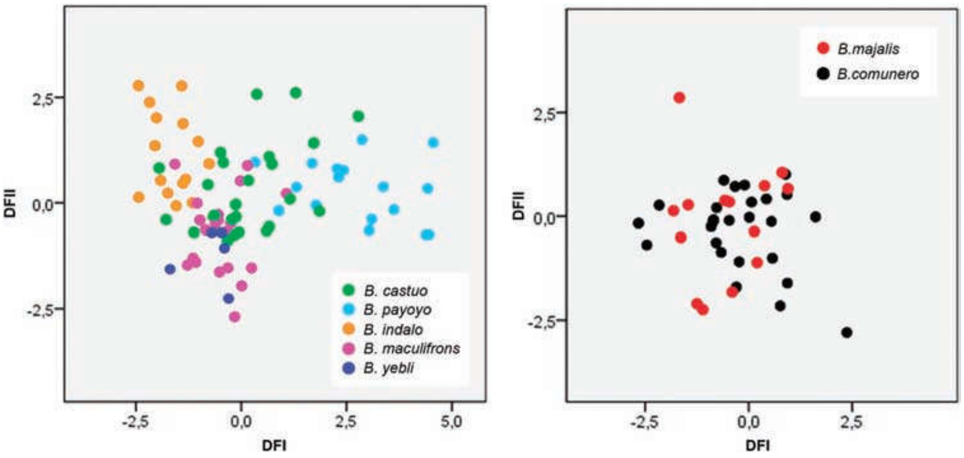

Figure 5. First two axes from Discriminant Function Analysis of eight size-corrected morphometric variables for *Berberomeloe majalis* species group (excluding *B. laevigatus*); point clouds of *B. majalis* and *B. comunero* have been extracted from the analysis and figured independently to facilitate visualization. Each species represented by colours as indicated in the legend.

conveyed by the name *B. majalis.* Under this situation we deem it necessary to redefine *B. majalis*, limiting it to a single morphologically defined phylogroup, and to treat each of the morphologically defined phylogroups depicted in our analyses as evolutionary independent species. Our taxonomic hypothesis results in *Berberomeloe* harbouring ten well-characterized evolutionary units, each of which can be considered as a taxonomic entity. Concordance between monophyletic phylogroups and morphological diagnostic traits also match the confirmed candidate species concept (Padial *et al.*, 2010). These results are more conservative than the output obtained by using molecular species delimitation methods.

The nominal taxon, *B. majalis*, needs to be redefined in a restrictive sense. *Berberomeloe majalis* was described by Linnaeus based on at least two morphologically distinct specimens (LINN 6662 and LINN 6663; LSL), both therefore syntypes. These specimens do not have a label that could link them to Linnaeus' (1758) published type localities: '… Europa australiore; … America…; … Africa…' (see: Day & Fitton, 1978). Since these specimens match the generally adopted concept of *B. majalis* (Bologna, 1989, 1991; García-París, 1998; García-París *et al.*, 2010), we consider that it is realistic to treat them as the types of the species.

Each of the two Linnean specimens correspond to different morphological species, therefore any of those two species could bear the name *B. majalis*. In order to solve this taxonomic problem, and according to the International Code of Zoological Nomenclature (ICNZ, 1999), the fixation of a lectotype is necessary. As lectotype we selected the specimen LINN 6662, morphologically assignable to the phenotype present in the Iberian Southern Plateau populations (lineage A). Once the nominal taxon was fixed to a specific clade, we revalidated two former synonyms (see: e.g. Bologna, 1989, 1991, 2008; García-París *et al.*, 2010): ***Berberomeloe laevigatus* (Olivier, 1797) comb. nov.** (type locality: 'Catalogne'), for north-eastern Iberian populations (mainly Aragon and Catalonia), and ***Berberomeloe maculifrons* (Lucas, 1847) comb. nov.** (type locality: 'environs de Bougie et d`Orán', Algeria), for populations distributed from eastern Morocco to Tunisia. We have described the remaining evolutionary and distinguishable lineages as new species, raising the diversity within *Berberomeloe* from two to ten species. New species are named herein after cultural or historical icons that might be identified with their geographic distribution.

In conclusion, we have identified two species groups: (1) *Berberomeloe majalis* species group formed by *B. majalis* (lineage A), *B. laevigatus* (lineage H), *B. maculifrons* (lineage C) and five new species (lineages B, D, E, F, G) and (2) *Berberomeloe insignis* species group, including *B. insignis* (lineage I) and a new species (lineage J). Each of these species is treated in detail in the accounts section below. Apart from the first, we have omitted description of morphological features common for all species in the genus. Synonymic lists only include synonyms and combinations, not misidentifications or other considerations (see: García-París *et al.*, 2010).

SPECIES ACCOUNTS

BERBEROMELOE MAJALIS (LINNAEUS, 1758)

Meloe majalis Linnaeus, 1758: 419. Terra typica: 'in Europa australiore; in America…; in Africa…'.

Downloaded from https://academic.oup.com/zoolinnean/article-abstract/189/4/1249/5714599 by 81263633 user on 05 August 2020

Meloe majalis var. *sanguineus* Escherich, 1889: 334. Terra typica: 'Cuenca'.
Trichomeloe majalis (Linnaeus, 1758): MacSwain, 1956: 71.
Berberomeloe majalis (Linnaeus, 1758): Bologna, 1989: 361.

Type material examined

Syntypes of *Meloe majalis* Linnaeus, 1758 (LSL, photographs) (not sexed). LINN 6662, labelled: 2 *majalis* [handwritten white label]; 2 [printed white label]. LINN 6663, not labelled. Lectotype: LINN 6662 (designated here).

Holotype of *Meloe majalis* var. *sanguineus* Escherich, 1889 (MNHAT) (not sexed). Specimen labelled: Cuenca Castilien 87. K. [printed white label]; *maculifrons* Lucas [handwritten white label]; *majalis* v. *sanguineus* Escherich [handwritten white label]. Figured in García-París *et al.* (2010: 170, fig. 2).

Lectotype designation and nomenclatural comments: The type series of *Meloe majalis* Linnaeus, 1758 consists of two dry-preserved specimens (syntypes) held in the collection of the Linnean Society of London at Burlington House. We examined several photographs of both specimens (available at http://linnean-online.org/), which are catalogued as LINN 6662 and LINN 6663. Revision of qualitative features indicates that LINN 6662 and LINN 6663 do not represent the same taxonomic unit, differing mainly in the width of the tergal red bars and in the punctures of the pronotum. While the identity of LINN 6663 is difficult to ascertain without manipulation and close examination of the specimen, the specimen LINN 6662 can be morphologically assigned to the central-southern Iberian plateau clade (lineage A). So, under the provisions of article 74 of the International Code of Zoological Nomenclature and Declaration 44, Amendment of article 74.7.3 (ICZN, 1999, 2003), we designate the specimen LINN 6662 as lectotype of *Meloe majalis* Linnaeus, 1758, fixing the unique bearer of the name to the taxon corresponding to lineage A (central-southern Iberian plateau).

Likewise, the study of the holotype of *B. majalis* var. *sanguineus* Escherich, 1889 confirms the synonymy of this variety with *B. majalis s.s.* (see: García-París *et al.*, 2010).

Description: Berberomeloe majalis s.s. presents the general traits of the genus (see: Bologna, 1989, 1991) and it is characterized as follows:

Length (frons to posterior border of elytra), 10–20 mm; maximum total length among preserved, studied specimens, 60 mm. General coloration black, usually with red or orange transverse bars on the posterior margin of each abdominal terga, except VII and VIII. Tegument of the head and pronotum finely microreticulated, semi-glossy. Head with punctures dispersed, similar to those of pronotum but sparser; medium-sized punctures over the temples; middle line subtle but perceptible at the vertex. Antennae (male) with antennomeres III–X subtrapezoidal, not especially expanded at inner apexes; antennomeres V and VI subdentiform, with a yellowish, distinct but diffused area in the inner apex; antennomere XI of normal width, widely cleft at the apex, with the inner end pointed. Pronotum subquadrate, with lateral sides weakly or barely convergent in its posterior two-thirds; presence of two types of punctures, small and medium-sized, all over its surface; puncture density low to medium, mostly covering the sides and fore angles; middle longitudinal line finely impressed. Elytral surface with shallow and dispersed punctures; tegument with fine but marked longitudinal corrugations. Abdomen black, usually with a wide red-orange coloured transverse bar at the caudal margin of each terga, except VII and VIII. Male genitalia (Fig. 6C–F) with tegmen (parameres + phallobasis) evenly sclerotized; parameres moderately elongated, length similar or a little longer than phallobase, with distal lobes relatively elongated in lateral view; median lobe (aedeagus) with two similar, acute ventral hooks far from the apex, and well separated between each other; apex obliquely truncated in lateral view; endophallic hook slender. Female genitalia with sclerotized spicules in the inner side of the bursa copulatrix.

Variability: Body length highly variable, from 10 to 20 mm. Morphometric variability is shown in Table 2. Colour intensity of the transverse bar variable, from light-red to blood-red. Populations composed only by entirely black specimens have been recorded in some geographically localized areas in the province of Ciudad Real (Piedrabuena and Carrión de Calatrava) (Bravo *et al.*, 2017). Some specimens show a single, small red spot on the frons, diffuse and little marked (e.g. holotype of *Meloe majalis* var. *sanguineus*). A slight variation in the density of the puncturation of head and pronotum was observed across populations. *Berberomeloe majalis* presents variability in the width of coloured transverse tergal bars, but on average they are relatively wide (ratio 'total width of the second tergum/width of the transverse bar of the second tergum' between 1.04 and 2.03, average = 1.6, SD = 0.27, *N* = 23). Specimens from Penyagolosa (Castellón) show wider coloured transverse tergal bars and deeper punctures. Individuals recently emerged from pupal stage present a non-expanded abdomen, almost completely covered by the elytra; abdomen expands and increases in volume as they start feeding (as reported by Cortés-Fossati, 2018a for *B. payoyo*;

Downloaded from https://academic.oup.com/zoolinnean/article-abstract/189/4/1249/5714599 by 81263633 user on 05 August 2020

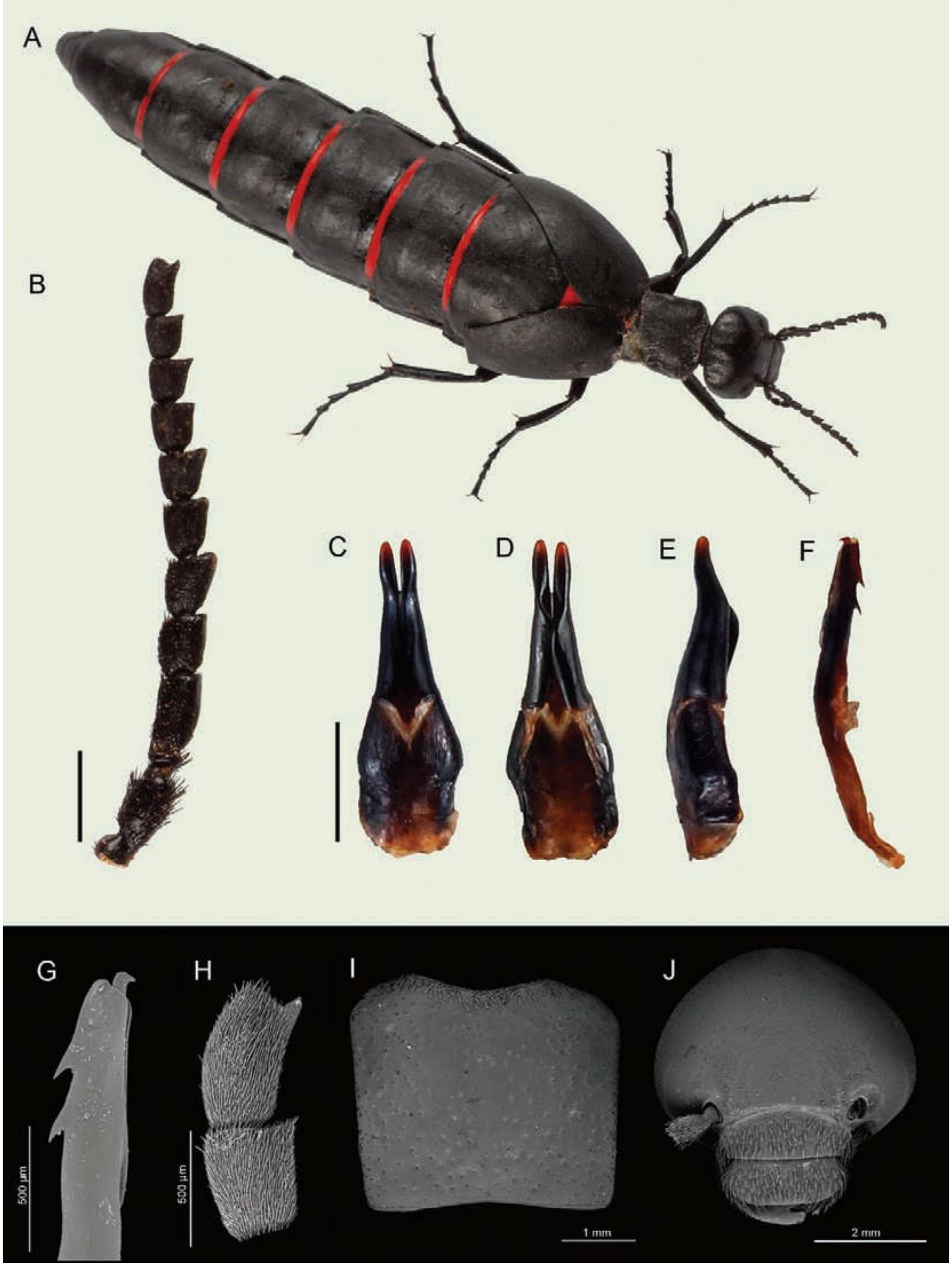

Figure 6. Habitus and morphological details of *Berberomeloe majalis* from Villafranca de los Caballeros, Ciudad Real (A) and La Guardia, Toledo (B–J). A, dorsal view of a female; B, male antenna; C, D, E, dorsal, ventral and lateral view of male genitalia, showing parameres and phallobase; F, lateral view of aedeagus; G, SEM micrographs of distal part of aedeagus; H, SEM micrographs of two last antennomeres; I, SEM micrographs of pronotum, dorsal view; J, SEM micrographs of head, frontal view.

pers. obs., under laboratory conditions). This pattern of individual abdominal size change is present in all the species of *Berberomeloe*.

Diagnosis: Berberomeloe majalis can be distinguished from all other species of *Berberomeloe* by the following combination of characters (Fig. 6): (1) abdomen with

Downloaded from https://academic.oup.com/zoolinnean/article-abstract/189/4/1249/5714599 by 81263633 user on 05 August 2020

Table 2. Mean and standard deviation (SD) of the morphometric measurements (in mm) from studied *Berberomeloe* specimens (excluding *B. laevigatus* and *B. insignis*)

	Berberomeloe castuo			***Berberomeloe payoyo***			***Berberomeloe indalo***			***Berberomeloe yebli***		
	Mean	**SD**	***N***	**Mean**	**SD**	***N***	**Mean**	**SD**	***N***	**Mean**	**SD**	***N***
Pronotum length	2.74	0.66	29	3.11	0.7	21	3.21	0.47	17	2.64	0.33	9
Pronotum proximal width	3.6	0.89	29	4.38	1.08	21	4.53	0.58	17	3.47	0.41	9
Pronotum distal width	3.27	0.79	29	4	0.98	21	3.92	0.55	17	3.25	0.44	9
Head width	4.37	1.09	29	5.1	1.24	21	5.43	0.77	17	4.13	0.6	9
Width of the second tergal bar	4.01	1.16	28	4.68	1.09	18	7.99	1.47	15	4.28	0.78	7
Width of the third tergal bar	4.31	1.21	28	4.97	1.27	19	8.39	1.34	15	4.75	0.76	8
Longitude of metafemur	4.07	1	25	4.71	1.05	20	5.24	0.7	17	3.75	0.41	6
Longitude of elytra	7.59	1.68	29	9.22	2.07	20	9.44	1.36	17	7.48	1.04	9
	Berberomeloe maculifrons			***Berberomeloe majalis***			***Berberomeloe comunero***			***Berberomeloe tenebrosus***		
	Mean	**SD**	***N***	**Mean**	**SD**	***N***	**Mean**	**SD**	**N**	**Mean**	**SD**	***N***
Pronotum length	2.79	0.53	39	2.83	0.51	29	2.81	0.6	44	2.98	0.5	11
Pronotum proximal width	3.72	0.74	39	3.69	0.66	28	3.63	0.86	44	4.07	0.64	11
Pronotum distal width	3.42	0.66	39	3.35	0.59	29	3.35	0.8	44	3.38	0.6	11
Head width	4.46	0.98	39	4.48	0.82	29	4.41	1.04	44	4.57	0.8	11
Width of the second tergal bar	6.05	1.2	33	4.72	1.34	24	4.97	1.43	35	0	0	11
Width of the third tergal bar	6.47	1.35	32	5.21	1.37	24	5.4	1.51	35	0	0	11
Longitude of metafemur	4.52	0.75	24	4.36	0.75	18	4.1	0.86	33	4.36	0.71	11
Longitude of elytra	8	1.71	35	7.88	1.48	29	7.79	1.67	44	7.78	1.08	11

red-coloured transverse bars of medium to large width in the posterior margin of tergites I–VI; (2) punctures on the head small to medium-sized, rounded, shallow, isolated from each other, but relatively dense; (3) pronotum subquadrate with rounded, not particularly expanded, fore angles and with lateral margins weakly converging backwards; (4) pronotum surface usually homogeneously punctured, with two types of puncturation, small and medium-sized, generally non-confluent; (5) male genitalia with the apex of the median lobe obliquely truncated in lateral view; (6) male antennomere XI wide; and (7) male antennomeres VII and IX moderately expanded on the inner apical side.

Distribution and notes on natural history: Berberomeloe majalis occurs in most of the central and eastern regions of the Iberian Peninsula, covering the Meseta Sur and most of the Sistema Ibérico Meridional Mountain Range, over the following Spanish provinces (Fig. 2): Madrid (limited to the south-eastern border), central and eastern Toledo and Ciudad Real, Albacete, Cuenca, Guadalajara (mostly in the south-east), Teruel, Castellón, Valencia and Jaén (north of the province). Distributional limits are yet to be defined in detail. It occurs across a wide spectrum of substrates, from limestone and gypsum soils to granitic formations (see: Vera, 2004). It is present in different habitat types, mostly open areas, including cereal fields, steppes, Mediterranean shrublands and Mediterranean open forests (Fig. 7). Most records are located within the meso-Mediterranean bioclimatic level and, to a lesser extent, at the supra-Mediterranean, in regions with ombrotype from dry to humid (see: Rivas-Martínez, 1987; Rivas-Martínez *et al.*, 2002).

Biological aspects of *B. majalis* are poorly known, but they are expected to be similar to the ones described generically for *B. majalis s.l.* (previous to this study) by Beauregard (1890), Bologna (1989, 1991), Cros (1912, 1913, 1921, 1928) and Górriz Muñoz (1878, 1882).

BERBEROMELOE CASTUO SÁNCHEZ-VIALAS *ET AL.*, SP. NOV.

LSID: urn:lsid:zoobank.org:act:3528014D-4F1E-488D-AAA1-CF26421FE5DB

Holotype: Female: Spain, Extremadura, Cáceres, Losar de la Vera, paraje de Valcamello, 40°6’44.44”N, 5°36’27.63”W, 15 May 2016, Conrado Sánchez Díaz leg. [white label, handwritten]; MNCN_Ent 231422 [white label, printed]; ASV16079 [white label, printed]; Holotypus, *Berberomeloe castuo* Sánchez-Vialas, García-París, Ruiz & Recuero des. 2019 [white label, printed]. Preserved in absolute ethanol at the Entomological collection of the Museo Nacional de Ciencias Naturales, Madrid.

Downloaded from https://academic.oup.com/zoolinnean/article-abstract/189/4/1249/5714599 by 81263633 user on 05 August 2020

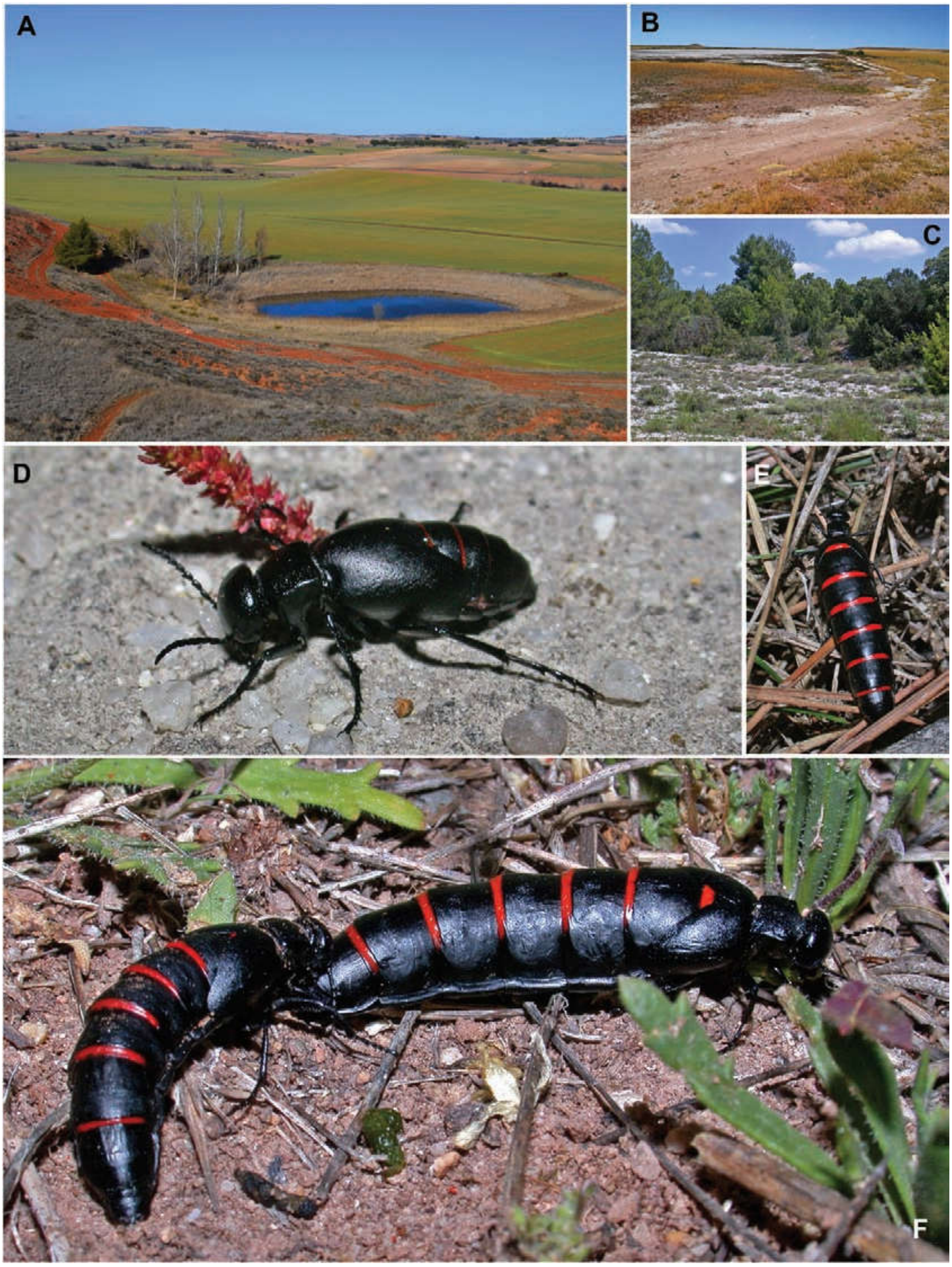

Figure 7. A–C, habitat of *Berberomeloe majalis*, Spain. A, Pozo Airón, La Almarcha, Cuenca; B, Pajares, Ciudad Real; C, Bascuñana, Cuenca. D, newly emerged specimen from Tembleque, Toledo; note the unexpanded abdomen. E, specimen from Penyagolosa, Castelló; unlike most populations, specimens from this region present characteristic wide transverse abdominal bars. F, *Berberomeloe majalis* courtship, Alcazar de San Juan, Ciudad Real.

Paratypes: Castillejo de Dos Casas (Salamanca), 30 May 2009, I. Doadrio leg. [printed white label]; MNCN_Ent 231423 [printed white label] (male, extracted genitalia, preserved dry).—Spain, Cáceres, Garrovillas, Monasterio de Santa Gracia, 23 May 2001, M. García-París leg., MAB166 [white label, printed];

Downloaded from https://academic.oup.com/zoolinnean/article-abstract/189/4/1249/5714599 by 81263633 user on 05 August 2020

MNCN_Ent 231424 [white label, printed] (female, extracted genitalia, preserved dry).—Cáceres, 1 km SE Arroyo de la Luz, 23 May 2001, NTM72, MAB121, M. Gª-París leg. [white label, printed]; MNCN_Ent 231425 [white label, printed] (female, extracted genitalia, preserved in ethanol).—Villablanca (Huelva) Hispania, 25 Mar. 1983, J. de Ferrer leg. [white label, printed and handwritten]; MNCN_Ent 231426 [white label, printed] (preserved dry).—Ávila, Villanueva Campillo, 15 June 2005, M. Gª-París leg, mel05111, Bm [white label, printed]; MNCN_Ent 231427 [white label, printed] (preserved in ethanol).—Spain, Cáceres, 6 km al S de Guijo de Coria, 16 April 2004, M. García-París, mel04022 [white label, printed]; MNCN_Ent 231428 [white label, printed] (preserved in ethanol).—Spain, Ourense: Lampaza-Pedrosa, 42°05’58.82’’N, 7°52’05.91”O, 718 m, 21 April 2012, mel12006, M. Gª-París & N. Percino leg. [white label, printed]; MNCN_Ent 231429 [white label, printed]; ASV16040 [white label, printed] (male, extracted genitalia, preserved in ethanol).—Castilblanco, Badajoz, España, 39°17’9.08”N, 5°4’59.35”W, 26/05/2016, D. Bermejo leg. [white label, handwritten]; MNCN_Ent 231430 [white label, printed] (preserved in ethanol).—Guadalupe, Cáceres, 12 May 1957 [white label, handwritten]; MNCN_Ent 232459 [white label, printed] (preserved dry).—Guadalupe, Cáceres, 12 May 1957 [white label, handwritten]; MNCN_Ent 232460 [white label, printed] (preserved dry).—Béjar, Salamanca, 960 m [white label, handwritten]; Expedición Instituto Español de Entomología, July 1954 [white label, printed]; *Berberomeloe majalis* Linnaeus, 1758, M. Gª-París det. 98 [printed]; MNCN_Ent 233399 [white label, printed] (preserved dry).—2 exx. Cáceres, Jarandilla de la Vera, 40°5’49.28”N, 5°38’4.33”W, 20/05/2018, A. Sánchez-Vialas & K. López-Estrada leg. [white label, handwritten]; MNCN_Ent 250985 and MNCN_Ent 250986, respectively [white labels, printed] (preserved in ethanol).—Cáceres, Serradilla, Garganta del Fraile (arroyo Trasierra), 360 m, 29N7473387E/44412418N [white label, handwritten]; mel08239 [white label, printed]; MNCN_Ent 250987 [white label, printed] (preserved in ethanol).—2 exx. labelled: Portugal, Granja, 38°18’9.95”N, 7°15’30.15”W, 185 m, 23 April 2016, A. Sánchez-Vialas leg. [white label, printed] (preserved in ethanol); MNCN_Ent 250988 and MNCN_Ent 250989, respectively [white labels, printed].—2 exx. labelled: Portugal, Barrancos, 38°8’26.45”N, 7°3’12.34”W, 300 m, 23 April 2016, A. Sánchez-Vialas leg. [white label, printed]; MNCN_Ent 250990 and MNCN_Ent 250991, respectively [white labels, printed] (preserved in ethanol).—Portugal, Odemira (Algarve), 10 May 2017, Daniel Escoriza leg. [white label, handwritten]; APP 17004 [white label, handwritten]; MNCN_Ent 250992 [white label, printed] (preserved in ethanol). All paratypes labelled: ‘Paratypus, *Berberomeloe castuo* Sánchez-Vialas, García-París, Ruiz & Recuero, des. 2019 [red labels for dry-preserved specimens, and white labels for ethanol-preserved specimens, all printed]’. All specimens are held at the Entomological collection of the Museo Nacional de Ciencias Naturales, Madrid. Total paratypes: 19 exx.

Etymology: The epithet is derived from Spanish *castúo*, referring to the inhabitants and language of Extremadura where the type locality of the species is situated. It is a noun in apposition.

Description of the holotype: Length (frons to posterior margin of elytra), 11.9 mm. Total length (including abdomen) of preserved holotype, 64 mm. Maximum width, 7.1 mm. Body robust. Voluminous and elongated abdomen. Reduced and convex elytra, wings absent. Coloration black all over body and appendages, with a narrow orange transverse bar in the posterior edge of each tergum, except VII and VIII, which are entirely black. Tegument of silky appearance, with fine, but apparent, microreticulation. Tibial spines and tarsal claws brownish. Black setae dispersed over the body, scattered on dorsal areas of head, thorax and abdomen. Head voluminous, broadly rounded and slightly wider than the pronotum (head maximum width: 5.5 mm). Temples wide and regularly rounded. Surface covered by numerous small to medium-sized punctures, almost uniformly distributed, rounded, deep marked, usually isolated from each other, but subconfluent on the frons (just below the midline) and temples. A longitudinal midline is finely impressed from the upper half of the frons to the vertex. Frontal side of the cephalic capsule slightly curved, with the surface above the antennal insertions markedly elevated and the disc region almost flat. Frons and temples almost glabrous, with a short seta on each puncture, and longer setae on the upper margin of the antennal insertion. Back of the head with moderately long, decumbent setae. Neck (sclerotized region between the posterior edge of the head and pronotum) laminar, semilunar, conspicuous, dense and deeply punctate, also with moderately long and decumbent setae. Eyes small, kidney-shaped and weakly swollen, with the upper and lower lobes of similar size; barely notched at the level of antennal insertions; minimum interorbital distance: 3.3 mm. Suture between frons and clypeus deeply marked, arcuate. Clypeus flat, subrectangular, transverse (2.7 mm wide by 1.0 mm long); punctures small and separated, almost absent in the fore region; long setae evenly distributed following the puncture pattern, directed forward, longer in the sides. Labrum–clypeus suture almost straight. Labrum transverse (2.7 mm wide by 1.1 mm long), slightly emarginated in the middle; punctures similar to those of the clypeus; setae

Downloaded from https://academic.oup.com/zoolinnean/article-abstract/189/4/1249/5714599 by 81263633 user on 05 August 2020

longer in the lobes, following the puncture pattern, oriented forward and curved towards the centre. Mandibles robust, longitudinally concave on outer side and notched in the distal region, glabrous in the apex, and basally pilose. Maxillary palpi with palpomere I longer than the others, subtroncoconical; II short, subcylindrical; III subtrapezoidal and dorsoventrally flattened; distal palpomere widest with a narrow excavation along the distal margin; setation moderately long in palpomeres I and II, shorter on the distal segment. Labial palpi with palpomere I subcylindrical; II troncoconical; III subtrapezoidal, with setation as on maxillary palpi. Antennae with eleven antennomeres, subcompressed, not reaching the pronotum base when extended backward. Antennomeres widened apically, with short black vestiture, mostly decumbent and with a few sparse setae erect, longer and semi-erect on antennomeres I–II; antennomere I slightly widened apically, subcylindrical (length: 0.8 mm); II short, subglobose (length: 0.3 mm); III (length: 0.8 mm) subcylindrical, slightly widened apically, rectangular; IV (length: 0.7 mm) shorter than III but equally wide, subrectangular; V (length: 0.7 mm) trapezoidal, wider than VI, with a wide and smooth apical tooth on the inner edge; VI (length: 0.7 mm) trapezoidal, with a wide and smooth apical tooth on the inner edge; VII (length: 0.6 mm) trapezoidal, wider than VI, with an acute apical tooth on the inner edge; VIII (length: 0.6 mm) trapezoidal, weakly dentate on inner edge apex; IX (length: 0.5 mm) trapezoidal, dentate on inner edge; X (length: 0.5 mm) trapezoidal, apical tooth slightly acute; XI (length: 0.6 mm) subconical, notched on apex. Pronotum subquadrate with subparallel sides, narrower behind (anterior side of pronotum: 4.9 mm; basal edge of pronotum: 4.4 mm; pronotum length on sagittal plane: 3.7 mm); anterior margin concavely curved, posterior margin slightly arcuate; fore and hind angles rounded; surface weakly convex with sides slightly elevated, with a fine and impressed longitudinal midline, and shallow, diffuse lateral depressions next to the fore angles, less marked next to the posterior ones. Pronotum base entire and finely bordered. Pronotum surface almost evenly covered with dense punctures; punctures of various sizes, rounded and relatively deep, close but mostly isolated from each other, occasionally confluent (on the sides), but not forming a corrugated or reticulated pattern. Dorsal surface of pronotum of glabrous appearance, with an isolated short seta in each puncture; anterior margin, adjacent to the neck, with numerous, moderately long setae. Mesonotum covered by the pronotum, showing only its posterior margin, straight and strongly punctate, with longitudinal wrinkles. Metanotum completely covered by elytra. Prosternum narrow, slightly extended posteriorly, pointed at the tip. Mesosternum with a triangular prolongation, extended posteriorly, ending in a rounded tip that extends to the level of the upper half of mesocoxae; lateral extensions narrow; surface covered by disperse short setae. Metasternum subtrapezoidal. Elytra reduced and convex, imbricated basally (the right over the left), longer than pronotum (length: 7.7 mm), divergent posteriorly and reaching the posterior edge of the second tergum; tegument glabrous, slightly corrugated longitudinally with impressed irregular vermicular lines and scarce, weakly marked, dispersed punctures. Abdomen voluminous. First tergum partly covered by elytra. Distal margin of tergites I–VI with an orange transverse bar, relatively narrow in comparison with the total width of the terga (width of the second tergum: 8.4 mm; width transverse bar of the second tergum: 4.9 mm); tergites VII and VIII entirely black. Dorsal surface of abdomen smooth, almost glabrous, with scarce, small and shallow punctures with a short seta on each puncture. Distal margin of last tergite with dense, short setae. Ventrites with sparse and slightly marked punctures mostly on the posterior half, with short and decumbent black setae, scattered but homogeneously distributed. Last ventrite rounded at the hind margin. Legs moderately robust, covered by decumbent and relatively long setae. Trochanters and coxae of middle legs overlap partially with hind coxae. Metafemur shorter than metatibia (metafemur length: 5.1 mm; metatibia length: 5.5 mm). Pro- and mesotibiae with two similar spurs, slender and straight; metatibial spurs dissimilar and divergent; inner spur spatulated, outer spur similar to those of fore- and mesotibiae. Tarsi long, with tarsomeres subcylindrical, slightly expanded distally and emarginated. Protarsi shorter than meso- and metatarsi. First tarsomere of metatarsus large, followed in size by second and third (metatarsal tarsomeres length, from inner to apical: 2.8, 1.6, 1.3, 1.4 mm). Tarsal ventral pads consisting on a dense, short and thick tuft of semi-erected setae. Metatarsomeres with relatively thick setae, distributed longitudinally through the dorsal side of each of them. Claws smooth, curved, with the lower lobe narrower and smaller. External genitalia formed by wide valvifers, which are approximately two times longer than the stylus. Stylus narrow and cylindrical with long setae. Inner surface of the bursa copulatrix with large sclerotized spicules and plates of irregular shape (Fig. 8A).

Male: Similar to the female, but differing from it in the form of the last abdominal tergite (VIII), which is emarginated at the hind margin, and in the antennomeres, clearly more dentate (Fig. 9B). Antennomere I slightly widened apically, subcylindrical; II short, cylindrical; III subrectangular, slightly widened apically; IV longer than III but equally wide, subrectangular; V subtriangular, wider

Downloaded from https://academic.oup.com/zoolinnean/article-abstract/189/4/1249/5714599 by 81263633 user on 05 August 2020

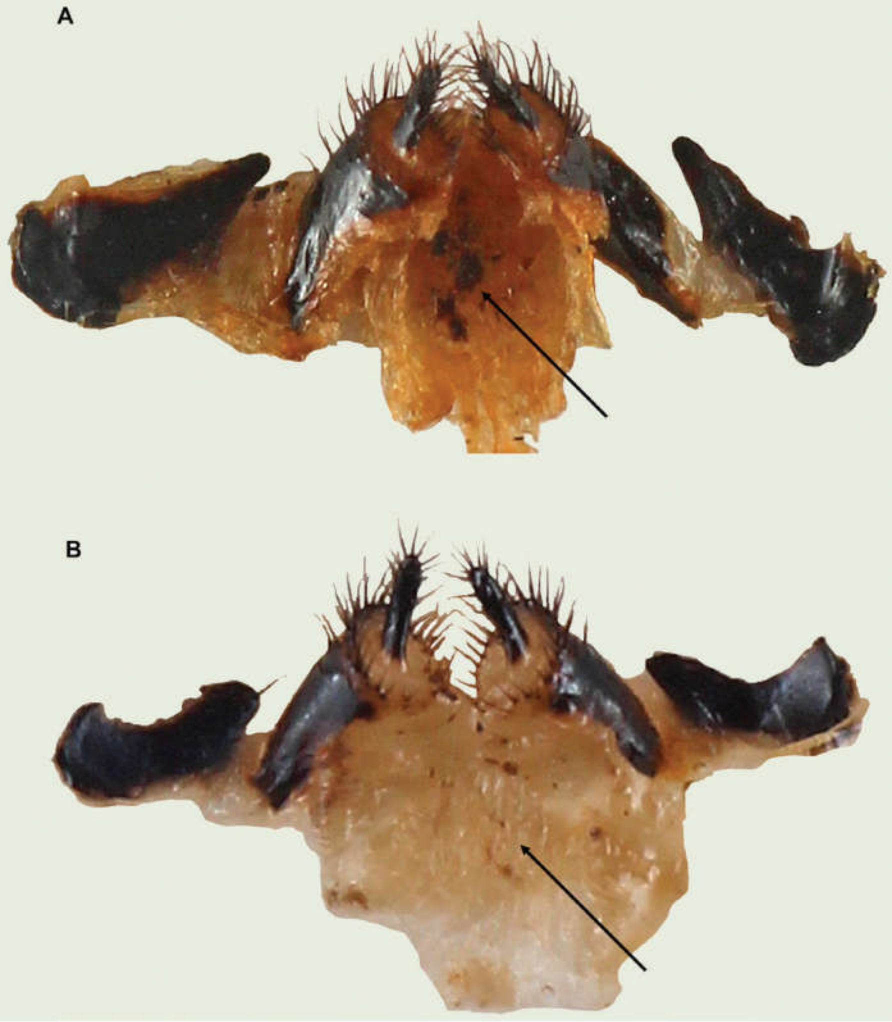

Figure 8. Female genitalia of (A) *Berberomeloe castuo* and (B) *B. indalo*, showing the valvifera and style over the inner side of the vagina. An arrow shows the place where sclerotized spicules are present (A) or absent (B).

than VI at apex, with a wide and rounded apical tooth on the inner edge; VI subtrapezoidal, with an apical tooth on the inner edge; VII trapezoidal, with an apical tooth on the inner edge; VIII trapezoidal, narrow than VII, weakly dentate on the apex of the inner edge; IX trapezoidal, moderately dentate on inner edge; X trapezoidal, narrower than IX, apical tooth slightly acute; XI subconical with subparallel sides, moderately slender, notched on apex. Male genitalia (Fig. 9C–G) with tegmen brownish; moderately elongated, relatively slender both on dorsal and lateral views. Phallobase longer than wide, a little shorter than the parameres, wider on dorsal view; maximum width at the middle. Parameres longer than wide, basally cylindrical; distal third formed by parameral lobes; setae scarce, applied against the tegument, on the central dorsal region of parameres. Parameral lobes separated by a longitudinal notch that extends to the middle of the dorsal surface of the parameres; apexes rounded, digitiform. Median lobe long, robust, flattened, truncated at the apex, with two acute ventral hooks, subequal, close to each other and separated from apex. Endophallic hook visible.

Variability: Body length (frons to posterior edge of elytra) highly variable, 8–17 mm; maximum total length among preserved, studied specimens, 64 mm. Morphometric variability shown in Table 2. Specimens from populations distributed along the south-western area of the Iberian Peninsula (southern Portugal and south-western Spain) are entirely black coloured. Specimens from populations located north of the Sistema Central mountain range, including northern Portugal and the provinces of Ourense, León and Zamora in Spain, usually present the abdominal transverse bars wider than southern and central populations, but variability of the coloured

Downloaded from https://academic.oup.com/zoolinnean/article-abstract/189/4/1249/5714599 by 81263633 user on 05 August 2020

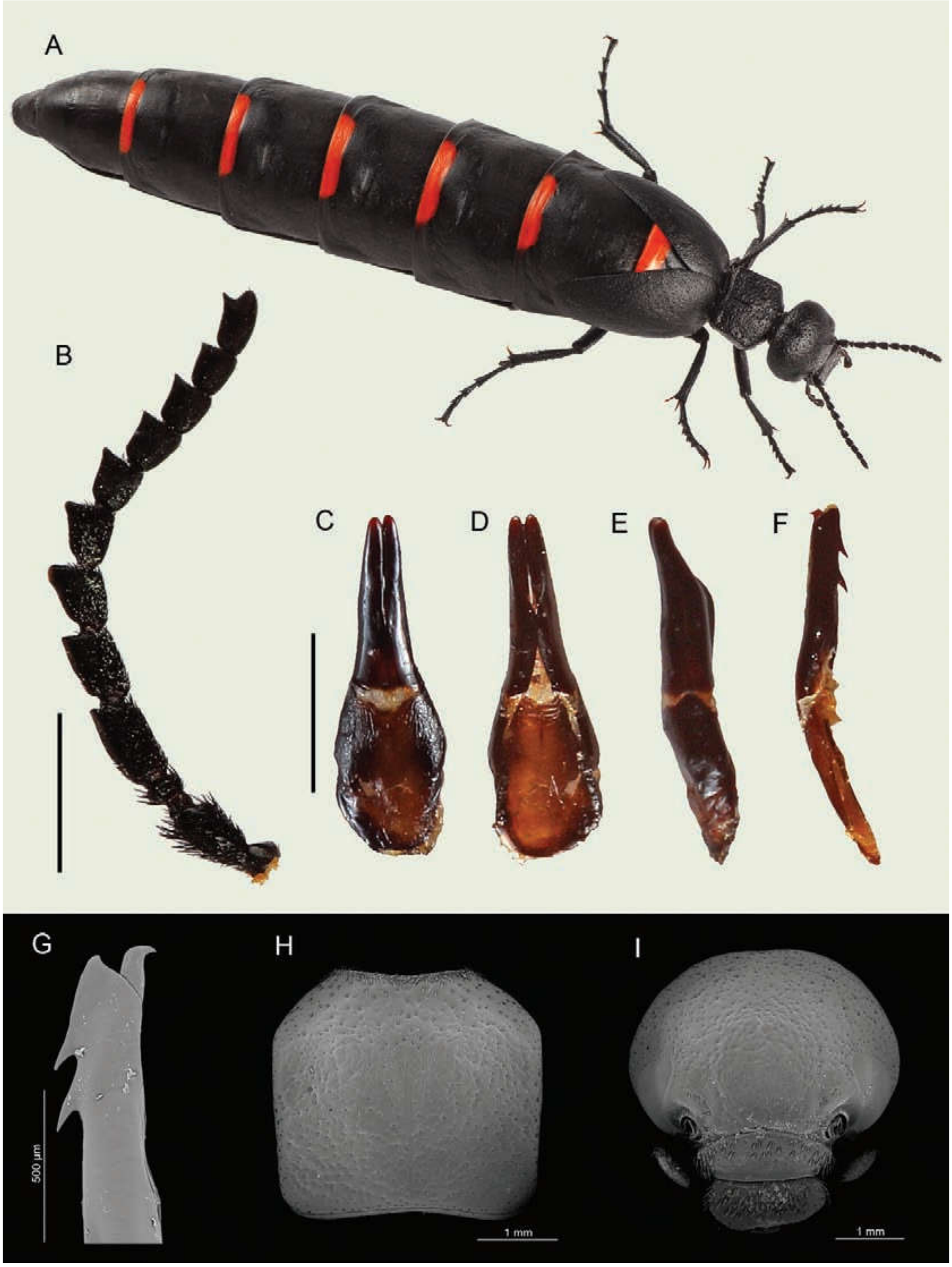

Figure 9. Habitus and morphological details of *Berberomeloe castuo* from Losar de la Vera, Cáceres (A), and Castilblanco, Badajoz (B–I). A, dorsal view of a female; B, male antenna; C, D, E, dorsal, ventral, lateral view of male genitalia, showing parameres and phallobase; F, lateral view of aedeagus; G, SEM micrographs of distal part of aedeagus, note the truncated shape of the apex; H, SEM micrographs of pronotum, dorsal view; I, SEM micrographs of head, frontal view.

bar width is relatively small (ratio ‘total width of the second tergum/width of the transverse bar of the second tergum’ between 1.68 and 2.50, average = 2.1, SD = 0.23, $N = 30$). Coloration of the abdominal transverse bars in live specimens is yellow to orange in most populations of the Extremadura Region, and deep red in areas north to

Downloaded from https://academic.oup.com/zoolinnean/article-abstract/189/4/1249/5714599 by 81263633 user on 05 August 2020

the Sistema Central mountain range. Some variability in the density of puncturation of the head and pronotum can be observed within populations, as well as in the width of parameral lobes.

Diagnosis: Berberomeloe castuo can be distinguished from all other species of *Berberomeloe* by the following combination of characters (Fig. 9): (1) narrow to very narrow coloured transverse tergal bars on the distal margin of tergites I–VI; (2) punctures on the head large to medium-sized, rounded, deep and close to each other; (3) pronotum surface almost homogeneously punctate; with two types of punctures, large and medium-sized, generally close to each other, of medium density; (4) fore angles of pronotum rounded, not especially expanded; (5) male genitalia with apex of median lobe obliquely truncated in lateral view and distal region of the parameres wide and relatively short in lateral view; (6) antennomere XI in males wide; and (7) antennomeres V–VII in males markedly expanded on its inner apical side.

Distribution and notes on natural history: Berberomeloe castuo is one of the most widely distributed species of the genus (Fig. 2). It ranges across most of the occidental half of the Iberian Peninsula, including all Portugal and the Spanish provinces of Huelva, Badajoz, Cáceres, western Toledo, Ávila, Salamanca, Zamora, León and Ourense. It is likely to occur in western areas of the provinces of Valladolid, Segovia and Ciudad Real. It occurs from almost sea level to 1345 m at La Cañada (province of Ávila); it occupies thermo-, meso- and supra-Mediterranean bioclimatic levels and, more locally (in the northernmost regions), the Montane Eurosiberian, with ombrotypes from dry to humid (Rivas-Martínez, 1987; Rivas-Martínez *et al.*, 2002). Geological substratum is diverse across its distribution area, but mainly siliceous, including granites, sandstones, gneisses and schists, generating acid soils (see: Vera, 2004). *Berberomeloe castuo* occupies several types of open habitats, including open pastures, shrublands (dominated by *Cistus* L., *Lavandula* L. or *Thymus* L.), farmland edges, forest edges (mostly dominated by *Pinus* L. or *Quercus* L.) and dehesas (cleared *Quercus* forests) (Fig. 10).

Biological aspects of this species are expected to be similar to the ones described for the genus by Bologna (1989, 1991). Adults are found from April to July.

BERBEROMELOE COMUNERO SÁNCHEZ-VIALAS *ET AL.*, **SP. NOV.**

LSID: urn:lsid:zoobank.org:act:CF638D73-6A93-4FAE-88D1-D548C0214D29

Holotype: Male: Spain, Madrid, Montejo de la Sierra, pastizal junto al pueblo, 24 April 1999, M. García-París leg. [printed white label]; MNCN_Ent 231431 [printed white label]; Holotypus, *Berberomeloe comunero* Sánchez-Vialas, García-París, Ruiz & Recuero des. 2019 [printed white label]. Preserved in absolute ethanol, held at the Entomological Collection of the Museo Nacional de Ciencias Naturales, Madrid.

Paratypes: Spain, Madrid, Montejo de la Sierra, pastizal junto al pueblo, 24 April 1999, MAB166, M. García-París leg. [white label, printed]; MNCN_Ent 231431 [white label, printed] (male, preserved in ethanol).—Spain, Madrid, Montejo de la Sierra, pastizal junto al pueblo, 24 April 1999, NTM120, M. García-París leg. [white label, printed]; MNCN_Ent 231433 (female, extracted genitalia, preserved dry).—Spain, Madrid, Montejo de la Sierra, pastizal junto al pueblo, 24 April 1999, M. García-París leg. [white label, printed]; MNCN_Ent 231432 [white label, printed]; 118 [white label, handwritten] (female, extracted genitalia, three legs separated, preserved dry).—Madrid, Rivas de Jarama (Urbanizaciones), 5 June 2009, mel09044, M. G^{a}-París & G. G^{a}-Martín leg. [white label, printed]; MNCN_Ent 231434 [white label, printed] (female, preserved in ethanol).—Área de Montarco, Rivas-Vaciamadrid (Madrid), 13 April 2006, J. I. López-Colón leg. [white label, handwritten]; MNCN_Ent 231435 [white label, printed] (preserved in ethanol).—Madrid, Alcalá de Henares, 16 May 2001 [white label, printed]; MNCN_Ent 233312 (preserved dry).—Madrid, Alcalá de Henares, 16 May 2001[white label, printed]; MNCN_Ent 233313 (preserved dry).—Madrid, Alcalá de Henares, 16 May 2001 [white label, printed]; MNCN_Ent 233314 (preserved dry).—Madrid, Leganés, 8 June 1990 [white label, handwritten]; *Meloe majalis* Linneo; ex. Colección M. de los Mozos; MNCN_Ent 173819 [white label, printed] (preserved dry).—Madrid, Barrio del Pilar, 21 April 1980, M. de los Mozos leg., entre hierbas [white label, handwritten]; *Meloe majalis* Linneo [white label, handwritten]; ex. Colección M. de los Mozos; MNCN_Ent 173820 [white label, printed] (preserved dry).—5 exx. MNCN_Ent 232449 to MNCN_Ent 232453 [white label, printed]; Madrid, Braojos, 24 April 2012, F. A. Montes leg. [white label, printed] (preserved dry).—Madrid, San Fernando de Henares, 16 May 2011, J. I. López-Colón leg. [white label, printed]; MNCN_Ent 232454 [white label, printed] (preserved dry).—Madrid, Ciudad Universitaria, 14 April [white label, handwritten]; *Berberomeloe majalis* Linnaeus, 1758 [white label, printed]; MNCN_Ent 233310 [white label, printed] (preserved dry).—Spain, Madrid, Rivas del Jarama, 13 March 1988, F. A. Montes leg. [white label, printed]; *Berberomeloe majalis* Linnaeus, 1758, M. G^{a}-París det. 98 [white label, printed]; 342 [white label, handwritten]; MNCN_Ent 233311 [white label, printed] (preserved dry).—Madrid, El Molar [white label, handwritten];

Downloaded from https://academic.oup.com/zoolinnean/article-abstract/189/4/1249/5714599 by 81263633 user on 05 August 2020

Figure 10. A, B, habitat of *Berberomeloe castuo*, Spain. A, dehesa ecosystem with cattle, Plasencia, Cáceres; B, Jarandilla de la Vera, Cáceres. D, E, specimens of *B. castuo* from Ramacastañas, Ávila and Agallas, Salamanca, respectively. C, specimen of *B. castuo* showing defensive behaviour from Cabezas Rubias, Huelva; note the lack of the coloured abdominal transverse bars, typical from the southern populations.

Berberomeloe majalis Linnaeus, 1758, M. Gª-París det. 98; 571 [white label, handwritten]; MNCN_Ent 233309 [white label, printed] (preserved dry).—2 exx. labelled: Madrid, Lozoyuela, 20 June 2002, I. Martínez-Solano & I. Sánchez [white label, handwritten]; MNCN_Ent 250993 and MNCN_Ent 250994, respectively [white

Downloaded from https://academic.oup.com/zoolinnean/article-abstract/189/4/1249/5714599 by 81263633 user on 05 August 2020

labels, printed] (preserved in ethanol).—Madrid, Montejo de la Sierra, 24 April 1999, NTM 121 [white label, handwritten]; MNCN_Ent 250995 [white label, printed] (preserved in ethanol).—Spain, Madrid, 4.5 Km E/SE de Rivas Vaciamadrid, 576 m, 40°18’54.46”N, 3°34’22.57”W, 11/V/2009, I. Martínez-Solano, C. Settani, E. Recuero leg. [white label, handwritten]; MNCN_Ent 250996 [white label, printed] (female, preserved in ethanol).—Spain, Madrid, Colmenar de Oreja, La Aldehuela, 726 m, 40°04’43.74”N, 3°23’57.14”O, 15 May 2012, mel12012, M. Gª-París leg. [white label, printed]; MNCN_Ent 250997 [white label, printed] (preserved in ethanol).—Madrid, Rivas de Jarama (Urbanizaciones), 5 June 2009, mel09041, M. Gª-París & G. Gª-Martín leg. [white label, printed]; MNCN_Ent 250998 [white label, printed] (preserved in ethanol).—Madrid, Rivas de Jarama (Urbanizaciones), 5 June 2009, mel09042, M. Gª-París & G. Gª-Martín leg. [white label, printed]; MNCN_Ent 250999 [white label, printed] (preserved in ethanol).—Madrid, Rivas de Jarama (Urbanizaciones), 5 June 2009, mel09043, M. Gª-París & G. Gª-Martín leg. [white label, printed]; MNCN_Ent 251000 [white label, printed] (preserved in ethanol).—3 exx. labelled: Segovia, Prádena, 7 May 2015, M. García-París leg. [white label, handwritten]; MNCN_Ent 251001, MNCN_Ent 251002 and MNCN_Ent 251003 respectively [white labels, printed] (preserved in ethanol). All paratypes labelled: ‘Paratypus, *Berberomeloe comunero* Sánchez-Vialas, García-París, Ruiz & Recuero, des. 2019 [red labels for dry-preserved specimens, and white labels for ethanol-preserved specimens, all printed]’. All specimens are held at the Entomological Collection of the Museo Nacional de Ciencias Naturales, Madrid.

Etymology: This species is named in remembrance of the ballad ‘Los Comuneros’ writen by Luis López Álvarez, published in 1972, and set to music by the folk music group ‘Nuevo Mester de Juglaría’ in 1976. This ballad narrates the tragic historical events that took place between 1520 and 1522 in Castille, in the area where the new species occur.

Description of the holotype: Length (frons to posterior margin of elytra), 7.3 mm. Total length (including abdomen) of preserved holotype, 31 mm. Maximum width, 5 mm. Moderately wide orange transverse bar in the posterior edge of each tergum except VII and VIII, which are entirely black. Tegument finely microreticulated, semi-glossy. Head maximum width, 2.4 mm. Surface covered by numerous, uniformly distributed punctures. Head punctures from medium-sized to large, rounded, deep marked, close to each other, confluent in temples. A longitudinal midline is impressed on the upper half of the frons, but faded at the vertex. Minimum interorbital distance, 1.5 mm. Clypeus 1.1 mm wide by 0.4 mm long. Labrum 1.1 wide by 0.4 mm long. Antennae with antennomeres widened apically but not strongly serrated, with short black vestiture, mostly decumbent and with a few sparse erect setae, longer and semi-erect on antennomeres I–II; antennomere I slightly widened apically, subcylindrical (length: 0.5 mm); II short, cylindrical (length: 0.2 mm); III (length: 0.4 mm) subcylindrical, slightly widened apically, rectangular; IV (length: 0.3 mm) shorter than III but equally wide, subrectangular; V (length: 0.3 mm) trapezoidal, wider than VI, with a wide and rounded apical tooth on the inner edge; VI (length: 0.3 mm) trapezoidal, with a rounded apical tooth on the inner edge; VII (length: 0.3 mm) trapezoidal, with an apical tooth on the inner edge; VIII (length: 0.3 mm) trapezoidal, narrow than VII, weakly dentate on the apex of the inner edge; IX (length: 0.3 mm) trapezoidal, similar to VIII, dentate on inner edge; X (length: 0.3 mm) trapezoidal, apical tooth slightly acute; XI (length: 0.4 mm) subconical, moderately wide, notched on apex. Pronotum subquadrate with subparallel sides, slightly narrower towards the base (anterior side of pronotum: 2.1 mm; posterior edge of pronotum: 2 mm; pronotum length on sagittal plane: 1.7 mm); fore angles rounded; anterior margin curved, posterior margin slightly arcuate; with an impressed longitudinal midline through the pronotum length and diffuse lateral depressions. Pronotum surface densely and homogenously punctate; punctures of various sizes, mostly large, rounded, and deep, close to each other, confluent and forming a corrugated or reticulated pattern. Dorsal surface of pronotum almost glabrous, with a short isolated seta in each puncture; anterior margin, adjacent to the neck, with numerous, moderately long setae. Elytra imbricated basally (the right over the left), length: 4.1 mm; tegument glabrous, slightly corrugated longitudinally with impressed irregular vermicular lines, with scarce, weakly marked, dispersed punctures. Distal margin of tergites I–VI with an orange transverse bar, moderately narrow in comparison with the total width of the terga (width of the second tergum: 4.8 mm; width transverse bar of the second tergum: 2.7 mm). Last ventrite notched. Metafemur longer than metatibia (metafemur length: 2.5 mm; metatibia length: 2 mm). Metatarsal tarsomeres length, from inner to apical: 2.2, 0.4, 0.4, 0.7 mm. Genitalia with tegmen brownish; moderately elongated, slender both on dorsal and lateral views. Phallobase longer than wide, length similar to the parameres; maximum width at the middle. Parameres longer than wide, basally cylindrical; distal third formed by parameral lobes; setae present on middle region of parameres. Parameral lobes separated by a longitudinal notch that extends to the middle of the dorsal surface of the parameres; apexes rounded. Median lobe long, robust, flattened, truncated at the apex in lateral view, with two acute ventral hooks;

Downloaded from https://academic.oup.com/zoolinnean/article-abstract/189/4/1249/5714599 by 81263633 user on 05 August 2020

ventral hooks similar and close to each other, separated from apex. Endophallic hook visible.

Female: Similar to male, but with the last abdominal ventrite rounded, not emarginated in its posterior margin and antennomeres less widened apically. Studied specimens present the inner surface of the bursa copulatrix with few and small sclerotized spicules, sometimes absent (similar to those of *B. indalo*, as figured in Fig. 8).

Variability: Body length (frons to posterior border of elytra) highly variable, from 7.3 to 20 mm; maximum total length among preserved, studied specimens, 54 mm. Morphometric variability is shown in Table 2. Some specimens have a single, small, red spot on the frons, diffuse and faintly marked. Colour of transverse bars in live specimens vary from orange to blood-red, but constant within each population. Populations composed exclusively of entirely black-coloured specimens are found in Madrid (Rivas de Jarama, Valdepiélagos, Talamanca, Daganzo de Arriba, Vicálvaro) and western Guadalajara (Uceda) (Bravo *et al.*, 2017; authors pers. obs.). *Berberomeloe comunero* presents a high variability in the width of coloured transverse tergal bars, but on average they are relatively wide (ratio 'total width of the second tergum/width of the transverse bar of the second tergum' between 1.32 and 2.34, average = 1.8, SD = 0.29, N = 31). Transverse bars are narrower in mountain populations from the provinces of Madrid and Segovia. Specimens with deeper punctures on the pronotum, forming a strongly corrugated pattern, are found over most part of the province of Madrid and eastern Segovia.

Diagnosis: Berberomeloe comunero can be distinguished from all other *Berberomeloe* species by the following combination of characters (Fig. 11): (1) medium-sized to moderately narrow, coloured, transverse tergal bars on the distal margin of tergites I–VI; (2) punctures on head large to medium-sized, rounded, deep and close to each other; (3) pronotum surface densely and homogeneously punctate, with two types of puncturation simultaneously, large and medium-sized, confluent or subconfluent, often forming a corrugated pattern; (4) fore angles of pronotum rounded and not especially expanded; (5) apex of the median lobe of male genitalia obliquely truncated in lateral view; and (6) antennomere XI in males wide, V–VII in males weakly expanded at its inner apical side.

Distribution and notes on natural history: Berberomeloe comunero is a euryecious species distributed over most of the northern Central Iberian Plateau, in the provinces of Madrid (except at its south-eastern edge), Burgos, Segovia, Guadalajara and most of Valladolid. According to the known localities, it occupies a wide elevational range from 522 m at Balcón del Tajo (Madrid) to 1440 m at Puerto de Somosierra (Madrid). It inhabits a wide range of geological formations, from limestone and gypsum of the highlands of the Northern Plateau to granite and gneisses at Sierra de Guadarrama, while micaceous schists, slates and quartzites from Somosierra to Sierra de Ayllón (Rivas-Martínez *et al.*, 1990; Vera, 2004). It occupies the meso- and supra-Mediterranean bioclimatic levels (see: Rivas-Martínez, 1987; Rivas-Martínez *et al.*, 2002). *Berberomeloe comunero* is found over an extensive variety of open habitats (Fig. 12), such as cereal fields (mostly wheat and barley), gypsum hills with dispersed *Quercus coccifera* L. trees, steppes, juniper groves and open oak (*Quercus rotundifolia* Lam., *Q. pyrenaica* Willd.) and ash (*Fraxinus angustifolia* Vahl) forests (Rivas-Martínez & Costa, 1970; Rivas-Martínez *et al.*, 1990). Biological aspects of this species are expected to be similar to the ones described for the genus by Bologna (1989, 1991). Adult specimens are found from March to July.

BERBEROMELOE INDALO SÁNCHEZ-VIALAS *ET AL.*, SP. NOV.

LSID: urn:lsid:zoobank.org:act:B103E98C-6BCD-42DC-95B5-46B267AF25F1

Holotype: Male: España, Almería, Las Casillas de Atochares, 36°52'53.0"N–2°10'13.2"W, 30 March 2008, 118 m, ALM08/15, E. Recuero & C. Settanni leg. [white label, printed]; MNCN_Ent 231436 [white label, printed]; Holotypus, *Berberomeloe indalo* Sánchez-Vialas, García-París, Ruiz & Recuero des. 2019 [white label, printed] (extracted genitalia). Preserved in absolute ethanol, held at the Entomological Collection of the Museo Nacional de Ciencias Naturales, Madrid.

Paratypes: España, Almería, Las Casillas de Atochares, 36°52'53.0"N–2°10'13.2"W, 30 March 2008, 118 m, E. Recuero & C. Settanni leg. [white label, printed]; MNCN_Ent 231437 [white label, printed]; ALM08/15 [white label, handwritten] (female, preserved in ethanol).— España, Almería, Las Casillas de Atochares, 36°52'53.0"N–2°10'13.2"W, 30 March 2008, 118 m, E. Recuero & C. Settanni leg. [white label, printed]; MNCN_Ent 231438 [white label, printed]; ALM08/15 [white label, handwritten] (male, preserved dry).— España, Almería, Las Casillas de Atochares, 36°52'53.0"N–2°10'13.2"W, 30 March 2008, 118 m, ALM08/15, E. Recuero & C. Settanni leg. [white label, printed]; MNCN_Ent 232588 [white label, printed] (preserved dry).— 5 exx. labelled: Almería, 2.5 km SE de Sorbas, Mirador del Karst en Yesos (carretera A8203 entre Campico y Sorbas), 37°05'73.4"N–2°05'15.7"W, 389 m, 28 March 2008,

Downloaded from https://academic.oup.com/zoolinnean/article-abstract/189/4/1249/5714599 by 81263633 user on 05 August 2020

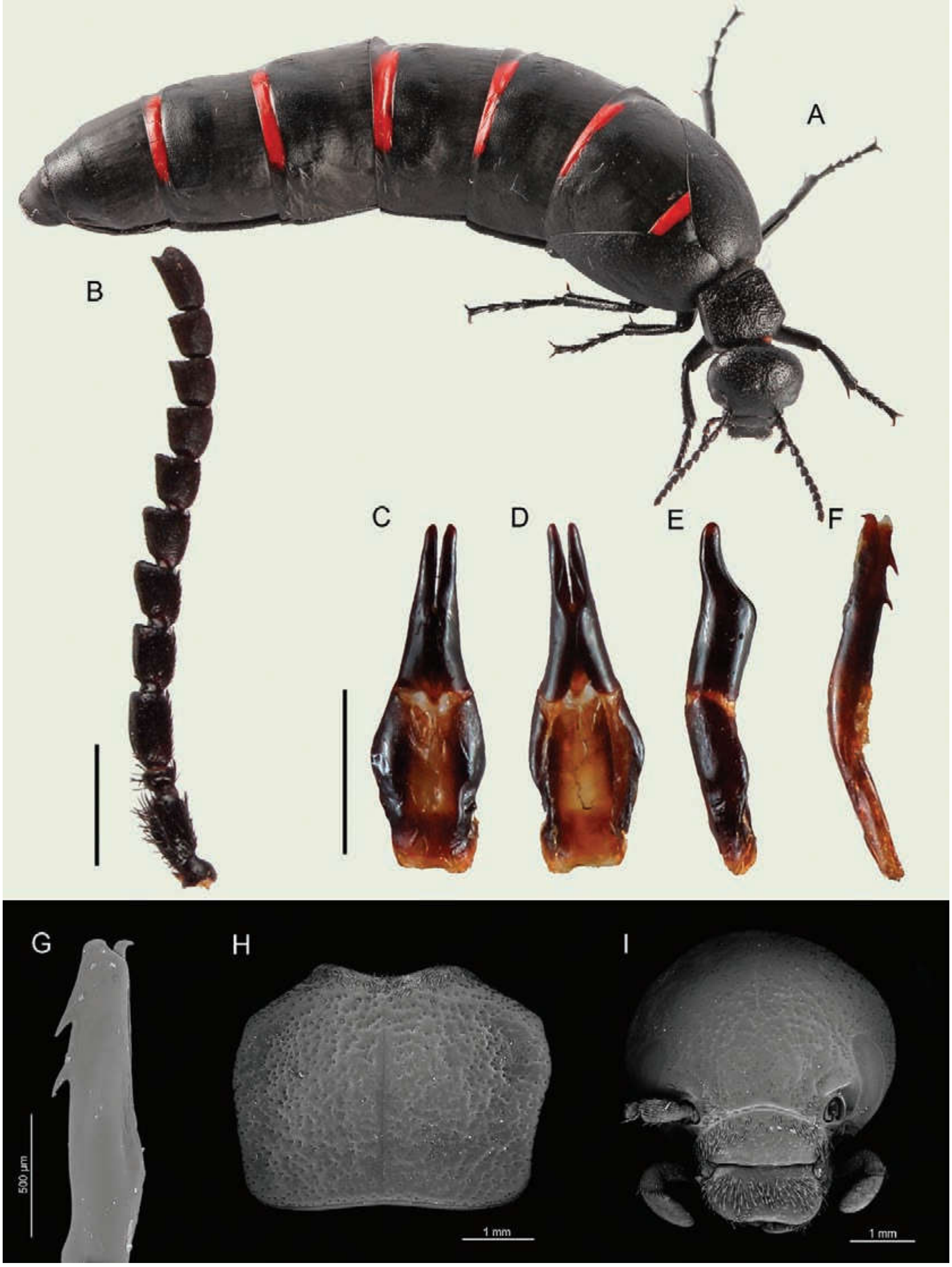

Figure 11. Habitus and morphological details of *Berberomeloe comunero* from Puebla de la Sierra, Madrid (A) and Canencia, Madrid (B–I). A, dorsal view of a female; B, male antenna; C, D, E, dorsal, ventral, lateral view of male genitalia, showing parameres and phallobase; F, lateral view of aedeagus; G, SEM micrographs of distal part of aedeagus; H, SEM micrographs of pronotum, dorsal view; I, SEM micrographs of head, frontal view.

E. Recuero & C. Settanni leg. [white label, printed]; MNCN_Ent 251004, MNCN_Ent 251005, MNCN_Ent 251006, MNCN_Ent 251007 and MNCN_Ent 251008, respectively [white labels, printed] (preserved in ethanol).— 3 exx. labelled: España, Almería, Las Casillas de Atochares, 36°52’53.0”N–2°10’13.2”W,

Downloaded from https://academic.oup.com/zoolinnean/article-abstract/189/4/1249/5714599 by 81263633 user on 05 August 2020

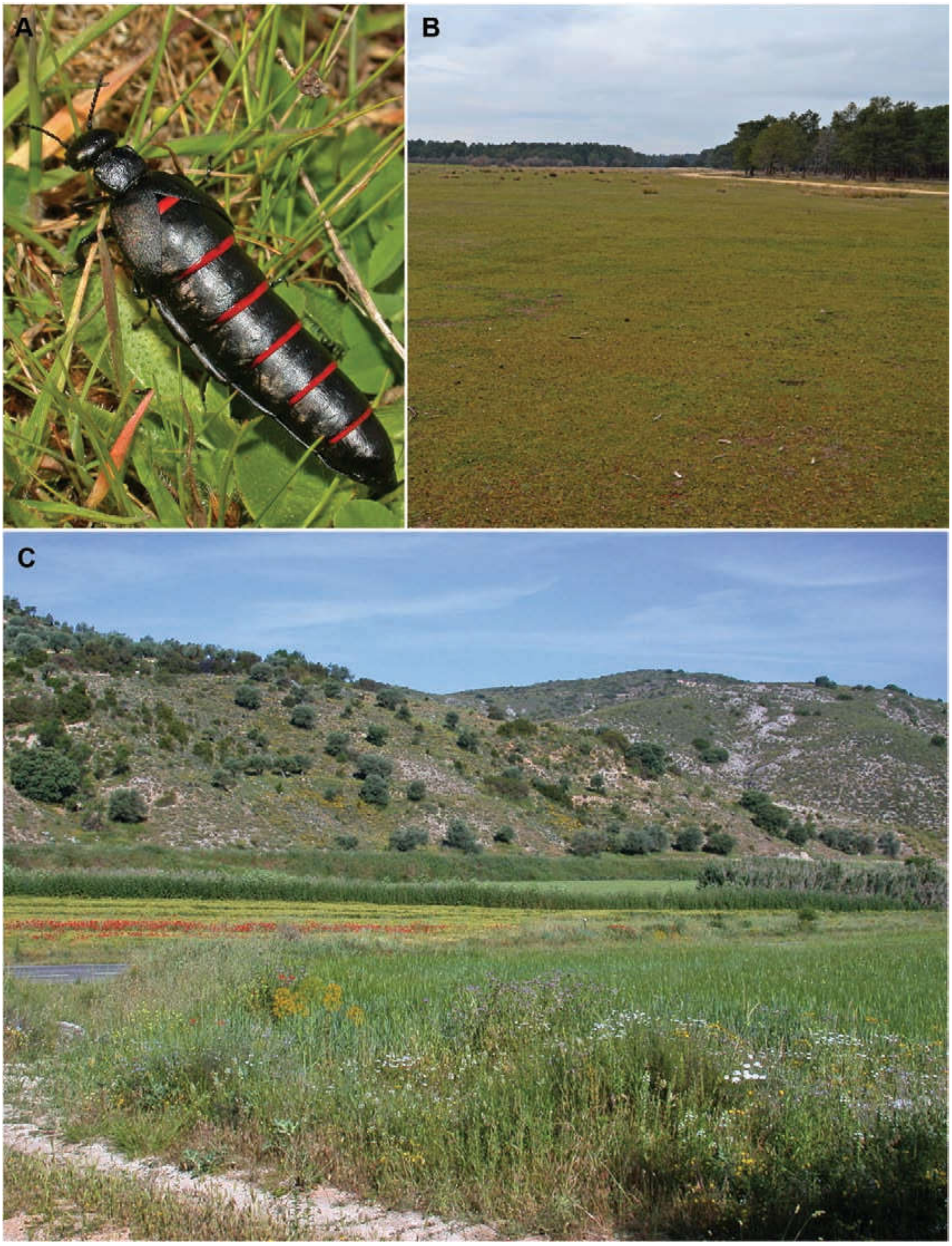

Figure 12. A, specimen of *Berberomeloe comunero* from Pinilla de los Moros, Burgos. B, C, habitat of *B. comunero,* Spain; B, Cantalejo, Segovia; C, Tielmes, Madrid.

30 March 2008, 118 m, E. Recuero & C. Settanni leg. [white label, printed]; ALM08/15 [white label, handwritten]; MNCN_Ent 251009, MNCN_Ent 251010 and MNCN_Ent 251011, respectively [white labels, printed] (preserved in ethanol).— 2 exx. labelled: España, Almería, entre Mojacar y Turres, carretera AL151, 37°08'77.9"N–1°52'19.3"W, 21 m, 27 March 2008, E. Recuero & C. Settanni leg. [white label,

Downloaded from https://academic.oup.com/zoolinnean/article-abstract/189/4/1249/5714599 by 81263633 user on 05 August 2020

printed]; ALM 08/1 [white label, handwritten]; MNCN_Ent 251012 and MNCN_Ent 251013, respectively [white labels, printed] (preserved in ethanol).— Almería, Campohermoso, 26 March 2001, NTM87, MAB 162, M. García-París leg. [white label, printed and handwritten]; MNCN_Ent 251014 [white label, printed] (preserved in ethanol).— España, Almería, La Mela, 28 March 2008, ALM08/6, E. Recuero & C. Settanni leg. [white label, printed]; MNCN_Ent 251015 [white label, printed] (preserved in ethanol). All paratypes labelled: 'Paratypus, *Berberomeloe indalo* Sánchez-Vialas, García-París, Ruiz & Recuero, des. 2019 [red labels for dry-preserved specimens, and white labels for ethanol-preserved specimens, all printed]'. All specimens are held at the Entomological Collection of the Museo Nacional de Ciencias Naturales, Madrid. Total paratypes: 15 exx.

Etymology: The epithet *indalo*, is the Spanish name for a prehistoric rock painting from the Late Neolithic or Copper Age representing a human figure with an arch over its arms and head. It was discovered at the Abrigo de Las Colmenas in Vélez-Blanco (Almería) by the archaeologist Manuel de Góngora Martínez in 1868. The Indalo figure has become the symbol for Almería province, where *Berberomeloe indalo* occurs. It is a noun in apposition.

Description of the holotype: Body length (frons to posterior margin of elytra), 11.7 mm. Total length (including abdomen) of preserved holotype, 45 mm. Maximum width, 7.6 mm. Wide orange transverse bars in the posterior edge of each tergum, except VII and VIII, which are entirely black. Tegument of silky appearance, with fine microreticulation, almost imperceptible. Head maximum width, 3.9 mm. Surface covered by scarce punctures almost uniformly distributed, small, rounded, shallow, and well separated from each other. A longitudinal midline, finely impressed, from the upper half of the frons to the vertex. Minimum interorbital distance, 2.2 mm. Clypeus, 1.8 mm wide by 0.9 long. Labrum, 1.8 mm wide by 0.7 mm long. Antennae with antennomeres widened apically, but not or barely dentate, with short black vestiture, mostly decumbent and with a few sparse, erect setae, longer and semi-erect on antennomeres I–II; antennomere I slightly widened apically, subcylindrical (length: 0.6 mm); II short, cylindrical (length: 0.3 mm); III (length: 0.6 mm) subcylindrical, slightly widened apically, rectangular, with a mildly invaginated area over the apical half on its inner side, whose surface is yellowish and covered by micropunctures with short, whitish pubescence; IV (length: 0.5 mm) shorter than III but equally wide, subrectangular, with a similar invaginated area on its inner surface; V (length: 0.5 mm) trapezoidal, wider than VI, poorly widened at apical region on the inner edge and weakly invaginated area similar to the previous two; VI (length: 0.5 mm) trapezoidal, with a poorly widened apical tooth on the inner edge; VII (length: 0.4 mm) trapezoidal, similar to VI; VIII (length: 0.4 mm) trapezoidal, narrower than VII, weakly dentate; IX (length: 0.4 mm) trapezoidal, similar to VIII, slightly dentate on inner edge; X (length: 0.4 mm) trapezoidal, narrower than IX; XI (length: 0.5 mm) subconical, moderately wide, notched on apex. Pronotum subquadrate, narrower posteriorly (anterior side of pronotum: 3.3 mm; basal edge of pronotum: 2.3 mm; pronotum length on sagittal plane: 2.3 mm); anterior margin curved, posterior margin slightly arcuate; fore angles prominent, obtusely pointed; with an impressed longitudinal midline through the pronotum length; surface with diffuse lateral depressions, close to the fore angles. Pronotum surface heterogeneously and sparsely punctured; punctures of various sizes, mostly medium and small, circular, well separated from each other, not confluent, sparse; medium sized punctures deep, located on the sides and along the midline. Dorsal surface of pronotum almost glabrous, with an isolated, short seta in each puncture; anterior margin, adjacent to the neck, with numerous, moderately long setae. Elytra length, 6.8 mm; tegument glabrous, slightly corrugated longitudinally with impressed irregular vermicular lines; with scarce, weakly marked, dispersed punctures. Distal margin of tergites I–VI with a wide orange transverse bar (width of the second tergum: 6.6 mm; width of transverse bar of the second tergum: 5.2 mm). Last ventrite notched at the hind margin. Metafemur longer than metatibia (metafemur length: 3.8 mm; metatibia length: 3.7 mm). Metatarsomeres length, from basal to apical: 1.9, 0.9, 0.8, 1.1 mm. Genitalia with tegmen brownish; moderately elongated, slender both on dorsal and lateral views. Phallobase longer than wide, length similar to the parameres; wider on dorsal view; maximum width at the middle. Parameres longer than wide, basally cylindrical; distal third formed by parameral lobes; setae present dorsally on the middle region, scarce, applied against the tegument. Parameral lobes digitiform, separated by a longitudinal notch that extends to the middle of the dorsal surface of the parameres; apexes rounded. Median lobe long, robust, flattened, weakly truncated at the apex in lateral view, with two similar, acute ventral hooks, not too close to each other and separated from apex. Endophallic hook visible.

Female: Similar to male, but with VIII abdominal ventrite rounded, not emarginated in its posterior margin, and with antennomeres clearly less dentate. Studied specimens present the inner surface of the bursa copulatrix without sclerotized spicules or plates (Fig. 8).

Downloaded from https://academic.oup.com/zoolinnean/article-abstract/189/4/1249/5714599 by 81263633 user on 05 August 2020

Variability: Body length variable (frons to posterior edge of elytra), 11 to 20 mm; maximum total length among studied, preserved specimens, 46 mm. Morphometric variability is shown in Table 2.

No entirely black-coloured specimens are known in *Berberomeloe indalo*. The orange to deep red bars of the abdominal tergites in live specimens are always wide (ratio 'total width of the second tergum/width of the transverse bar of the second tergum" between 1.09 and 1.35, average = 1.18, SD = 0.07, N = 17). There is some individual variability in puncturation density of head and pronotum. In some male specimens the inner apical angle of the antennomeres VI, VII, IX and XI present a yellowish coloration, similar to those of the invaginated areas of antennomeres IV and V. Presence of short setae scattered over the dorsal side of parameres varies at the individual level.

Diagnosis: Berberomeloe indalo can be distinguished from all other species of *Berberomeloe* by the following combination of characters (Fig. 13): (1) wide, coloured, transverse tergal bars on the distal margin of tergites I–VI; (2) punctures on the head small to medium-sized, rounded, shallow, sparsely distributed; (3) pronotum surface scarcely and heterogeneously punctured; with two types of punctures simultaneously, small punctures less than the half of diameter of the large ones, usually well separated from each other; large punctures predominantly arranged longitudinally along lateral borders and midline, close to each other; disc region smooth or finely punctured; (4) fore angles of pronotum prominent, obtusely pointed; (5) median lobe robust, with its apex wide and obliquely truncated in lateral view; (6) male antennomere XI wide; (7) male antennomeres IV and V substraight, poorly dentate, but swelled at their inner side and with a singular invaginated, yellowish area at the inner border; antennomeres V–IX relatively similar in shape.

Distribution and notes on natural history: Berberomeloe indalo is endemic to the south-eastern corner of the Iberian Peninsula, known only from eastern Almería, Spain (Fig. 2). According to the known records, it occurs in lowland areas (elevational range: 20–570 m) occupying the thermo-Mediterranean bioclimate level, with semi-arid ombrotype (200–350 mm average rainfall; see Rivas-Martínez, 1987; Valle, 2003; Valle *et al.*, 2004), and the meso-Mediterranean at the southern slopes of the Sierra de Filabres and Sierra de Gádor. However, the limits of its distribution, especially in the northern edge, are unknown. The lithological substrates are formed principally by gypsum marls, subsaline marls, schists and volcanic materials (see: Valle *et al.*, 2004; Vera, 2004). The habitat (Fig. 14, 15A) is constituted by steppes and badlands with semi-arid plant communities [mostly xerothermic scrubs of low coverage: *Ziziphus lotus* (L.) Lam., *Maytenus senegalensis* (Lam.) Exell, *Periploca angustifolia* Labill., *Pistacia lentiscus* L., *Chamaerops humilis* L., *Retama sphaerocarpa* (L.) Boiss., *Anthyllis cytisoides* L., *Rhamnus lycioides* L., *Gypsophila struthium* Loefl., *Macrochloa tenacissima* (L.) Kunth], and their respective stages of degradation (see: Mota *et al.*, 1997; García-París *et al.*, 1999; Valle, 2003; Valle *et al.*, 2004) and, in a lesser extent, by rainfed almond trees [*Prunus dulcis* (Mill.) Webb]. Adults are found from March to June (pers. obs.). *Berberomeloe indalo* has been found in microsympatry with *B. insignis* in several localities (García-París *et al.*, 1999; pers. obs.).

BERBEROMELOE LAEVIGATUS (OLIVIER, 1797)
COMB. NOV.

Meloe laevigatus Olivier, 1797: 650. Terra typica: 'Catalogne'
? *Meloe fissicornis* Górriz Muñoz, 1882:38. Terra typica: 'Cariñena (Aragon)'.

Our phylogenetic results recovered a distinctive clade grouping the specimens sequenced from or close to the Ebro Basin (Fig. 16), in the provinces of Zaragoza, Soria and the northern portion of Guadalajara. Although we lack morphological data, the phylogenetic results are clear about its independent evolutionary uniqueness. Therefore, we assigned this distinctive lineage to a separate species for which, tentatively, the available name *B. laevigatus* (Olivier, 1797), described from 'Catalogne' (see: García-París *et al.*, 2010), could be used (previously included in the synonymy of *B. majalis*; see: Bologna, 1989, 1991, 2008; García-París, 1998; García-París *et al.*, 2010). We have not been able to study the type material of *Meloe laevigatus*, so the tentative assignment of this available name to lineage H is based only on its geographic distribution with respect to the type locality of this nominal taxon. However, the definition of this taxon is tentative, as more extensive sampling for phylogeographic and morphological studies are needed to solve the taxonomic identity and systematics of north-eastern Iberian populations.

Based on a limited sample of specimens of *B. laevigatus* (see: Supporting Information, Appendix S1), we noted that it can be distinguished from all other species of *Berberomeloe* by a characteristic elytral puncturation based on deeper and denser punctures than the rest of congeneric species and also by the following combination of characters: (1) wide, coloured, transverse tergal bars on the distal margin of tergites I–VI; (2) punctures on the head medium-sized to large, rounded, deep and isolated from each other; (3) pronotum surface homogeneously punctured; (4) fore angles of pronotum not expanded, rounded or weakly marked; (5) male antennomere XI

Downloaded from https://academic.oup.com/zoolinnean/article-abstract/189/4/1249/5714599 by 81263633 user on 05 August 2020

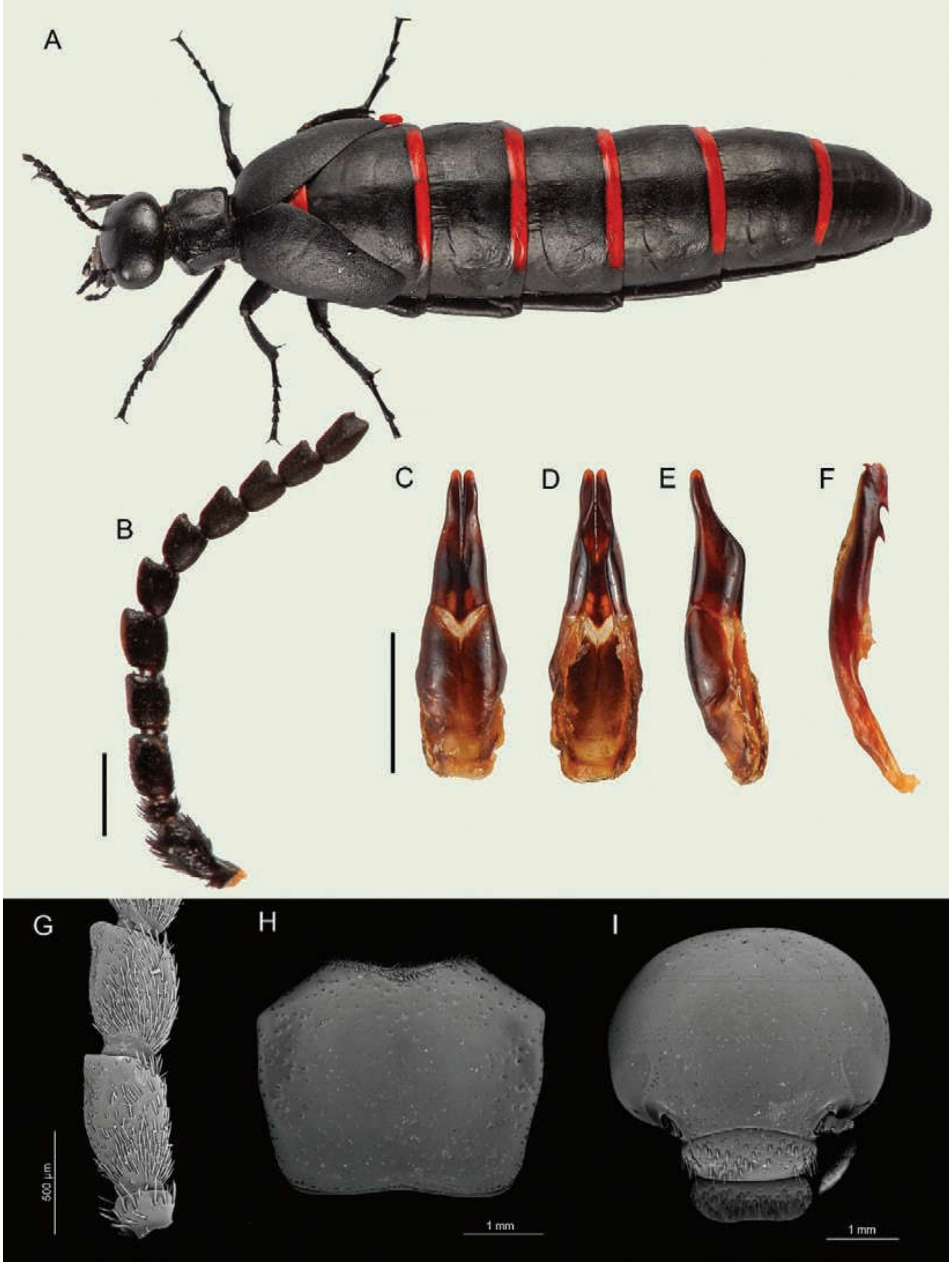

Figure 13. Habitus and morphological details of *Berberomeloe indalo* from Carboneras, Almería (A) and Casillas de Atochares, Almería (B–I). A, dorsal view of a female; B, male antenna; C, D, E, dorsal, ventral, lateral view of male genitalia, showing parameres and phallobase; F, lateral view of aedeagus; G, SEM micrographs of third and fourth antennomeres: note the longitudinal concave surface along the ventral side of each antennomere; H, SEM micrographs of pronotum, dorsal view; I, SEM micrographs of head, frontal view.

wide; and (6) male antennomeres IV and V moderately expanded on the inner apical side. However, an exhaustive morphological study, including a larger sample size, is necessary to unequivocally characterize the morphological diagnostic traits of the species.

Downloaded from https://academic.oup.com/zoolinnean/article-abstract/189/4/1249/5714599 by 81263633 user on 05 August 2020

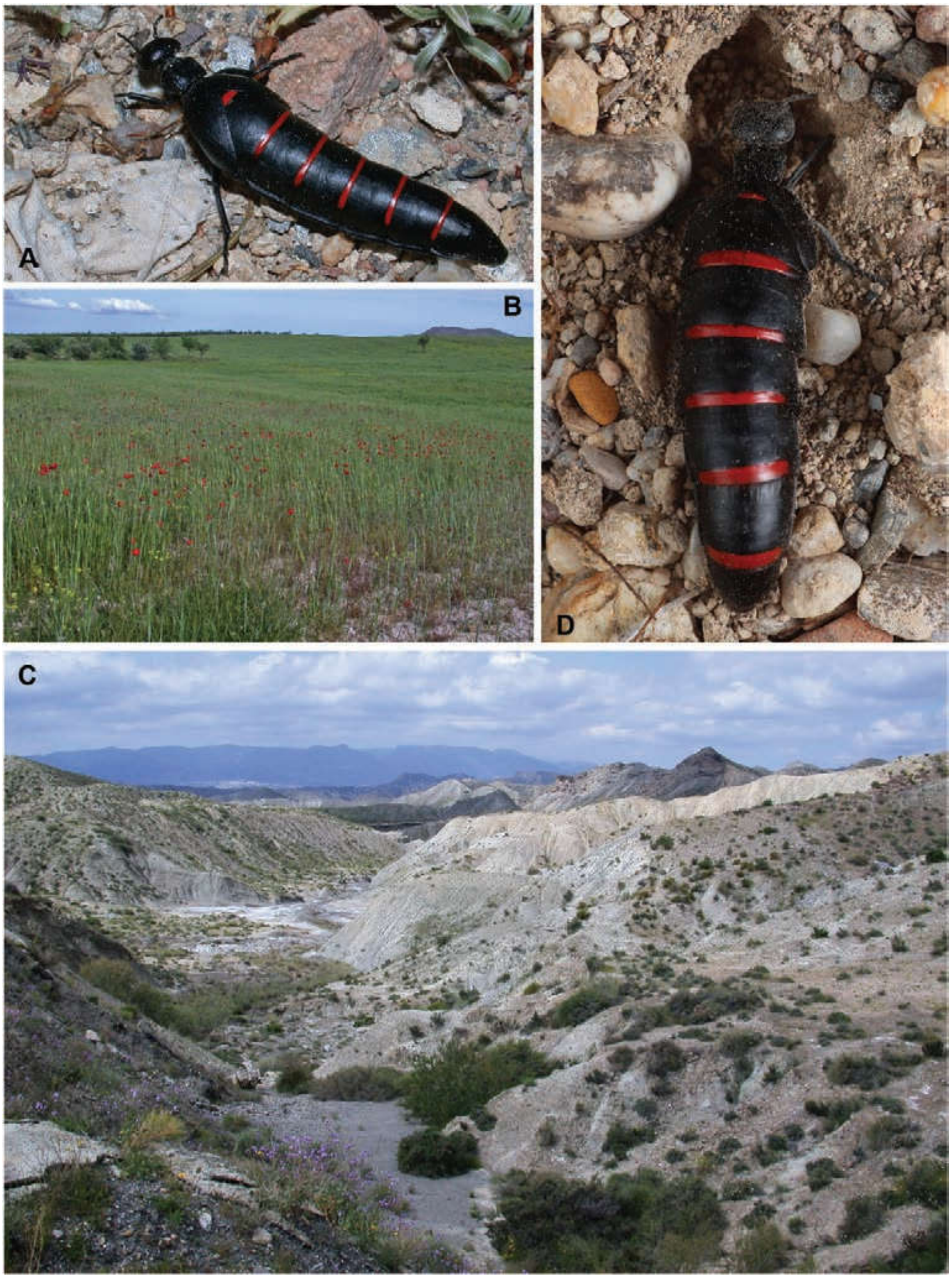

Figure 14. A, specimen of *Berberomeloe indalo* from Tonosa, Almería. B, C, habitat of *B. indalo*, Spain; B, cereal fields of Tonosa, Almería; C, Tabernas, Almería. D, female of *B. indalo* from Carboneras, Almería, digging a hole for oviposition.

BERBEROMELOE PAYOYO SÁNCHEZ-VIALAS *ET AL.*, **SP. NOV.**

LSID: urn:lsid:zoobank.org:act:DAAFDC7E-4B4E-4B01-A1B6-A8456B26BE4E

Holotype: Male: Manzanete, Cádiz, Sierra de Retín, 36°12’ N, 5°48’ W, 24 March 2011 [white label, handwritten];MNCN_Ent231455 [white label, printed]; Holotypus, *Berberomeloe payoyo* Sánchez-Vialas, García-París, Ruiz & Recuero des. 2019 [white label, printed] (extracted genitalia). Preserved in absolute ethanol, held at the Entomological Collection of the Museo Nacional de Ciencias Naturales, Madrid.

Paratypes: Cádiz: 2 km al S de Benalup de Sidonia, 19 April 2001, MAB124, NTM106, M. García-París y E. Recuero leg. [white label, handwritten]; MNCN_Ent

Downloaded from https://academic.oup.com/zoolinnean/article-abstract/189/4/1249/5714599 by 81263633 user on 05 August 2020

Figure 15. Two examples of habitat destruction of narrowly distributed species of *Berberomeloe*. A, greenhouses in Adra, Almería, Spain, extended over the habitat of *B. indalo*, one of the most threatened species of the genus. B, Surroundings of Bab Berred, Rif mountains, Morocco, cultivated with *Cannabis* over *B. yebli* range.

2314391 [white label, printed] (female, preserved dry).—Spain: Cádiz: 7 km SO de Benalup de Sidonia, 19 April 2001, MAB101, NTM56 E. Recuero & M. García-París leg. [white label, printed] MNCN_Ent 231440 [white label, printed] (preserved in ethanol).—Sª de las Nieves (Málaga), Spain, 25 April 1991, J. L.

Downloaded from https://academic.oup.com/zoolinnean/article-abstract/189/4/1249/5714599 by 81263633 user on 05 August 2020

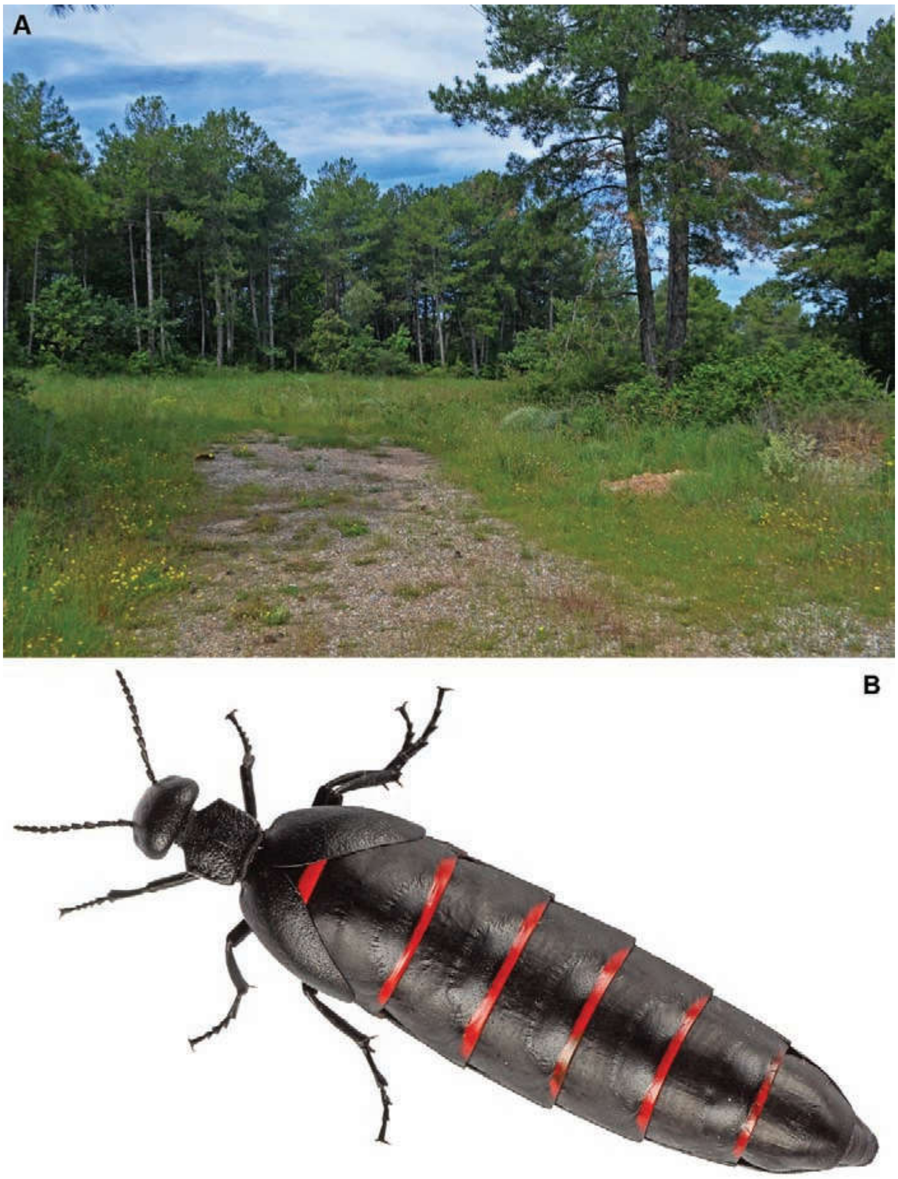

Figure 16. A, Solsona, Lleida, Spain, habitat of *Berberomeloe laevigatus*. B, habitus of *B. laevigatus* from Solsona, Lleida.

Ruiz leg. [white label, printed]; MNCN_Ent 231441 [white label, printed] (male, extracted genitalia, preserved dry).—S^{a} de las Nieves (Málaga), Spain, 25 April 1991, J. L. Ruiz leg. [white label, printed]; MNCN_Ent 231442 [white label, printed] (male, preserved dry).—San Roque (Cádiz), Hispania, J. de Ferrer leg., May 1973 [white label, handwritten]; MNCN_Ent 231443 [white label, printed] (female, preserved dry).—Cádiz, Facinas, 36°07’34.8”N 5°42’20.6”W, 19 June 2016, E. Recuero, J. Gutiérrez-Rodríguez, J. Esteban leg. [white label, printed]; MNCN_Ent 231444 [white label, printed] (female, preserved in ethanol).—Spain, Cádiz, 4 km al NE de San José del Valle, 19 April 2001, MAB101, NTM53, Recuero & M. García-París leg. [white label, printed]; MNCN_Ent 231445 [white label, printed] (male, preserved in ethanol).—3 exx. labelled: Sierra Carbonera [white label, handwritten]; *Berberomeloe majalis* Linnaeus, 1758, M. G^{a}-París det. 98 [white label, printed]; MNCN_Ent 233507–233509, respectively [white labels, printed] (preserved dry).—Spain, Cádiz, Conil de la Frontera, playa de Torre del Gallo, 36°17’48.9”N 6°07’09.3”W, 28 m, 13 April 2013, ber13010, M. García-París & N. Percino leg. [white label, printed]; MNCN_Ent 251016 [white label, printed] (female, preserved in ethanol).—Spain, Manzanete, Sierra de Retín,

Downloaded from https://academic.oup.com/zoolinnean/article-abstract/189/4/1249/5714599 by 81263633 user on 05 August 2020

24-III-2011 [white label, handwritten]; MNCN_Ent 251017 [white label, printed] (female, preserved in ethanol).—Cádiz, Paterna, 21 May 2017, A. Hinckley leg. [white label, handwritten]; APP17001 [white label, handwritten]; MNCN_Ent 251018 [white label, printed] (preserved in ethanol). All paratypes labelled: 'Paratypus, *Berberomeloe payoyo* Sánchez-Vialas, García-París, Ruiz & Recuero, des. 2019 [red labels for dry-preserved specimens, and white labels for ethanol-preserve specimens, all printed]'. All specimens are held at the Entomological Collection of the Museo Nacional de Ciencias Naturales, Madrid. Total number of paratypes: 13 exx.

Etymology: The epithet payoyo is Spanish for an endangered goat breed (cabra payoya; *Capra aegagrus hircus* Linnaeus, 1758) originating in the Sierra de Grazalema, Serranía de Ronda and adjacent areas in the provinces of Cádiz and Málaga. *Berberomeloe payoyo* and the payoya goat share their distribution range.

Description of the holotype: Length (frons to posterior margin of elytra), 12.9 mm. Total length (including abdomen) of preserved holotype, 64 mm. Maximum width, 8.8 mm. Narrow, orange, transverse bar present in the posterior edge of each tergum, except VII and VIII, which are entirely black. Tegument of semi-matt appearance, with a fine microreticulation. Head maximum width, 4.3 mm. Surface covered by small, rounded, shallow punctures, uniformly distributed, scarce. A longitudinal midline is finely impressed from the upper half of the frons to the vertex. Minimum interorbital distance: 2.7 mm. Clypeus 1.9 mm wide by 0.9 mm long. Labrum 1.8 mm wide by 0.9 mm long. Antennomeres widened apically, with short, black vestiture, mostly decumbent and with a few sparse setae erect, longer and semi-erect on antennomeres I–II; antennomere I slightly widened apically, subcylindrical (length: 0.6 mm); II short, cylindrical (length: 0.2 mm); III (length: 0.5 mm) subrectangular, slightly widened apically; IV (length: 0.6 mm) longer than III but equally wide, subrectangular; V (length: 0.5 mm) subtriangular, wider than VI at apex, with a wide and rounded apical tooth on the inner edge; VI (length: 0.5 mm) subtrapezoidal, with an apical tooth on the inner edge; VII (length: 0.4 mm) trapezoidal, with an apical tooth on the inner edge; VIII (length: 0.4 mm) trapezoidal, narrow than VII, weakly dentate on the apex of the inner edge; IX (length: 0.3 mm) trapezoidal, moderately dentate on inner edge; X (length: 0.4 mm) trapezoidal, narrower than IX, apical tooth slightly acute; XI (length: 0.5 mm) subconical with subparallel sides, moderately slender, notched on apex. Pronotum subquadrate with subparallel sides, barely narrower posteriorly (anterior side of pronotum: 3.7 mm; basal edge of pronotum: 3.6 mm; pronotum length on sagittal plane: 2.6 mm); anterior margin curved, posterior margin slightly arcuate; surface with an impressed longitudinal midline and showing shallow and diffuse lateral depressions next to the fore angles. Basis entire and finely bordered. Pronotum surface scarcely punctured, with punctures mainly concentrated on the sides, anterior region and, to a lesser extent, next to the midline and basis; punctures of various sizes, mostly medium and small to very small, circular, shallow, well separated, never confluent. Dorsal surface of pronotum almost glabrous, with an isolated seta in each puncture; anterior margin, adjacent to the neck, with numerous moderately long setae. Elytra imbricated basally (the right over the left); length, 7.5 mm; tegument glabrous, wrinkled longitudinally with impressed irregular vermicular lines, with scarce, weakly marked, dispersed punctures. Distal margin of tergites I–VI with an orange, transverse bar, moderately narrow in comparison with the total width of the terga (width of the second tergum: 7.4 mm; width of the transverse bar of the second tergum: 3.5 mm). Last ventrite notched at hind margin. Metafemur shorter than metatibia (metafemur length: 3.9 mm; metatibia length: 4.1 mm). Metatarsomere length, from inner to apical: 2, 1, 0.8, 1.1 mm. Genitalia with tegmen brownish; moderately elongated, slender on both dorsal and lateral views. Phallobase longer than wide, length similar to the parameres; maximum width at the middle. Parameres longer than wide, basally cylindrical; distal third formed by parameral lobes; scarce setae, decumbent, present on the mid-dorsal region. Parameral lobes weakly curved, wide and moderately short in lateral view, separated by a longitudinal notch that extends to the middle of the dorsal surface of the parameres; with apexes rounded, digitiform. Median lobe long, robust, flattened, truncated dorsally at the apex in lateral view, with two acute ventral hooks, close to each other and separated from apex. Endophallic hook visible.

Female: Similar to male, but with ventrite VIII rounded, not emarginated along the posterior margin, and with less dentate antennomeres. Studied specimens present the inner surface of the bursa copulatrix with large sclerotized spicules or plates (similar to those of *B. castuo*, as figured in Fig. 8).

Variability: Body length (frons to posterior border of elytra) highly variable, 10 to 20 mm; maximum total length among preserved, studied specimens, 64 mm. Morphometric variability is shown in Table 2. Some specimens, especially the largest ones, show a single, small, red spot on the middle of the frons, diffuse and poorly marked. Populations formed by entirely black

Downloaded from https://academic.oup.com/zoolinnean/article-abstract/189/4/1249/5714599 by 81263633 user on 05 August 2020

coloured specimens of *B. payoyo* are localized in Sierra Carbonera (southeastern Cádiz). Transverse coloured bars on the posterior edge of abdominal terga can be red (in most populations) or less often yellow-orange (as in Montecorto, Málaga). Variation in the width of the transverse bar is limited (ratio 'total width of the second tergum/width of the transverse bar of the second tergum' between 1.85 and 2.45, average = 2.11, SD = 0.17, *N* = 20). Slight individual variability in the density of punctures on the head and pronotum, and in the width of parameral lobes. Setation over parameres is variably present or absent in specimens from the same population.

Diagnosis: Berberomeloe payoyo can be distinguished from all other species of *Berberomeloe* by the following combination of characters (Fig. 17): (1) narrow, coloured, transverse tergal bars on the distal margin of tergites I–VI; (2) punctures on the head small, rounded, poorly impressed and well separated from each other; (3) pronotum surface scarcely punctate, with two types of punctures, which are generally medium and small to very small, poorly impressed and well separated from each other; medium-sized punctures located specially at the edges; pronotal disc almost smooth; (4) fore angles of pronotum not expanded, rounded or weakly marked; (5) male genitalia with median lobe obliquely truncated at dorsal edge in lateral view, and distal region of the parameres wide and relatively short in lateral view; (6) male antennomere XI wide; and (7) male antennomeres V–VII moderately expanded on the inner apical side.

Distribution and notes on natural history: Berberomeloe payoyo is distributed over southern Iberia, in the Spanish provinces of Cádiz, Málaga and western Granada (Andalusia), south to the Guadalquivir basin. It is an euryecious species that occurs from the coast (Zahara de los Atunes, Barbate, Puerto Real, at the province of Cádiz) to the mountain areas (elevational range: 5–1100 m) along the western Penibetic Mountain Range (Sierra de Grazalema, Serranía de Ronda, Sierra de Las Nieves, and Sierra Tejeda), usually at thermo- and meso-Mediterranean bioclimate levels, locally at the supra-Mediterranean, with ombrotypes mainly subhumid to humid (see: Rivas-Martínez, 1987; Valle *et al.*, 2004). The geology in these areas is complex, dominated by neogene-quaternary coastal–subcoastal sands, limestones (including karst complexes), dolomites, sandstones, schists and clays (e.g. see: Vera, 2004). The species can be found in an extensive variety of habitats, with preference for open areas (Cortés-Fossati, 2018a; sub *B. majalis*) (Fig. 18), from coastal sandy soils with *Juniperus* L., more or less open oak forests (with *Quercus suber* L., *Q. rotundifolia*, *Q. faginea* Lam. and, to a lesser extent, *Q. canariensis* Willd. and *Q. coccifera*) and their stages of degradation on mountain slopes and lowlands, open pine forest (*Pinus pinea* L., *P. halepensis* Mill., *P. pinaster* Ait.), different types of thermo- and meso-Mediterranean scrub formations [including *Calicotome villosa* (Poir.) Link, *Erica arborea* L., *Retama sphaerocarpa*, *Genista* L., *Cytisus* Desf., *Halimium* (Dunal) Spach, *Cistus*, *Lavandula*, etc.], open scrubs with pastures in rolling hills dominated by *Pistacia lentiscus* and *Chamaerops humilis* and meadows (see: Valle, 2003). Cortés-Fossati (2018a) recorded this species (as *B. majalis*) in suburban landscapes with degraded vegetation in southern Cádiz. Adults are found mostly from March to June (Cortés-Fossati, 2018a, 2018b; sub *B. majalis*; pers. obs.). It has been recorded on 04 January 2018 in Manzanete, Cádiz (A. Hinckley pers. obs.), representing the earliest record of adult emergence for the genus.

BERBEROMELOE MACULIFRONS (LUCAS, 1847)
COMB. NOV.

Meloe maculifrons Lucas, 1847: 399. Terra typica: Environs de Bougie et d`Oran (Lucas, 1847).
Meloe maculicollis Reitter, 1872: 176. Terra typica: Oran (Reitter, 1872).
Meloe majalis var. *frontalis* Baudi, 1878: 355. Terra typica: Oran…, Constantina (Baudi, 1878).
Type material examined: Holotypus of *Meloe maculicollis* Reitter, 1872 (HNHM): Oran [white label, handwritten]; Holotypus 1872 *Meloë maculicollis* Reitter [white label bordered in red, partially handwritten, presumably added by Z. Kaszab]; [folded white label not transcribed]; *Meloe majalis* ab. *maculicollis* Rtt. det dr. Kaszab [white label, partially handwritten]. Figured in García-París *et al.* (2010: 169, fig. 1).

Taxonomic and nomenclatural comments: We revised topotype specimens of *Meloe maculifrons* (MNHNP, MNCN) from Oran surroundings (species type locality). These specimens show morphological characteristics typical of the eastern Moroccan lineage of *Berberomeloe*. Based on this morphological similarity, geographic proximity and similar habitat, we allocate the eastern Moroccan lineage to *Berberomeloe maculifrons*. In Morocco, this species extends from the Middle Atlas and eastern regions of the Rif to the Algerian border. Additional revised specimens from northern central Algeria (Theniet El Had) present a strong similarity with the western Algerian specimens of *B. maculifrons*. However, additional molecular and morphological studies are needed to evaluate the identity of the populations from eastern Algeria to Tunisia (Bologna, 1991).

Downloaded from https://academic.oup.com/zoolinnean/article-abstract/189/4/1249/5714599 by 81263633 user on 05 August 2020

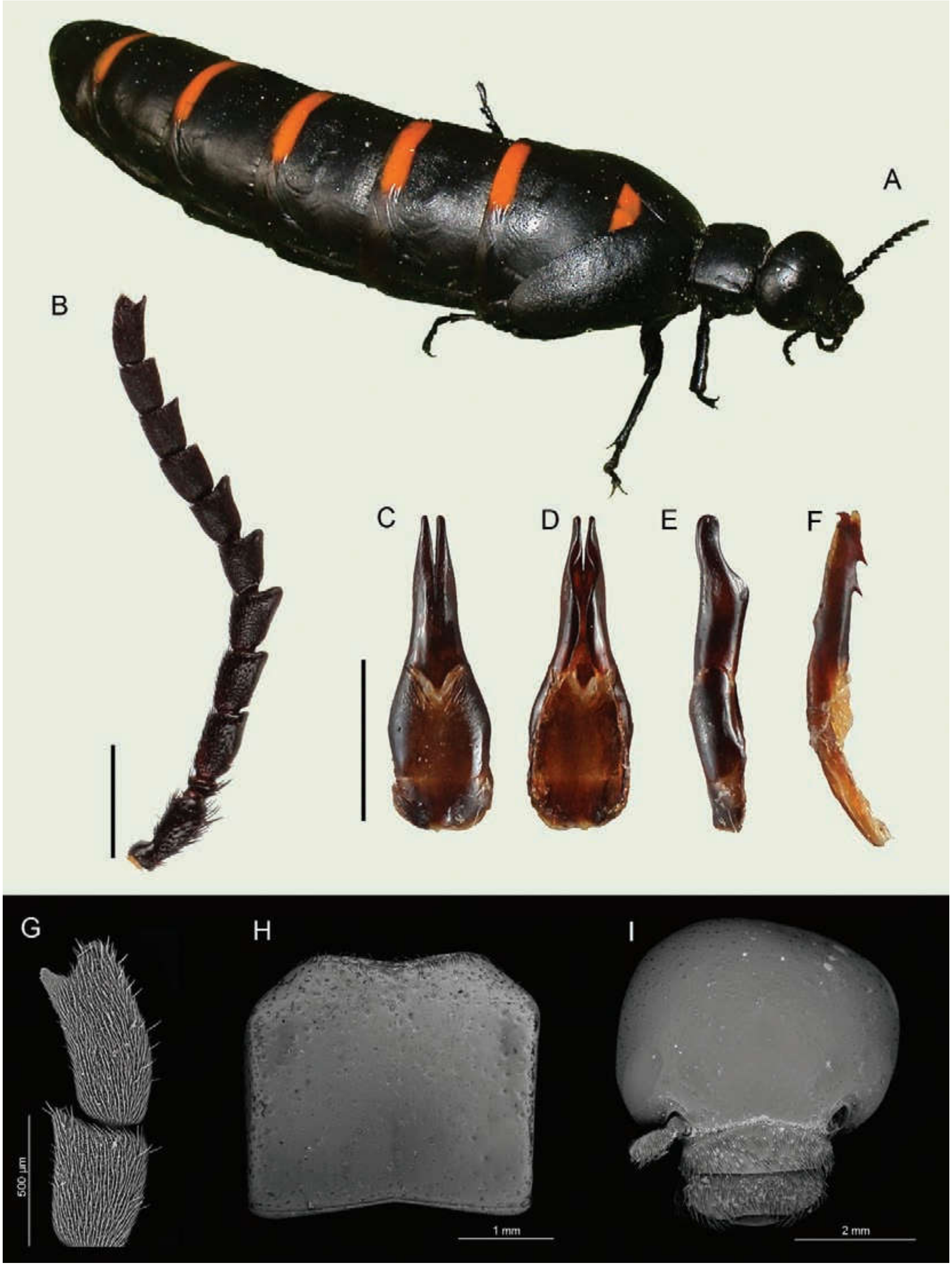

Figure 17. Habitus and morphological details of *Berberomeloe payoyo* from Montecorto, Málaga (A) and Medina Sidonia, Cádiz (B–I). A, dorsal view of a male; B, male antenna; C, D, E, dorsal, ventral, lateral view of male genitalia, showing parameres and phallobase: note the width of the lobes at lateral view; F, lateral view of aedeagus; G, SEM micrographs of the two last antennomeres; H, SEM micrographs of pronotum, dorsal view; I, SEM micrographs of head, frontal view.

Bologna (1989) figured specimens from Tebessa, eastern Algeria (sub *B. majalis*), that could represent *B. maculifrons*.

Description: Berberomeloe maculifrons presents the general characteristics of the genus (see: Bologna 1989, 1991) and the following diagnostic features: Body

Downloaded from https://academic.oup.com/zoolinnean/article-abstract/189/4/1249/5714599 by 81263633 user on 05 August 2020

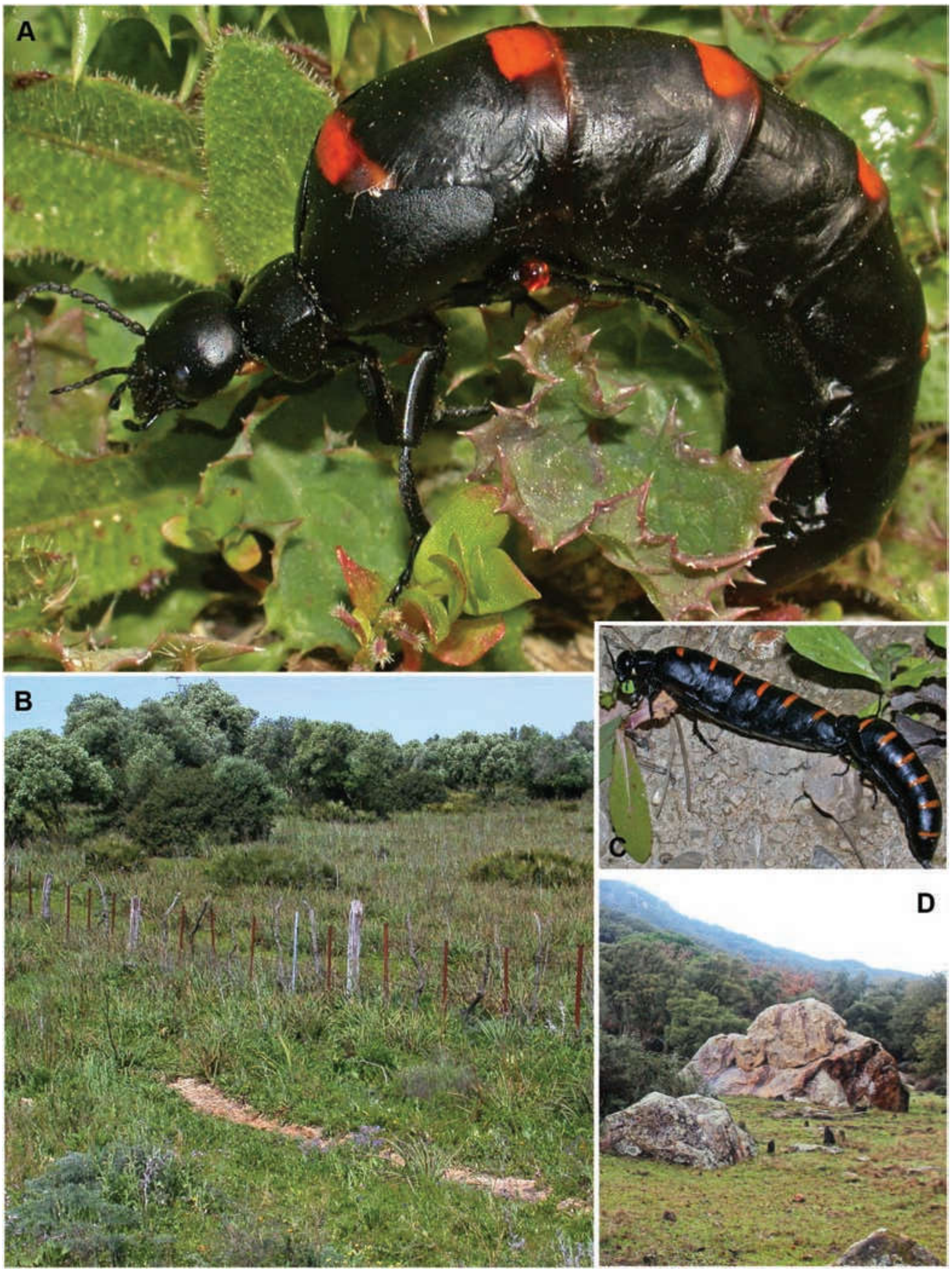

Figure 18. A, specimen of *Berberomeloe payoyo* in defensive behaviour at Malcocinado, Cádiz; note the reddish drop of haemolymph with cantharidin released in the metafemur-metatibia joint. B, courtship behaviour of *B. payoyo* at Montecorto, Málaga. C, D, habitats of *B. payoyo*, Spain; C, Medina Sidonia, Cádiz; D, Los Barrios, Cádiz.

length (frons to posterior border of elytra), 10 to 20 mm. General coloration black, always with red stripes on the posterior margin of each abdominal terga except VII and VIII (no entirely black-coloured specimens have been recorded), and usually with a diffuse red blotch in the disc of the frons. Tegument of head and pronotum finely microreticulated, shiny; surface with two types of puncturation simultaneously, similar to that of the pronotum, but less dense; mid-longitudinal line present from the middle of the frons to the vertex, thin and shallow. Antennomere IV elongated, subrectangular, with subparallel sides; V, VI, VII and IX trapezoidal

Downloaded from https://academic.oup.com/zoolinnean/article-abstract/189/4/1249/5714599 by 81263633 user on 05 August 2020

or subtriangular, strongly dentate; X subtrapezoidal, barely dentate; XI elongate, slightly arched and strongly emarginated at apex (Fig. 19). Pronotum subquadrate, lateral sides convergent in the posterior two-thirds, basis markedly arcuate; surface generally with two rounded depressions near the anterior angles and sometimes

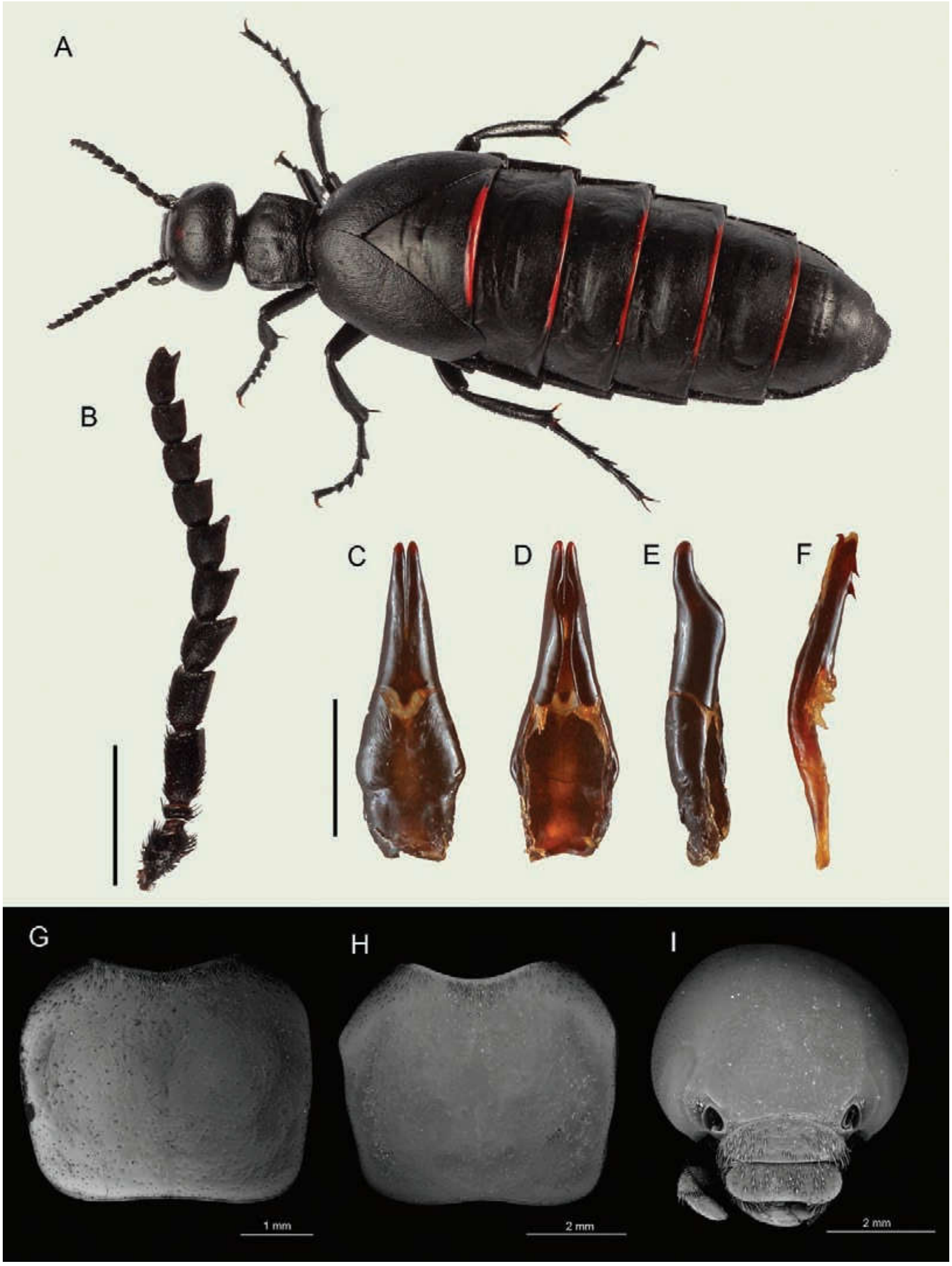

Figure 19. Habitus and morphological details of *Berberomeloe maculifrons* from Fez, Morocco (A), Saidia, Morocco (B–F, H) and Ifrane, Morocco (G). A, dorsal view of a male; B, male antenna; C, D, E, dorsal, ventral, lateral view of male genitalia, showing parameres and phallobase; F, lateral view of aedeagus; G, H, SEM micrographs of pronotum, dorsal view, of specimens from populations located at the Middle Atlas and at the eastern side of Moulouya river basin, respectively: note the deep puncturation in the middle atlas form; I, SEM micrographs of head, frontal view.

Downloaded from https://academic.oup.com/zoolinnean/article-abstract/189/4/1249/5714599 by 81263633 user on 05 August 2020

also on the posterior ones; with two types of punctures simultaneously, ranging from small to medium-sized in populations from the eastern Moulouya river basin, to medium-sized to large punctures in the populations of the Middle Atlas; puncture density low or medium in the Eastern Moulouya populations and medium-high in the Middle Atlas populations, with the largest punctures located over the pronotum edges; punctures in the disc sparse and smaller; some specimens from the Middle Atlas (Ifrane–Azrou surroundings) present deep and dense punctures on the pronotum, forming a semi-corrugated pattern; mid-longitudinal line conspicuous, strongly impressed, covering almost the entire length of the pronotum. Elytra with semi-glossy tegument and well-marked longitudinal wrinkles; punctures subtle and dispersed over the whole surface, difficult to appreciate. Male genitalia (Fig. 19C–F) with tegmen evenly sclerotized; parameres relatively elongated, slightly shorter than phallobase, with distal lobes short and wide in lateral view; median lobe with two acute similar hooks far from apex, relatively close to each other; apex obliquely truncated in lateral view; endophallic hook slender.

Variability: Body length (frons to posterior border of elytra) highly variable, 10 to 20 mm; maximum total length among preserved, studied specimens, 55 mm. Morphometric variability is shown in Table 2. The coloured bars of abdominal terga present individual colour variability in live specimens, from yellow-orange to deep red. Width of the coloured transverse tergal bars highly variable, but on average, relatively narrow (ratio 'total width of the second tergum/width of the transverse bar of the second tergum' between 1.17 and 1.95, average = 1.43, SD = 0.15, $N = 33$). Frontal red spot variable in width and intensity, sometimes absent or, on the contrary, expanded sideways, almost reaching the temples; in some specimens, pronotum may present two diffuse reddish spots on the sides of the disc (e.g. holotype of *Meloe maculicollis* Reitter; see: García-París *et al.*, 2010: 169, fig. 1). Weak individual differences have been detected in the dentation of the antennomeres, usually more marked in larger specimens. Pronotum shape variable individually, with fore angles more or less rounded. Pronotal puncturation also variable in density, size and depth, with two different phenotypes geographically structured (see description above) (Fig. 19G, H).

Diagnosis: Berberomeloe maculifrons can be distinguished from all other species of *Berberomeloe* by the following combination of characters (Fig. 19): (1) abdomen with medium width transverse bars, orange to red-coloured in the posterior margin of tergites I–VI; (2) punctures on head small to medium-sized, rounded, shallow, isolated; variation between western and eastern Moulouya populations has been described above; (3) pronotum surface homogeneously punctured, with two types of puncturation simultaneously; punctures small to medium and relatively shallow (Moulouya basin populations) or medium to large and deep (Middle Atlas and eastern Rif populations); (4) antennomeres V–VII and IX trapezoidal or subtriangular, strongly dentate in their inner apex; (5) male antennomere XI wide; and (6) male genitalia with parameres relatively elongated; median lobe obliquely truncated at apex in lateral view, with similar hooks relatively distant from the apex, close to each other.

Distribution and notes on natural history: This species ranges across eastern and central Morocco, from the Middle Atlas mountain range and the eastern slopes of the Rif Mountains to the Moulouya River basin (Fig. 2), extending eastward along northern Algeria probably to Tunisia (Bologna, 1991). *Berberomeloe maculifrons* inhabits different habitat types, from semi-arid Mediterranean scrublands [e.g. *Ziziphus lotus*, *Chamaerops humilis*, *Retama sphaerocarpa*, *Tetraclinis articulata* (Vahl) Masters, *Rosmarinus officinalis* L., *Pistacia lentiscus*, *Launea arborescens* (Batt.) Murb., *Lavandula*, *Artemisia* L.] in north-eastern Morocco and arid steppes in the eastern Moulouya region, Debdou plains and Rekkan plateau (with grazed steppes of *Macrochloa tenacissima*), to highland grasslands and open forest edges of *Cedrus atlantica* (Endl.) Manetti ex Carrière, *Quercus rotundifolia*, *Q. faginea* and *Juniperus thurifera* L. in the Middle Atlas (see: Benabid, 1985, Benabid & Fennane, 1994). It also occurs in reforested open forests (*Pinus*), cereal fields, and olive groves in the Fez region (Fig. 20, pers. obs.). It occupies thermo-, meso- and supra-Mediterranean bioclimatic levels, in regions with arid to hyperhumid ombrotypes (Benabid, 1985; Le Houerou, 1989; Sebbar *et al.*, 2013).

Adult life period can last up to 50 days (Cros, 1912; sub *M. majalis*). Gravid females can lay approximately 1500 eggs in each clutch (Cros, 1912; sub *M. majalis*). Notes on the behaviour, courtship, and larval development are described in Cros (1912, 1913; sub *M. majalis*) from Algerian populations. Adult phenology extends from March to July (Bologna, 1991; sub *B. majalis*, referred to Magrebian populations, and pers. obs.).

BERBEROMELOE YEBLI SÁNCHEZ-VIALAS *ET AL.*, SP. NOV.

LSID: urn:lsid:zoobank.org:act:C412DC8D-17FA-4937-9DEA-91D9766517D5

Holotype: Male: Carretera P-4702 entre Zinat y Moulay Abdeselam, Addrou, Región Tánger-Tetouan,

Downloaded from https://academic.oup.com/zoolinnean/article-abstract/189/4/1249/5714599 by 81263633 user on 05 August 2020

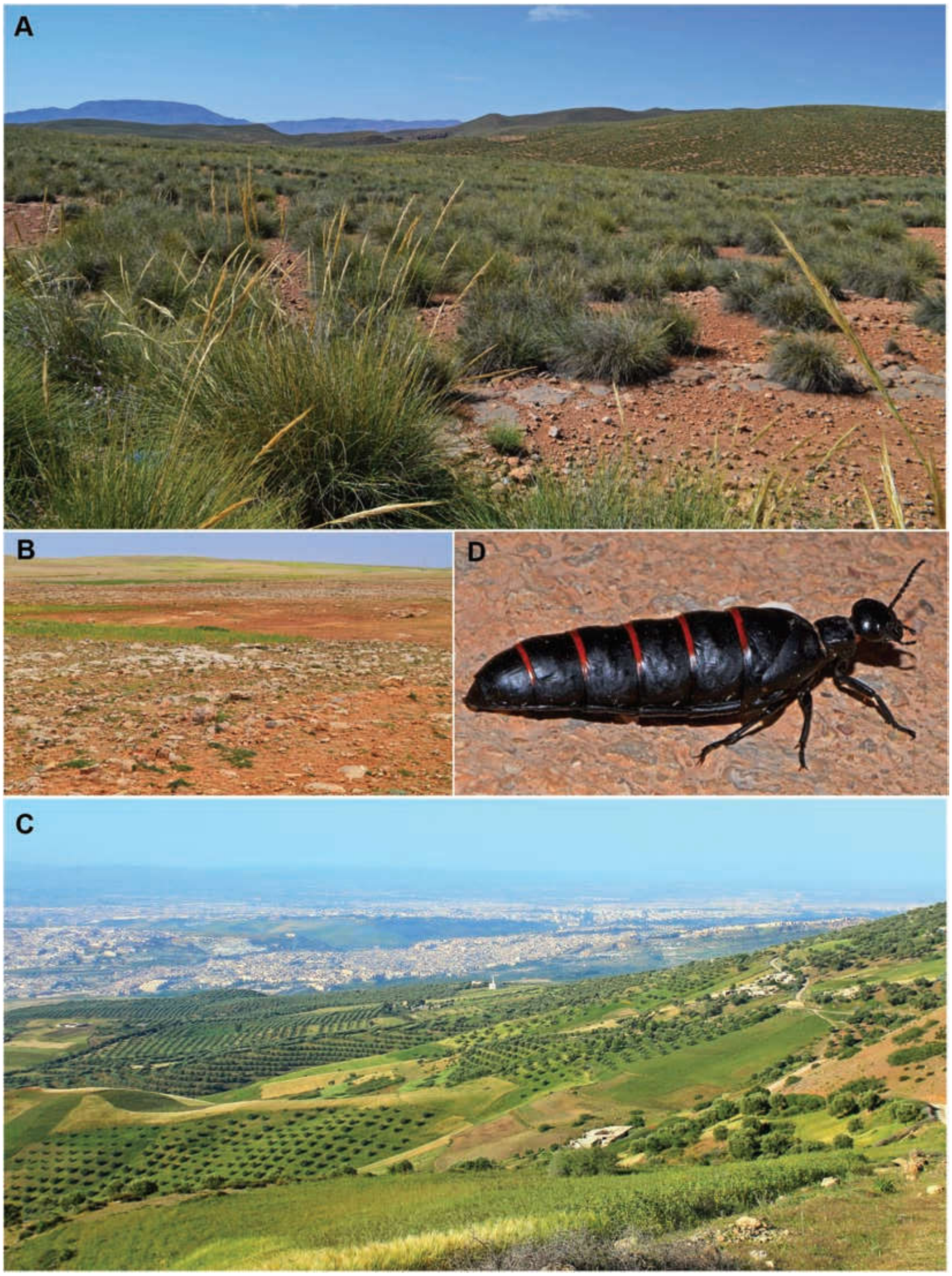

Figure 20. A–C, habitat of *Berberomeloe maculifrons*, Morocco: A, Enjil; B, 10 km South of Debdou; C, Fez surroundings, view from Jbel Zalagh. D, specimen of *B. maculifrons* from Enjil.

Marruecos, 35°22’04”N 5°32’17”W, 513 m, 12 May 2017, J. L. Ruiz leg. [white label, printed]; MNCN_Ent 231447 [white label, printed]; Holotypus, *Berberomeloe yebli* Sánchez-Vialas, García-París, Ruiz & Recuero des. 2019 [white label, printed]. Preserved in absolute ethanol, held at the Entomological Collection of the Museo Nacional de Ciencias Naturales, Madrid.

Paratypes: Carretera P-4702 entre Zinat y Moulay Abdeselam, Addrou, Región Tánger-Tetouan,

Downloaded from https://academic.oup.com/zoolinnean/article-abstract/189/4/1249/5714599 by 81263633 user on 05 August 2020

Marruecos, 35°22’04”N 5°32’17”W, 513 m, 12 May 2017, J. L. Ruiz leg. [white label, printed] (female, preserved in ethanol).— Marruecos, Derdara, 29 May 2013, J. L. Ruiz leg. [white label, handwritten]; MNCN_Ent 231448 [white label, printed] (male, extracted genitalia, preserved dry).—Smir-M´Diq, (Marruecos), 11 April 1990, J. L. Ruiz leg. [white label, printed]; MNCN_Ent 231449 [white label, printed] (female, preserved dry).—Marruecos, Yebel Tiziren, Bab-Berred, Rif Central, 35°00’34.23” N, 4°53’57.28” W, 1480 m., 13 May 2017, J. L. Ruiz leg. [white label, handwritten]; MNCN_Ent 231450 [white label, printed] (preserved in ethanol).—Tánger, M. Escalera [white label, printed]; *Meloe majalis* L. [white label, handwritten]; 609 [white label, handwritten]; MNCN_Ent 175293 [white label, handwritten] (preserved dry).—Tetuán [white label, printed]; *M. majalis* [white label, handwritten]; 625 [white label, handwritten]; MNCN_Ent 175294 [white label, printed] (preserved dry).—Tetuán a Ceuta [white label, printed]; 628 [white label, handwritten]; MNCN_Ent 175297 [white label, printed] (preserved dry).—Tánger, M. Escalera [white label, printed]; 614 [white label, handwritten]; MNCN_Ent 175299 [white label, printed] (preserved dry).—Tánger, M. Escalera [white label, printed]; 615 [white label, handwritten]; MNCN_Ent 175300 [white label, printed] (preserved dry).—Tánger, M. Escalera [white label, printed]; 616 [white label, handwritten]; MNCN_Ent 175301 [white label, printed] (preserved dry).— Bab Taza, El Ajmas, Yebala, June 1930, Exp. C. Bolivar [white label, printed]; MNCN_Ent 175302 [white label, printed] (preserved dry).—Tánger, M. Escalera [white label, printed]; 618 [white label, handwritten]; MNCN_Ent 175303 [white label, printed] (preserved dry).—Tánger, M. Escalera [white label, printed]; 603 [white label, handwritten]; MNCN_Ent 175309 [white label, printed] (preserved dry).—Tánger, 1897 [white label, printed]; *M. majalis* L. [white label, printed]; 597 [white label, handwritten]; MNCN_Ent 175310 [white label, printed] (preserved dry).—Tánger, 1897 [white label, printed]; 598 [white label, handwritten]; MNCN_Ent 175311 [white label, printed] (preserved dry).—Morocco, Tánger, June 1905, Escalera [white label, printed]; 599 [white label, handwritten], MNCN_Ent 175312 [white label, printed] (preserved dry).—Llano Malalien, Morocco, Ferrer Andreu leg. [white label]; *Meloe majalis* L., Pardo Alcaide det. 64 [white label, printed]; MNCN_Ent 233307 [white label, printed] (preserved dry).—Morocco, carretera P-4702, hacia Moulay Abdeselam, Parque Regional Bou-Hachem (Beni-Aros), Yebala, 35°22’05”N 5°32’15”W, 513 m, 29 April 2011, J. L. Ruiz leg. [white label, handwritten]; MNCN_Ent 251019 [white label, printed] (preserved in ethanol).—Moulay Abdeselam, 27 May 2006 [white label, handwritten]; ASV16010 [white label, printed]; MNCN_Ent 251020 [white label, printed] (preserved in ethanol).—Moulay Abdeselam, 27 May 2006 [white label, handwritten]; ASV16011 [white label, printed]; MNCN_Ent 251021 [white label, printed] (preserved in ethanol).—Morocco, 8 km NW Moulay Abdeselam, 35°22’11”N 5°33’56.8”W, 30 May 2013, E. Recuero, P. Mas-Peinado, R. García-Roa leg. [white label, printed]; MNCN_Ent 251022 [white label, printed] (preserved in ethanol).—Morocco, Bounezal, 35°36’19.1”N 5°29’29.4”W, 31 May 2013, E. Recuero, P. Mas-Peinado, R. García-Roa leg. [white label, printed]; MNCN_Ent 251023 [white label, printed] (preserved in ethanol).—Carretera entre Tetuán y Khemis Anyera. P4701, Provincia Fashs Anjera, Morocco, 35°38’13.93”N 5°29’52.96”W, 63 m, 30 April 2018, J. L. Ruiz & M. Cámara leg. [white label, handwritten]; MNCN_Ent 251024 [white label, printed] (preserved in ethanol).—Bab-Taza [white label, handwritten]; ASV16006 [white label, printed]; MNCN_Ent 251025 [white label, printed] (preserved in ethanol).—Morocco, Chefchaouen, 35°11’34.5”N 5°18’38.5”W, 29 April 2003, C. Settanni, R. Sindaco, A. Venchi leg. [white label, handwritten]; ASV16003 [white label, printed]; MNCN_Ent 251026 [white label, printed] (preserved in ethanol). All paratypes labelled: ‘Paratypus, *Berberomeloe yebli* Sánchez-Vialas, García-París, Ruiz & Recuero, des. 2019 [red labels for dry-preserved specimens, and white labels for ethanol-preserved specimens, all printed]’. All specimens are held at the Entomological Collection of the Museo Nacional de Ciencias Naturales, Madrid. Total paratypes: 25 exx.

Etymology: The specific epithet *yebli* (a masculine noun, in apposition), refers to the male natives of the ‘Yebala’ region (in Arabic, ‘mountains region’), located in north-western Morocco and coinciding for the most part with the distribution range of the species.

Description of the holotype: Length (frons to posterior margin of elytra), 8.1 mm. Total length (including abdomen) of preserved holotype, 29 mm. Maximum width, 5.4 mm. Moderately wide orange transverse bars in the posterior edge of each tergum, except VII and VIII, which are entirely black. Tegument of glossy (head, thorax and legs) or semi-glossy (elytra and abdomen) aspect, with fine microreticulation, almost imperceptible. Head maximum width, 2.8 mm. Surface covered by numerous punctures uniformly distributed. Head punctures vary from medium- to large-sized, rounded, deep marked, close to each other, confluent in temples. A longitudinal midline is finely impressed from the upper half of the frons to the vertex. Minimum interorbital distance: 1.7 mm. Clypeus 1.3 mm wide by 0.5 long. Labrum 1.3 mm wide by 0.5 long. Antennae with antennomeres widened apically, with short black vestiture, mostly decumbent and with a few sparse setae erect, longer

Downloaded from https://academic.oup.com/zoolinnean/article-abstract/189/4/1249/5714599 by 81263633 user on 05 August 2020

and semi-erect on antennomeres I–II; antennomere I slightly widened apically, subcylindrical (length: 0.5 mm); II short, cylindrical (length: 0.2 mm); III (length: 0.5 mm) subcylindrical, slightly widened apically, rectangular; IV (length: 0.4 mm) shorter than III but equally wide, subrectangular; V (length: 0.3 mm) trapezoidal, wider than VI, with a wide and rounded apical tooth on the inner edge; VI (length: 0.3 mm) trapezoidal, with an apical tooth on the inner edge; VII (length: 0.3 mm) trapezoidal, wider than VI, with a marked and sharp apical tooth on the inner edge; VIII (length: 0.3 mm) trapezoidal, narrow than VII, weakly dentate on the apex of the inner edge; IX (length: 0.3 mm) trapezoidal, wider than VIII, sharply dentate on inner edge; X (length: 0.3 mm) trapezoidal, narrower than IX, apical tooth slightly acute; XI (length: 0.4 mm) subconical, moderately slender, notched on apex. Pronotum subquadrate with subparallel sides, slightly narrower at the anterior portion (anterior edge of pronotum: 2.1 mm; basal edge of pronotum: 2.6 mm; pronotum length on sagittal plane: 2.2 mm); anterior margin curved, posterior margin slightly arcuate; with an impressed fine longitudinal midline through the pronotum length; surface with diffuse and slightly pronounced lateral depressions behind the anterior angles. Pronotum surface deeply punctured; punctures of various sizes, mostly large, circular and deep, close to each other, some confluent, providing a corrugated appearance. Dorsal surface of pronotum almost glabrous, with an isolated short seta in each puncture; anterior margin, adjacent to the neck, with numerous, moderately long setae. Elytra imbricated basally (the right over the left); length, 4.9 mm; tegument glabrous, slightly wrinkled longitudinally with impressed irregular vermicular lines, with scarce, weakly marked, dispersed punctures. Distal margin of tergites I–VI with an orange transverse bar, moderately narrow in comparison with the total width of the terga (width of the second tergum: 4.8 mm; width transverse bar of the second tergum: 3.1 mm). Last ventrite notched. Metafemur as long as metatibia (metafemur length: 2.7 mm; metatibia length: 2.7 mm). Metatarsomere length, from inner to apical: 1.4, 0.6, 0.5, 0.7 mm. Genitalia with tegmen brownish; moderately elongated, slender both on dorsal and lateral views. Phallobase longer than wide, length similar to the parameres; wider on dorsal view; maximum width at the middle. Parameres longer than wide, basally cylindrical; distal third formed by parameral lobes; scarce setae, applied against the tegument, present on the mid-dorsal area. Parameral lobes separated by a longitudinal notch that extends to the middle of the dorsal surface of the parameres; apexes rounded. Median lobe long, robust, flattened, with rounded apex in lateral view and two acute ventral hooks; ventral hooks similar, close to each other and well separated from apex. Endophallic hook visible.

Female: Similar to male, but with the last abdominal ventrite (VIII) rounded, not emarginated in its posterior margin, and less dentate antennomeres. Studied specimens present the inner surface of the bursa copulatrix with few but conspicuous sclerotized spicules or plates (similar to those of *B. castuo*, as figured in Fig. 8).

Variability: Body length variable (frons to posterior edge of elytra): 12–18 mm; maximum total length among preserved, studied specimens, 40 mm. Morphometric variability is shown in Table 2. No entirely black specimens have been found. Variability of the tergal red bar width is moderate (ratio 'total width of the second tergum/width of the transverse bar of the second tergum' between 1.32 and 1.95, average = 1.65, SD = 0.23, N = 10). There is slight individual variation in the density of punctures on the head and pronotum.

Diagnosis: Distinguished from all other species of *Berberomeloe* by the following combination of characters (Fig. 21): (1) medium-sized, coloured, transverse tergal bars on the distal margin of I to VI tergites; (2) punctures of the head large- to medium-sized, rounded, deep and close to each other; (3) pronotum surface homogeneously punctate, with two types of punctures simultaneously, large and medium-sized, usually close to each other, often forming a rough pattern; (4) fore angles of pronotum not expanded, rounded; (5) apex of the median lobe of male genitalia rounded in lateral view; (6) male antennomere XI wide; and (7) male antennomeres V–VII expanded, clearly dentate, on the inner apical side.

Distribution and notes on natural history: Berberomeloe yebli is endemic to northern Morocco (Fig. 2). It is distributed over the Tingitanian Peninsula (mostly the Yebala region), including the Western and Central Rif. Across this area, *B. yebli* is found from almost sea level (Tangier and Smir-M'Diq), to 1480 m (Yebel Tiziren and Bab-Berred). The ombrotype of its geographic area of occupancy varies from subhumid to hyperhumid, at bioclimatic levels from thermo- to supra-Mediterranean (see: Benabid, 1982, 1985; Abdelilah & Taiqui, 2015). The geology of this region is complex (Betic-Rifian Arc), characterized mainly by sandstones, limestones and schists (Sanz de Galdeano, 1997).

It occurs over an extensive variety of open field habitats (Fig. 15B, 22) such as meadows and cultivated fields (*Cannabis* L., cereals), xerophile Mediterranean scrubs (*Chamaerops humilis*, *Pistacia lentiscus*,

Downloaded from https://academic.oup.com/zoolinnean/article-abstract/189/4/1249/5714599 by 81263633 user on 05 August 2020

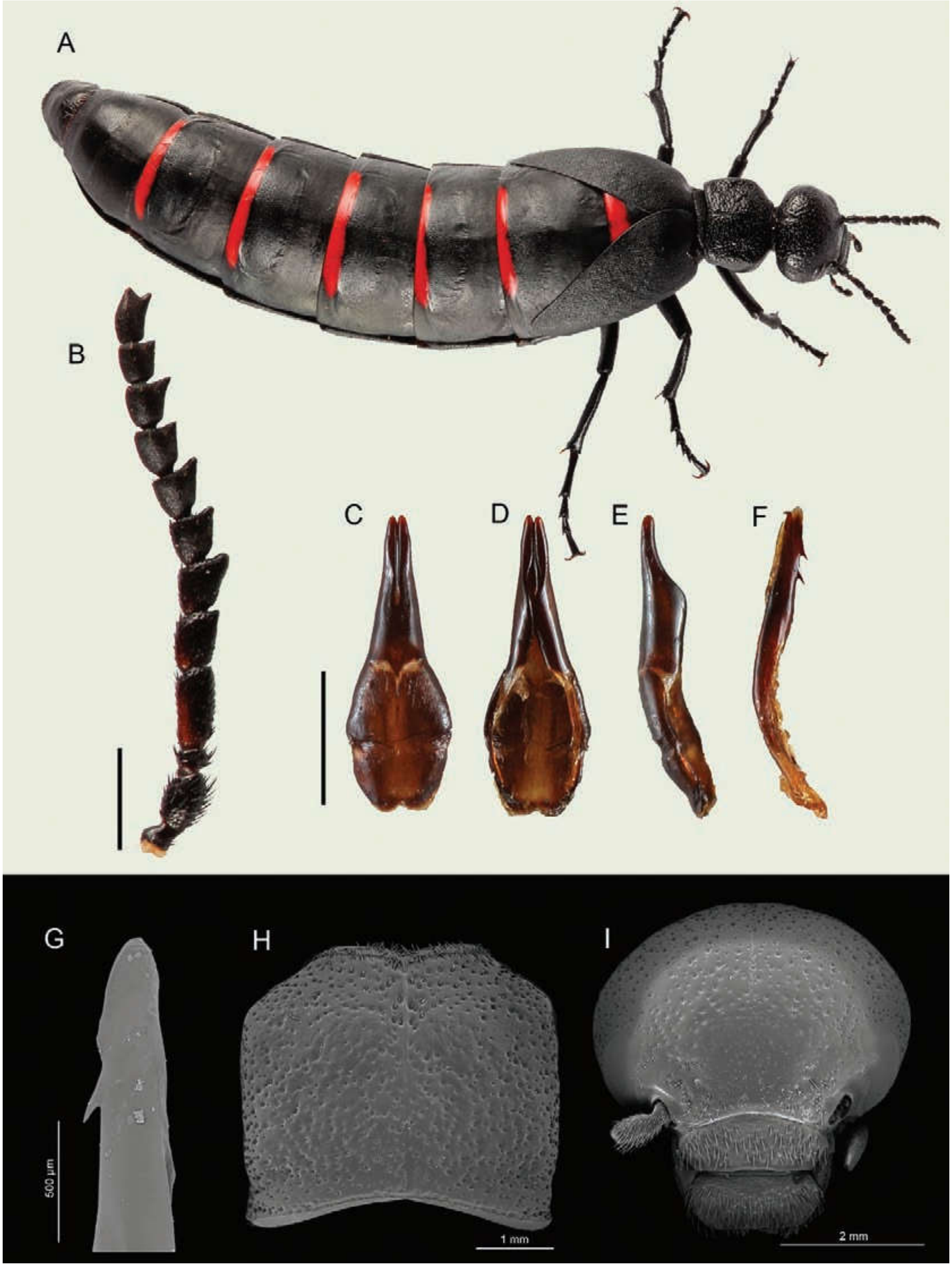

Figure 21. Habitus and morphological details of *Berberomeloe yebli* from Moulay Abdessalam, Morocco (A–B) and Bab Taza (C–I). A, dorsal view of a male; B, male antenna; C, D, E, dorsal, ventral, lateral view of male genitalia, showing parameres and phallobase: F, lateral view of aedeagus; G, SEM micrographs of distal part of aedeagus; note the rounded apex with the lateral distal hook broken; H, SEM micrographs of pronotum, dorsal view; I, SEM micrographs of head, frontal view.

Calicotome villosa (Poir.) Link, *Phillyrea* and *Cistus*), forest edges and open forests, mainly formed by oaks (*Quercus suber*, *Q. faginea*, *Q. pyrenaica* and *Q. rotundifolia*), wild olive-trees (*Olea europaea* L. var. *sylvestris* Brot.), pines (*Pinus pinaster*, *P. pinea* and *P. halepensis*) and, localized in mountains, *Cedrus*

Downloaded from https://academic.oup.com/zoolinnean/article-abstract/189/4/1249/5714599 by 81263633 user on 05 August 2020

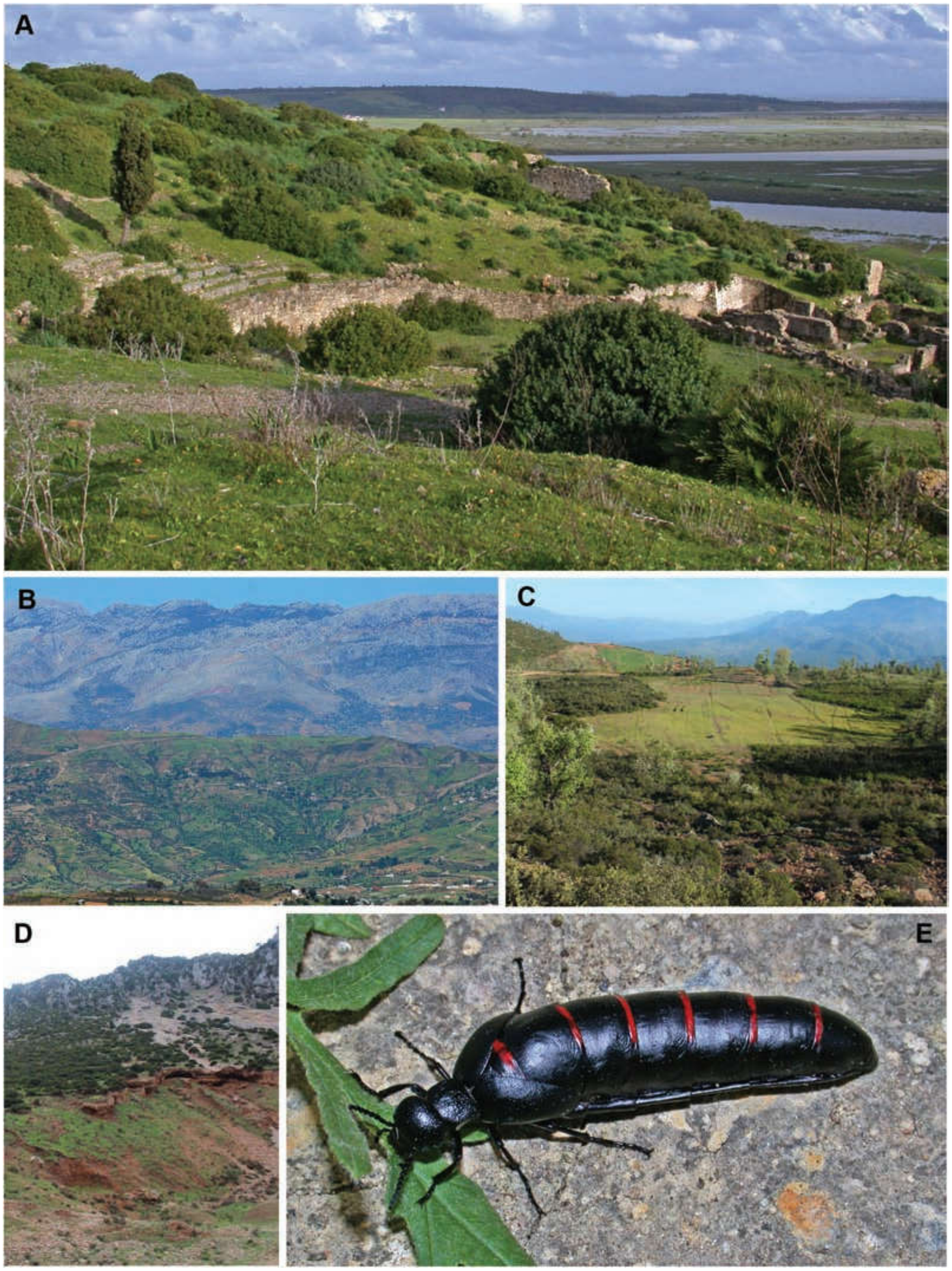

Figure 22. A–D, habitats of *Berberomeloe yebli*, Morocco: A, Lixus, province of Larache; B, Rif Mountains; C, Ketama surroundings; D, South of Tetouan. E, specimen of *B. yebli* from Moulay Abdeselam.

atlantica (see: Benabid, 1982, 1984; Benabid & Fennane, 1994; Charco, 1999). Adults are found from March to June (pers. obs.).

BERBEROMELOE INSIGNIS (CHARPENTIER, 1818)

Meloe insignis Charpentier *in* Germar, 1818: 258.

Terra typica: 'Spanien'.

Berberomeloe insignis (Charpentier, 1818): García-París, 1998: 99.

Diagnosis: Berberomeloe insignis can be distinguished from all other species of *Berberomeloe* by the following combination of characters (Fig. 23): (1) entirely black

Downloaded from https://academic.oup.com/zoolinnean/article-abstract/189/4/1249/5714599 by 81263633 user on 05 August 2020

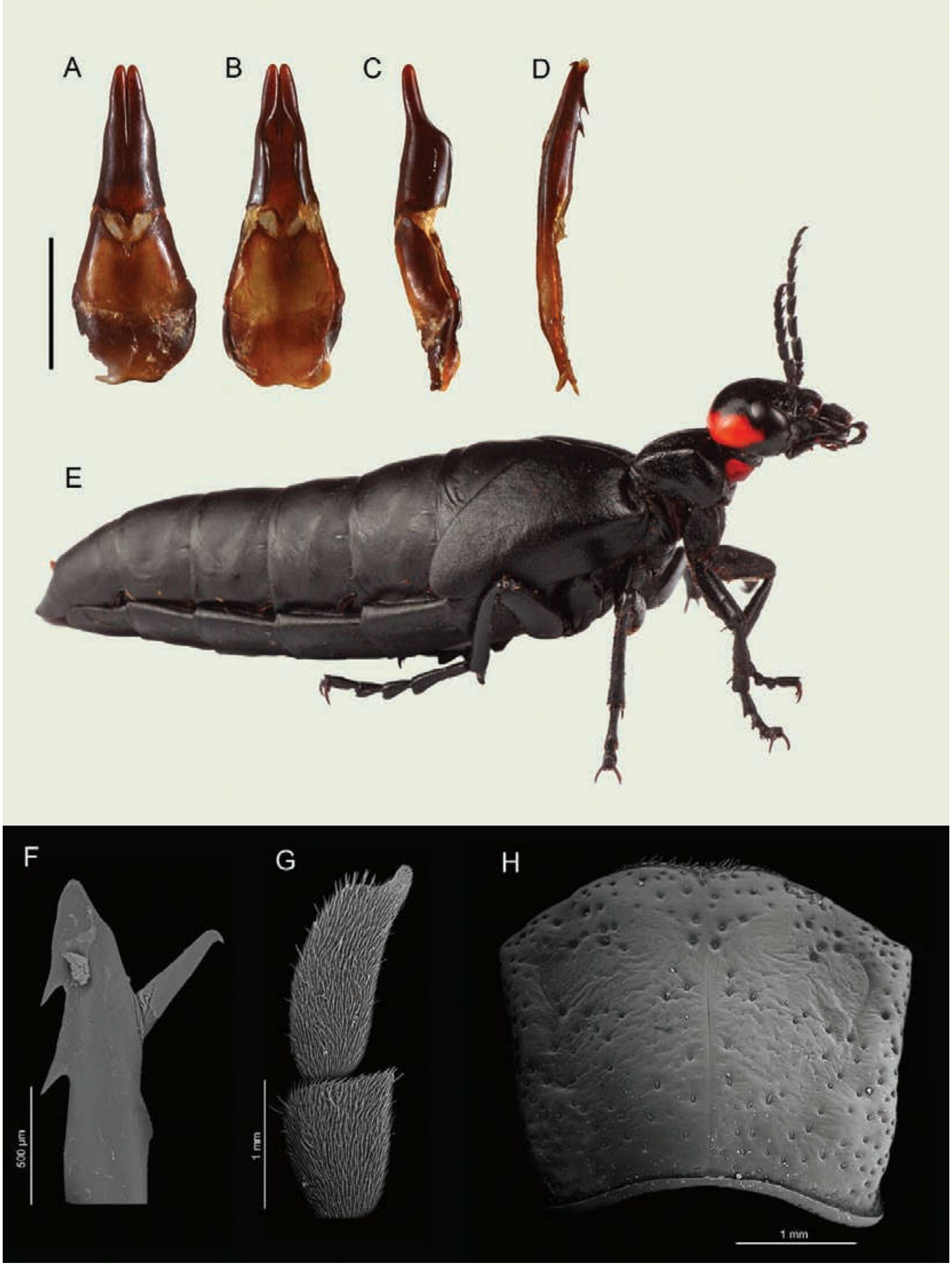

Figure 23. Habitus and morphological details of *Berberomeloe insignis* from Sierra Alhamilla, Almería (A–D), Las Palas, Murcia (E) and Morata, Murcia (F–H). A, B, C, dorsal, ventral, and lateral view of male genitalia, showing parameres and phallobase; D, lateral view of aedeagus; E, lateral view of a male; F, SEM micrographs of distal part of aedeagus; note the stretched and rounded apex, and variability compared with Figure 23D; G, SEM micrographs of the two last antennomeres; H, SEM micrographs of pronotum, dorsal view.

abdomen; (2) presence of isolated symmetrical red blotches on the head temples; an additional red blotch on the frons is also present in some populations; (3) punctures on the head generally small to medium-sized, rounded, shallow and mostly isolated from each other; (4) pronotum surface heterogeneously

Downloaded from https://academic.oup.com/zoolinnean/article-abstract/189/4/1249/5714599 by 81263633 user on 05 August 2020

punctured; with medium or large-sized punctures, deep and located mainly on the sides and along the midline area; disc region almost smooth, with isolated punctures; (5) fore angles of pronotum expanded, obtuse, well-marked; (6) antennomere XI slender (both in males and females); (7) antennomeres VII and IX strongly dentate on the inner apical side, especially in males; and (8) male genitalia with apex of the median lobe markedly narrow. A detailed description of the species was provided by García-París (1998).

Variability: Total length (frons–last abdominal ventrite) varies from 12 to 49 mm (García-París & Ruiz, 2008). García-París (1998) figured the interpopulation variability regarding the shape and extension of the red blotch of the head temples. Populations from southern Almería, particularly the surroundings of Tabernas, present an additional single red blotch in the middle of the frons. Among examined specimens certain variability has been observed in head and pronotum puncturation density, as well as in male genitalia, i.e. in width and length of parameral lobes and in size and shape of apical hook of aedeagus (Fig. 23D, F).

Distribution and notes on natural history: Berberomeloe insignis is a species endemic to south-eastern Spain, including the coastal provinces of Murcia, Almería and Granada (García-París, 1998; García-París & Ruiz, 2011a). It occurs mostly over the 'Murciano-almeriense' phytochorological province, but it also extends westward to the Betic phytochorological province (see: Rivas-Martínez, 1987; Valle *et al.*, 2004) along the southern foothills of Sierra Nevada, where the species reach its western distributional limit at the surroundings of Jete, Motril, Órgiva and Polopos (Granada) (García-París & Ruiz, 2008, 2011a; Ruiz & García-París, 2013).

Berberomeloe insignis generally inhabits lowland areas, from sea level to 900 m of elevation at Fiñana (Almería) (García-París *et al.*, 1999, 2003; García-París & Ruiz, 2008, 2011a), at thermo- and meso-Mediterranean bioclimate levels, with semi-arid (200–350 mm average rainfall) to dry (350–600 mm average rainfall) conditions (see: Rivas-Martínez, 1987; Valle *et al.*, 2004). The habitat (Fig. 24) is mainly constituted by steppes and, to a lesser extent, by open fields with scrubs and no tree cover, with the exception of open *Pinus* formations or almond fields (García-París & Ruiz, 2008, 2011a). Most parts of its range are dominated by xerophytic flora, such as *Periploca laevigata* Ait., *Maytenus senegalensis*, *Ziziphus lotus*, *Pistacia lentiscus*, *Chamaerops humilis*, *Macrochloa tenacissima*, *Anthyllis cytisoides*, *Thymelaea hirsuta* (L.) Endl. and *Thymus*, among others (García-París & Ruiz, 2008, 2011a).

Adults are diurnal and feed on diverse plants, such as flowers of *Convolvulus* L. (García-París *et al.*, 1999). Males search for females actively and courtship is similar to that of the *B. majalis* species group (García-París & Ruiz, 2008). García-París *et al.* (1999) recorded several localities where *B. insignis* co-occur with *B. indalo* (referred to as *B. majalis*), but interspecific courtship was not observed.

BERBEROMELOE TENEBROSUS SÁNCHEZ-VIALAS *ET AL.*, SP. NOV.

LSID: urn:lsid:zoobank.org:act:7402C214-00A6-4C4A-BE83-44584C7C518E

Holotype: Male: Almería, Calar Alto (37°12'39"N 2°36'26"W, 1927 m), 6 May 2005, mel 05048 Bi, M. Gª-París leg. [white label, printed]; MNCN_Ent 231451 [white label, printed]; Holotypus, *Berberomeloe tenebrosus* Sánchez-Vialas, García-París, Ruiz & Recuero des. 2019 [white label, printed] (genitalia extracted). Preserved in absolute ethanol, held at the Entomological Collection of the Museo Nacional de Ciencias Naturales, Madrid.

Paratypes: Peñones S. Fco (de San Francisco), Sierra Nevada, Granada, España, 2400 m, 30SVG656065, 10 June 1990, P. Barranco (leg.) [white label, printed]; MNCN_Ent 231452 [white label, printed] (male, preserved dry).—Puerto de la Ragua, 2000 m., Sierra Nevada, Granada, España, 21 May 2005, J. M. Barreda leg. [white label, printed]; MNCN_Ent 231453 [white label, printed] (female, preserved dry).—Peñones de S. Francisco, Albergue Universitario, Sierra Nevada (Granada), 2500 m; 25 June 1992, J. L. Ruiz leg. [white label, printed]; MNCN_Ent 231454 [white label, printed] (female, extracted genitalia, preserved dry).—Almería, Puerto de la Ragua, 8-V-2017, D. Escoriza leg. [white label, handwritten]; APP 17005 [white label, handwritten]; MNCN_Ent 251028 [white label, printed] (preserved in ethanol).—Almería, Puerto de Escúllar, Sierra de los Filabres, 8 May 2010, M. García-París leg. [white label, handwritten]; ASV16080 [white label, printed]; MNCN_Ent 251029 [white label, printed] (preserved in ethanol).—Granada, Borreguilillo, Pradollano, 10 July 2009, M. G. Rollán & J. París leg. [white label, printed]; ASV16075 [white label, printed]; MNCN_Ent 251027 [white label, printed] (preserved in ethanol).—Granada, carretera del Veleta, Km 41, 2800 m, 15 June 2007, M. G. Rollán leg. [white label, handwritten]; ASV16071 [white label, printed]; MNCN_Ent 251030 [white label, printed] (preserved in ethanol).—El Chorrillo, Granada, 8 July 1984, A. Compte leg. [white label, printed] (preserved dry).—Río Guadalfeo, Granada, July 1974, A. Compte leg. [white label, handwritten]; MNCN_Ent 233473 [white label, printed] (preserved dry).—2 exx labelled:

Downloaded from https://academic.oup.com/zoolinnean/article-abstract/189/4/1249/5714599 by 81263633 user on 05 August 2020

Figure 24. A, B, specimens of *Berberomeloe insignis* from Tabernas, Almería and Polopos, Granada, respectively. C–E, habitats of *Berberomeloe insignis*, Spain; C, Pulpí, Almería; D, Gergal, Almería; E, Las Palas, Murcia.

Residencia Universitaria Veleta, Granada, 5 July 1974, A. Compte leg. [white label, printed]; MNCN_Ent 233475 and MNCN_Ent 233476, respectively [white labels, printed] (preserved dry).—Granada, Pradollano, Sierra Nevada, 2000 m, 21 June 1996, J. París leg. [white label, print]; *Berberomeloe majalis* Linnaeus, 1758 [white label, print]; 355 [white label, handwritten]; MNCN_Ent 233472 [white label,

Downloaded from https://academic.oup.com/zoolinnean/article-abstract/189/4/1249/5714599 by 81263633 user on 05 August 2020

printed] (preserved dry).—Granada, Pradollano, Sierra Nevada, 2000 m, 17 June 83, M. García-París leg. [white label, print]; *Berberomeloe majalis* Linnaeus, 1758 [white label, print]; 357 [white label, handwritten]; MNCN_Ent 233468 [white label, printed] (preserved dry).—10 exx labelled: Sierra Nevada, VII-1936, Escalera [white label, printed]; *Berberomeloe majalis* Linnaeus, 1758, M. G^{a}-París det. 98 [white label, printed]; [white label, handwritten: numbered from 527 to 536]; MNCN_Ent 233458–233466 respectively [white labels, printed] (preserved dry).—Loma del tlfno [Teléfono], Sierra Nevada, 17 July 1972 [white label, handwritten]; *Berberomeloe majalis* Linnaeus, 1758, M. G^{a}-París det. 98 [white label, printed]; 538 [white label, handwritten]; MNCN_Ent 233469 [white label, printed] (preserved dry).—Veleta, Sierra Nevada, 27-VI-62; *Berberomeloe majalis* Linnaeus, 1758, M. G^{a}-París det. 98 [white label, preserved dry]; MNCN_Ent 233470 [white label, printed] (preserved dry).— Güejar- Sierra [white label, handwritten]; *Berberomeloe majalis* Linnaeus, 1758, M. G^{a}-París det. 98 [white label, printed]; 540 [white label, handwritten]; MNCN_Ent 233471 [white label, printed] (preserved dry).—All paratypes labelled: 'Paratypus, *Berberomeloe tenebrosus* Sánchez-Vialas, García-París, Ruiz & Recuero, des. 2019 [red labels for dry-preserved specimens, and white labels for ethanol-preserved specimens, all printed]'. All specimens are held at the Entomological Collection of the Museo Nacional de Ciencias Naturales, Madrid. Total paratypes: 26 exx.

Etymology: The epithet is derived from the Latin adjective *tenebrosum*, dark, gloomy, shrouded in darkness, referring to the dark appearance of this species due to the entirely black coloration that characterizes this taxon.

Description of the holotype: Length (frons to posterior margin of elytra), 9.4 mm. Total length (including abdomen) of preserved holotype, 33 mm. Maximum width, 6.3 mm. Coloration black all over the body and appendages. Tegument finely microreticulated, semi-matt. Head maximum width, 3.5 mm. Surface covered by numerous punctures uniformly distributed. Head punctures small to medium-sized, rounded, shallow and isolated from each other. A longitudinal midline is finely impressed from the upper half of the frons to the vertex. Minimum interorbital distance, 2.1 mm. Clypeus, 1.8 mm wide by 0.6 mm long. Labrum, 1.7 mm wide by 0.6 mm long. Antennomeres widened apically, with short black vestiture, mostly decumbent and with a few sparse setae erect, longer and semi-erect on antennomeres I–II; antennomere I slightly widened apically, subcylindrical (length: 0.4 mm); II short, cylindrical (length: 0.1 mm); III (length: 0.5 mm) subcylindrical, slightly widened apically, rectangular; IV (length: 0.5 mm) similar to III, subrectangular; V (length: 0.5 mm) trapezoidal, wider than VI, with a wide and rounded apical tooth on the inner edge; VI (length: 0.4 mm) trapezoidal, with an apical tooth on the inner edge; VII (length: 0.4 mm) trapezoidal, wider than VI, with an expanded apical tooth on the inner edge; VIII (length: 0.4 mm) trapezoidal, narrower than VII, weakly dentate on its outer edge of apex; IX (length: 0.4 mm) trapezoidal, wider than VIII, markedly dentate on inner edge; X (length: 0.3 mm) trapezoidal, apical tooth slightly acute; XI (length: 0.4 mm) subconical, slender, notched on apex. Pronotum subquadrate with subparallel sides, narrower posteriorly (anterior edge of pronotum: 3.1 mm; basal edge of pronotum: 2.6; pronotum length on sagittal plane: 2.2 mm); anterior margin curved, posterior margin slightly arcuate; fore angles expanded, obtusely pointed; with an impressed longitudinal midline and marked but diffuse lateral depressions. Pronotum surface heterogeneously punctate; punctures of various sizes, sparse, mostly medium and small, circular, well separated from each other, not confluent; medium sized punctures deep, located on the lateral borders and along midline. Dorsal surface of pronotum almost glabrous, with an isolated small seta in each puncture; anterior margin, adjacent to the neck, with numerous moderately long setae. Elytra length, 4.9 mm; tegument glabrous, slightly wrinkled longitudinally with impressed irregular vermicular lines, with scarce, weakly marked, dispersed punctures. Abdomen entirely black, without red stripes on the terga. Last ventrite notched. Metafemur shorter than metatibia (metafemur length: 3.3 mm; metatibia length: 3.4 mm). Metatarsal tarsomeres length, from inner to apical: 1.7, 0.8, 0.7, 0.9 mm. Genitalia with tegmen (see Fig. 25C–F) brownish; moderately elongated, slender both on dorsal and lateral views. Phallobase longer than wide, length similar to the parameres; wider on dorsal view; maximum width in the middle part. Parameres longer than wide, basally cylindrical; distal third formed by parameral lobes; scarce setae present on mid-dorsal region. Parameral lobes relatively long and narrow, separated by a longitudinal notch that extends to the middle of the dorsal surface of the parameres; apexes rounded. Median lobe long, robust, flattened, with rounded apex in lateral view and two acute ventral hooks, close to each other and separated from apex. Endophallic hook visible.

Female: Similar to male, but with the last abdominal ventrite rounded, not emarginated in its posterior margin, and less dentate antennomeres. Studied specimens present the inner surface of the bursa copulatrix without sclerotized spicules or plates (similar to those of *B. indalo*, as figured in Fig. 8B).

Downloaded from https://academic.oup.com/zoolinnean/article-abstract/189/4/1249/5714599 by 81263633 user on 05 August 2020

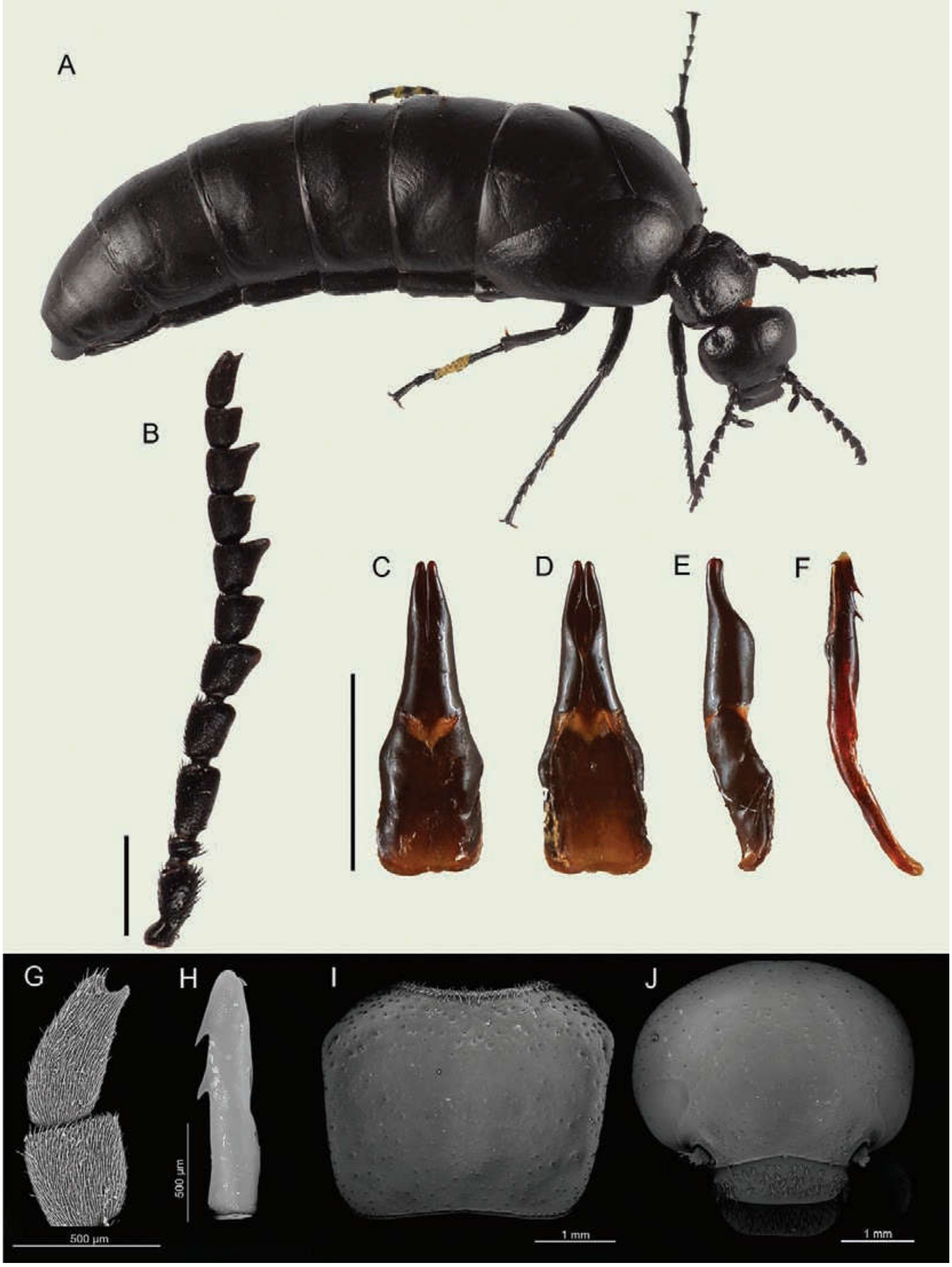

Figure 25. Habitus and morphological details of *Berberomeloe tenebrosus* from Sierra Nevada, Granada (A) and Calar Alto, Almería (B–J). A, dorsal view of a male; B, male antenna; C, D, E, dorsal, ventral, lateral view of male genitalia, showing parameres and phallobase; F, lateral view of aedeagus; G, SEM micrographs of the two last antennomeres; H, SEM micrographs of distal part of aedeagus; note the rounded shape of the apex; I, SEM micrographs of pronotum, dorsal view; J, SEM micrographs of head, frontal view.

Variability: Body length variable (frons to posterior edge of elytra), 12–16 mm; maximum total length among preserved, studied specimens, 42 mm. Morphometric variability is shown in Table 2. The density and distribution of the head and pronotum punctures show weak individual variability.

Downloaded from https://academic.oup.com/zoolinnean/article-abstract/189/4/1249/5714599 by 81263633 user on 05 August 2020

Diagnosis: Berberomeloe tenebrosus can be distinguished from all other species of *Berberomeloe* by the following combination of characters (Fig. 25): (1) entirely black head and abdomen; (2) punctures on the head small to medium-sized, rounded, shallow and mostly isolated from each other; (3) pronotum surface heterogeneously punctate; with medium-sized punctures, deep and located on the sides and along the midline area; disc region smooth or finely impressed; (4) fore angles of pronotum moderately expanded; (5) apex of the median lobe rounded; (6) male antennomere XI slender; and (7) male antennomeres VII and IX markedly expanded on the inner apical side.

Distribution and notes on natural history: Berberomeloe tenebrosus is found in Sierra Nevada and Sierra de Los Filabres mountain ranges (provinces of Almería and Granada) (Fig. 2), within an elevation range from 1250 m (0.6 km west of Ferreira) to 3000 m (surroundings of Pico Veleta), mostly at supra- and oro-Mediterranean bioclimatic levels, and locally at meso- and crioro-Mediterranean levels, with subhumid to humid ombrotypes (see: Rivas-Martínez, 1987; Molero-Mesa *et al.*, 1992; Valle, 2003; Valle *et al.*, 2004).

In Sierra Nevada, *B. tenebrosus* generally inhabits montane open fields such as alpine meadows, open high mountain scrubland and stony soils, dominated by formations of *Genista versicolor* Boiss. ex Steud. (Fig. 26) and, at higher elevation, by formations of *Juniperus communis* L., mainly on siliceous substrate (González-Megías *et al.*, 2004; Ruiz & García-París, 2013, as 'betic group' of *B. majalis*). It can be found also at forest edges, composed mostly of *Pinus sylvestris*, *Quercus pyrenaica* and *Q. rotundifolia* (see: Valle, 2003; Ruiz & García-París, 2013). In the foothills of the northern slopes of Sierra Nevada, at 1250 m, it has been found in almond (*Prunus dulcis*) fields (pers. obs.). In Sierra de los Filabres (Almería), it is also found in open grasslands with *Genista versicolor* formations, and on *P. sylvestris* and *Q. rotundifolia* forest edges (Peñas *et al.*, 1995).

It has been found feeding on *Genista versicolor* flowers, although it is probably polyphagous, like most members of the genus (Bologna, 1991). Adults are found from April to August (Ruiz & García-París, 2013).

COMPARATIVE MORPHOLOGY OF SPECIES OF *BERBEROMELOE*

The clade formed by *B. insignis* and *B. tenebrosus* differs from all the taxa of the *B. majalis* species group in the absence of coloured, transverse tergal bars, the morphology of antennomeres, with slenderer male antennomere XI, and, in general, with much stronger apical teeth in male antennomeres. *Berberomeloe insignis* can be distinguished from *B. tenebrosus* and the other congeneric species, among other traits, by the presence of symmetrical red blotches on the temples of the head. *Berberomeloe tenebrosus* and *B. insignis* differ from *B. castuo*, *B. comunero*, *B. yebli*, *B. laevigatus*, *B. maculifrons*, *B. majalis* and *B. payoyo* in the clearly expanded fore angles of the pronotum, comparatively more elongated than in the other species, in the pronotum puncturation and in the slenderer distal region of the median lobe of the male genitalia.

Within the *B. majalis* species group, the conspicuously narrow, coloured tergal bars represent, by itself, a diagnostic character to differentiate *B. castuo* and *B. payoyo* from all other species, whereas pronotum puncturation differentiate *B. castuo*, *B. comunero* and *B. yebli*, with usually deeply marked punctures, from *B. majalis*, *B. payoyo*, *B. indalo* and *B. maculifrons* (except Middle Atlas populations), usually presenting subtler marked punctures. The shape of the distal part of male genitalia median lobe is truncated in most of the *B. majalis* species group except in *B. yebli*, in which it is rounded. The puncturation of elytra could represent a diagnostic trait to differentiate *B. laevigatus* from the other congeneric species.

Additional morphological traits to identify each species are presented in the following key:

KEY TO ADULT *BERBEROMELOE* SPECIES (*B. LAEVIGATUS* NOT INCLUDED)

Berberomeloe laevigatus is excluded from the key. We have not been able to study its type material and an exhaustive morphological study, with larger sample size, is necessary to identify unequivocally the morphological diagnostic traits of this species (see *B. laevigatus* account above).

1. Last antennomere (XI) markedly narrowed from the middle towards the apex (more obvious in males) with converging sides (Figs 23G, 25B, G), about half as wide as antennomere X at the apex; VII and IX strongly toothed (Figs 23, 25G). Abdomen always entirely black. Male genitalia with median lobe clearly narrowed in its distal region (Figs 23D, F, 25F, H). Exclusively south-eastern Iberian Peninsula 2

\- Last antennomere (XI) not or barely narrowed towards the apex (narrower in males), with subparallel sides; VII and IX weakly or moderately toothed (Fig. 6B, H). Abdomen usually with red or orange transverse stripes (except specimens of some localized populations, which present the abdomen entirely black). Male genitalia with median lobe obliquely truncated and wide (Fig. 8G) or rounded and narrowed (Fig. 21G) at the apex (depending on the species). All Iberian Peninsula and north-western Africa 3

Downloaded from https://academic.oup.com/zoolinnean/article-abstract/189/4/1249/5714599 by 81263633 user on 05 August 2020

2. Head always with red temples; an additional red spot on the frons is present in some populations (Figs 23E, 24A, B). Pronotum longer, with well-marked, sharp fore angles (Fig. 23H)................................... *B. insignis*
- Black head, always without any trace of red blotches (Figs 25A, 26E, F). Pronotum shorter, strongly transverse, with rounded fore angles (Fig. 25I) .... *B. tenebrosus*
3. North African species..4
- Iberian species 5
4. Puncturation of head and pronotum dense, with thick and deep punctures that form a confluent or subconfluent pattern of rugose appearance (Fig. 21H). Male genitalia with parameral lobes of tegmen long and narrow in lateral view; distal region of median lobe relatively narrowed towards the apex (Fig. 21G). North-western Morocco (central and western Rif and adjacent areas)... *B. yebli*
- Puncturation of head and pronotum usually scattered, sparse, especially on pronotal disc, not rugose neither subconfluent, formed by small and medium-sized shallow punctures, (Fig. 19G, H) (populations from Middle Atlas have denser and deeper punctures, but always in lower density than in *B. yebli*). Male genitalia with parameral lobes of tegmen shorter and wider in lateral view; distal region of median lobe obliquely truncated, not markedly narrowed, towards the apex (Fig. 19F). Eastern and central Morocco, western and central Algeria... *B. maculifrons*
5. Pronotal puncturation dense, formed mostly by thick and deep punctures and by others about half thick but also deep and more scarce, usually forming a corrugated or rugose pattern; medium longitudinal groove of pronotum deep and clearcut (Fig. 11H)... *B. comunero*
- Pronotal puncturation dense or scarce, but never rugose or corrugated; medium longitudinal groove of pronotum shallow and inconspicuous, often absent...6
6. Posterior edge of abdominal tergites I–VI usually with a narrow red or orange bar (ratio ‘total width of the second tergite/width of the transverse bar of the second tergite’ in *B. castuo* between 1.68 and 2.5, average = 2.1, SD = 0.23; in *B. payoyo* between 1.85 and 2.45, average = 2.11, SD = 0.17), except specimens at some localized populations from southern Portugal and Cadiz Province (Spain), that are entirely black (Figs 9A, 17A). Sides of the pronotum subparallel and fore angles barely expanded, widely rounded (Figs 9H, 17H). Tegmen (male genitalia) with parameral lobes wide, broadly rounded at apex (Fig. 9G). Western Iberian Peninsula, Cadiz Province and western Betic Mountains (Sierra de Grazalema, Serranía de Ronda, Sierra de Las Nieves, and Sierra Tejeda)...7
- Posterior edge of abdominal tergites usually with a wide red bar (ratio ‘total width of the second tergite/width of the transverse bar of the second tergite’ in *B. majalis* between 1.04 and 2.03, average = 1.6, SD = 0.27; in *B. indalo* between 1.09 and 1.35, average = 1.18, SD = 0.07), except in some localized populations of *B. majalis* from the province of Ciudad Real, where individuals have the abdominal tergites entirely black) (Fig. 6A). Sides of the pronotum convergent towards back and fore angles marked and sharp (*B. indalo*, Fig. 13H) or sides of the pronotum subparallel and fore angles closely rounded (*B. majalis*, Fig. 6I). Tegmen (male genitalia) with parameral lobes relatively narrow (Fig. 6E). Eastern and central Iberian Peninsula.8
7. Pronotum surface rather convex (in lateral view), with abundant and deep punctures; disc clearly punctured (Fig. 9H). Western Iberian Peninsula (north of Guadalquivir river basin)...................................... *B. castuo*
- Pronotum surface almost flat (in lateral view), finely and sparsely punctate; disc almost smooth (Fig. 17H). Cádiz province and western Betic Mountain Range (south of Guadalquivir river basin)................. *B. payoyo*
8. Male antennomeres IV and V subparallel, poorly dentate, swelled and with a singular yellowish depressed sensitive area at their inner border; antennomeres VI–IX relatively similar in shape and feebly serrated (Fig. 13B). Fore angles of pronotum prominent, obtusely pointed (Fig. 13H); pronotal puncturation partly dense, heterogeneously arranged (denser towards the sides, disc almost smooth). Red bars of the abdominal tergites usually wide (ratio ‘total width of the second tergite/width of the transverse bar of the second tergite’ between 1.09 and 1.35, average = 1.18, SD = 0.07). Median lobe of male genitalia robust, broad at apex (Fig. 13F). Eastern of Almería province .... *B. indalo*
- Male antennomere IV subparallel and V dentate, not specially swollen and lacking a depressed sensitive area at their inner border; antennomeres VI–IX more serrated (Fig. 6B). Fore angles of pronotum obtuse, closely rounded (Fig. 6I); pronotum surface formed by relatively dense but isolated punctures, homogeneously arranged (disc always punctate). Red bars of the abdominal tergites with a ratio ‘total width of the second tergite/width of the transverse bar of the second tergite’ between 1.04 and 2.03, average = 1.6, SD = 0.27. Median lobe of male genitalia slender, not especially widened to the apex (Fig. 6F, G). Central and eastern Iberian Peninsula.. *B. majalis*

Downloaded from https://academic.oup.com/zoolinnean/article-abstract/189/4/1249/5714599 by 81263633 user on 05 August 2020

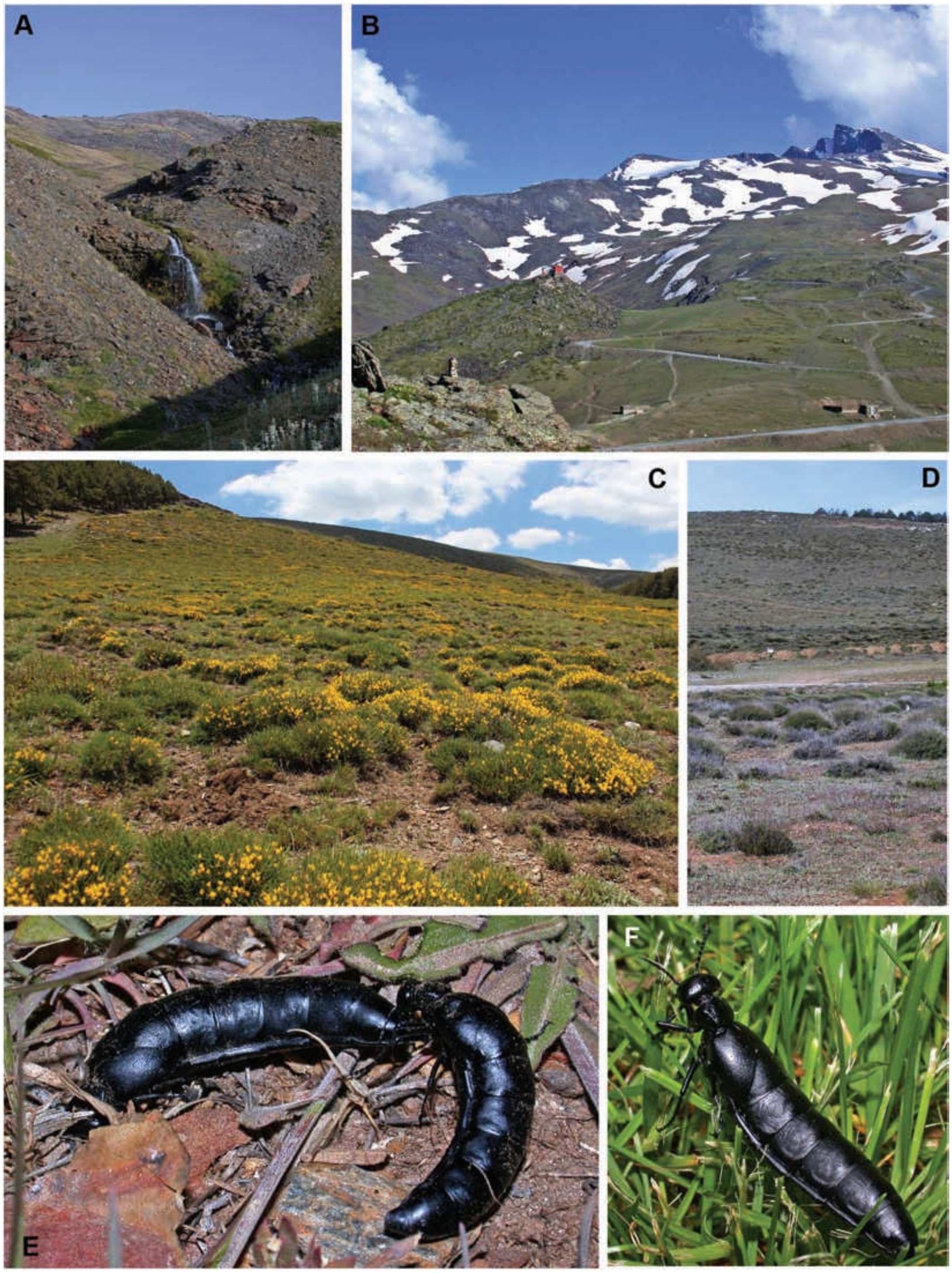

Figure 26. A–D, habitat of *Berberomeloe tenebrosus*, Spain: A, Río San Juan, Borreguiles, Sierra Nevada, Granada; B, El Veleta, view from Peñones de San Francisco, Sierra Nevada, Granada; C, Puerto de la Ragua, Sierra Nevada, Granada; D, Puerto de Escúllar, Sierra de Baza, close to Sierra de los Filabres, Granada. E, courtship of *B. tenebrosus* from Puerto de la Ragua, Almería. F, specimen of *B. tenebrosus* from Calar Alto, Sierra de los Filabres, Almería.

Downloaded from https://academic.oup.com/zoolinnean/article-abstract/189/4/1249/5714599 by 81263633 user on 05 August 2020

DISCUSSION

BIOGEOGRAPHY AND EVOLUTIONARY HISTORY OF THE GENUS *BERBEROMELOE*

Our results show that within the Iberian Peninsula and Northern Africa, no contemporaneous geographical barriers account for the divergence and distribution boundaries found across taxa in the *Berberomeloe majalis* species group. Traditionally considered geographical barriers to explain processes of vicariance and long-term geographic isolation, including Iberian and North African mountain systems, river basins, and the Gibraltar strait marine barrier, are older than our time estimates for the divergence between species of *Berberomeloe* (Vergés & Fernàndez, 2006; Mas-Peinado *et al*., 2018). Diversification within the *B. majalis* species group started in the Plio–Pleistocene transition, but according to our data, most speciation events occurred during the Early Pleistocene. This geological period is characterized by a succession of glacial and interglacial cycles (Hewitt, 1996), probably leading to the current allopatric or parapatric distribution patterns. Geographic isolation would have been favoured by changes in ecological suitability of large parts of the Iberian Peninsula during glacial maxima (Gómez & Lunt, 2007), including the formation of barriers impermeable to dispersal along ice-covered mountain systems (Hewitt, 1996). Isolation of populations induced by glacial maxima may have occurred recurrently along the Pleistocene, but the duration of each of these events must have been relatively sort, allowing for the formation of secondary contact areas during interglacial periods (Waters *et al*., 2013). In this context, speciation should benefit from rapid evolution of reproductive isolation among allopatrically initiated lineages (Carstens & Knowles, 2007).

The effects of Pleistocene glaciations in speciation processes and diversity patterns has long been a subject of interest for evolutionary biologists (Taberlet *et al*., 1998; Brown & Diesmos, 2002; Hewitt, 2004; Schmitt, 2007; Esselstyn *et al*., 2009; Rull, 2015). Currently, there is no doubt that Quaternary glacial cycles have been a most important factor in shaping patterns of both inter- and intraspecific diversity (e.g. Hewitt 1996, 1999, 2000; Avise, 2000; Cardoso & Vogler, 2015; Gómez & Lunt, 2007; Recuero & García-París, 2011). However, their role in promoting speciation has been debated, from those that considered them as a major speciation force (Rand, 1948; Johnson & Cicero, 2004), to others arguing that species differentiation mostly predated Pleistocene times and that Quaternary glaciations did not trigger speciation processes and were at most responsible for modelling intraspecific diversity (Klicka & Zink, 1997; Zink *et al*., 2004). Current evidence shows abundant examples of both scenarios from diverse groups and regions (Avise *et al*., 1998; Hewitt, 2000). Among western Mediterranean Basin Coleoptera, there are groups, such as *Pimelia* Fabricius, 1775 (Tenebrionidae), with dominating pre-Pleistocene species differentiation (Mas-Peinado *et al*., 2018), and others, such as Iberian Dytiscidae, with most species having originated allopatrically in Pleistocene glacial refugia (Ribera & Vogler, 2004). Our results agree better with those shown by species of Dytiscidae, pointing to the existence of multiple general patterns of speciation linked to Pleistocene glacial cycles among different taxonomic groups.

Currently, several *Berberomeloe* species present parapatric distribution patterns and consequently, there are areas of potentially overlapping distributions (Fig. 2). In this sense, different regions within the Iberian Peninsula are of particular interest to study the processes involved in the maintenance of species boundaries (e.g. exclusive competition, assortative mating, demographic processes, pre- and post-zygotic reproductive barriers) (Butlin & Smadja, 2018): southern Sierra Nevada slopes, where *B. insignis* and *B. tenebrosus* occur, the south-eastern Mediterranean coast in Almeria, that presents sympatric populations of *B. insignis* and *B. indalo*, the area between Extremadura and Castilla la Mancha, where *B. majalis* and *B. castuo* are likely in contact, and similarly in southern Madrid, where the ranges of *B. majalis* and *B. comunero* are intermixed. Future research should focus on these contact zones and potential hybrid populations to characterize the evolutionary processes promoting the strong cohesion between morphological and genetic characters maintained through the Quaternary.

The two African species of *Berberomeloe* clearly belong to the *B. majalis* species group, although our phylogenetic analyses could not resolve if they form a monophyletic group. According to our results, they should have one or two common ancestors in the Iberian Peninsula, and arrived in Northern Africa through a single or two independent dispersal events. In any case, colonization seems to have occurred after the formation of one of the main western Mediterranean geographical barriers: the Gibraltar Strait (Mas-Peinado *et al*., 2018). Overseas dispersal between Africa and Europe has been invoked to explain the existence of related lineages on both sides of the Gibraltar Strait, even in poorly dispersing organisms, such as amphibians (Gutiérrez-Rodríguez *et al*., 2017). However, recent research seems to confirm the past existence of a more or less continuous land bridge from south-eastern Iberia to the eastern Rif, formed by a volcanic arch that was fully formed by the end of the Miocene, about 6.2–5.3 Mya (Booth-Rea *et al*., 2018). From this time, the land bridge must have started to open, but the existence of large

Downloaded from https://academic.oup.com/zoolinnean/article-abstract/189/4/1249/5714599 by 81263633 user on 05 August 2020

islands in the Alboran Sea through the Pliocene and until the early Pleistocene (Booth-Rea *et al.*, 2018), together with the complex tectonic and sedimentary dynamics in the area (Martínez-García *et al.*, 2013), may have facilitated a dispersal route between the two continents for *Berberomeloe* and other terrestrial, non-flying organisms.

PATTERNS OF MORPHOLOGICAL DIVERSIFICATION

Morphometric analyses within the *B. majalis* species complex show uneven differentiation levels across taxa. There is a gross overlap in morphometric space between most of the species. *Berberomeloe indalo* and *B. payoyo*, two closely related, allopatric species along the Mediterranean coast show independent morphometric spaces with no overlap between them. Although allopatric, closely related taxa are generally difficult to separate on the basis of morphometric traits (Dayan & Simberloff, 2005; Darwell & Cook, 2017; Moritz *et al.*, 2017), *B. indalo* and *B. payoyo* show both deep qualitative and quantitative morphological differences. This unexpected pattern could be driven by processes triggered by the co-occurrence of *B. indalo* with *B. insignis*. However, we could not find evidence linking differentiated morphological traits to the ecology of *B. insignis* or *B. indalo*. Fine-scale studies (integrating data on their biology and ecology) are needed to infer if morphometric differences found between *B. indalo* and *B. payoyo* are related to ecological evolutionary processes or are just the result of locally triggered, random processes.

The discovery of *B. tenebrosus* as sister to *B. insignis*, supports the existence of deep phylogenetic diversification associated with evident, but limited, morphological change. *Berberomeloe tenebrosus* was previously included in *B. majalis*, because their distinctive morphological traits were once considered phenotypic variability across a widely distributed species (García-París, 1998; García-París *et al.*, 2003; Ruiz & García-París, 2013).

Berberomeloe tenebrosus inhabits the high elevation areas of the Sierra Nevada and Sierra de los Filabres where no other *Berberomeloe* species occur, but populations of the lowland *B. insignis* often present strict sympatry with *B. indalo* (García-París *et al.*, 1999, 2003) suggesting that past interactions with congeneric species could have promoted the marked morphological differentiation of *B. insignis* vs *B. tenebrosus*. This pattern is concordant with the hypothesis of sympatry as a driver of morphological differentiation (Moritz *et al.*, 2017). Divergence in ecological niches might facilitate establishing sympatric populations of closely related species, which eventually could result in morphological differentiation between sympatric taxa, even in species complexes characterized by morphological stasis (Vodă *et al.*, 2015; Darwell & Cook, 2017; Moritz *et al.*, 2017). There is no evidence of ecological niche differentiation between imaginal stadium in sympatric *B. insignis* and *B. indalo*; larval biology is still largely unknown in these species, but larval morphological differentiation is also larger between *B. insignis* and the *B. majalis* complex than among the species of the *B. majalis* complex (Settanni *et al.*, 2009). The most conspicuous morphological traits differentiating adult beetles in sympatric *B. insignis* and *B. indalo* are sexual characters such as the shape of the antennae and genitalia, but also patterns of disruptive coloration in the head and abdomen, which could have facilitated assortative mating in initial speciation stages, as has been shown in groups as different as fishes or butterflies (Puebla *et al.*, 2007; Merrill *et al.*, 2012; Whitney *et al.*, 2018). Morphological differentiation in sympatric *Berberomeloe* could have been more related to reproductive rather than to ecological character displacement, allowing for an early reinforcement of reproductive barriers (Brown & Wilson, 1956; Pfennig, 2009).

Additional incipient speciation processes have been detected within some of the proposed taxa. *Berberomeloe maculifrons* presents two geographically separated morphotypes: a Middle Atlas form, characterized by deeper puncturation of the pronotum, and an eastern form that ranges east of the Moulouya river (eastern Morocco) to western Algeria, characterized by having finer pronotal punctures. Similarly, within *B. castuo*, two morphotypes differing in the width of the tergal bars have been found, separated by the Sistema Central Mountains. These two instances of intraclade morphological differentiation are coupled with some degree of phylogeographic structure, indicating the existence of recent processes of differentiation. However, more detailed studies, using additional molecular markers, are needed to analyse these processes.

Patterns of abdominal coloration show extensive intraclade variation in the *Berberomeloe majalis* species group. The presence of populations composed of entirely black specimens next to populations formed only of barred specimens supports the hypothesis that relaxation of selective pressures (that previously maintained the disruptive coloration) is allowing the rapid evolution of black phenotypes in different geographic areas and within different species or lineages of the *B. majalis* species group (Bravo *et al.*, 2017). These authors found populations of *B. majalis* and *B. comunero* consisting entirely of black-coloured specimens (without transverse red bars) locally isolated among otherwise red-barred populations. We additionally find populations entirely composed of black specimens within *B. castuo* (covering a large

Downloaded from https://academic.oup.com/zoolinnean/article-abstract/189/4/1249/5714599 by 81263633 user on 05 August 2020

area in southern Portugal and south-western Spain), within *B. payoyo* (in a localized population in the province of Cádiz) and within *B. laevigatus* (in a small area in the province of Huesca). These results confirm that the origin of black phenotypes in the *B. majalis* species complex is a recent phenomenon and as Bravo *et al.* (2017) stated, the presence of coloured bars is the ancestral state for the complex. On the other hand, the discovery of the completely black *B. tenebrosus* within the *B. insignis* species group, suggests that the ancestral abdominal pattern of this species group was entirely black. As mentioned above, the evolution of red blotches on the head of *B. insignis* could be more related to intraspecific recognition and assortative mating than to disruptive coloration patterns as the tergal bands in the *B. majalis* complex. However, the true function of these traits remains to be tested. The ancestral coloration pattern of the abdominal terga for the genus is not clear; red-barred in *B. majalis* group, black in *B. insignis* group, but in any case, the existence of multiple independent events of loss/gain of disruptive coloration (both in abdominal tergal plates and in the head) are evident along the cladogenetic history of the genus (Bravo *et al.*, 2017).

Qualitative traits seem to be the most informative source for taxonomy in *Berberomeloe*. The use of phenotype-based traits to diagnose species is a relatively general trend among aposematic taxa (Brower, 1996; Brown *et al.*, 2011; Posso-Terranova & Andrés, 2018). Geographic variability of qualitative morphological traits is structured in markedly similar patterns to the geographic structure of mitochondrial lineages, and in consequence, concordance between mitochondrial and qualitative-trait defined units allows the existence of cryptic species in *Berberomeloe* (*sensu* Kress *et al.*, 2015) to be rejected. A large part of the underestimation of real diversity (Struck *et al.*, 2018) comes from morphologically undifferentiated taxa (i.e. cryptic species), but sometimes underestimation is rather a consequence of lack of adequate examination of character variation (Ortuño & Arribas, 2018; Rodríguez-Flores *et al.*, 2018), as it is also evident here for *Berberomeloe*.

SYSTEMATICS AND TAXONOMY OF THE GENUS *BERBEROMELOE*

Berberomeloe encompasses some of the largest and most conspicuous species of Coleoptera of the Western Palaearctic (Bologna, 1989; García-París, 1998; García-París & Ruiz, 2008, 2011a; Percino-Daniel *et al.*, 2013; García-París *et al.*, 2016), but despite their remarkable appearance, our results reveal the existence of unexpected multiple geographically structured and morphologically well-differentiated evolutionary lineages within it, indicating a gross underestimation of *Berberomeloe* diversity as reflected in its traditional taxonomic composition.

Berberomeloe is not formed of only two reciprocally monophyletic species (García-París, 1998). *Berberomeloe tenebrosus*, formerly included within *B. majalis* (Sierra Nevada population; García-París *et al.*, 2003; Ruiz & García-París, 2013), is phylogenetically closer to *B. insignis* than to any of the taxa in the *B. majalis* species group. This result, which is concordant with the morphometric analysis based on larval traits (Settanni *et al.*, 2009), is highly supported by molecular phylogenetic analyses, rendering the traditional concept of *B. majalis* paraphyletic. Additionally, there are multiple morphologically distinguishable mitochondrial lineages, that can be considered independent species using the evolutionary species concept (Wiley, 1978; Wiley & Mayden, 2000) within an integrative taxonomy framework (Padial *et al.*, 2010).

It is remarkable that the species diversity of one of the largest Coleoptera in the western Mediterranean Region has gone unnoticed and eluded the attention of taxonomists for almost 130 years. Our results match several previous studies that have revealed a taxonomic underestimation of the actual diversity in well-prospected regions, such as the western Mediterranean (Ibáñez *et al.*, 2006; Stöck *et al.*, 2008; Kaliontzopoulou *et al.*, 2011; Fitze *et al.*, 2012; Recuero *et al.*, 2012). This underestimation of diversity highlights the Linnean shortfall (Brito, 2010), i.e. the lack of taxonomic knowledge as one of the main problems to resolve before conservation plans can be developed and implemented. In this sense, the split of a formerly widespread species as *B. majalis* into multiple species, some of them with highly restricted geographical ranges, such as *B. indalo*, *B. yebli*, *B. payoyo* and *B. tenebrosus*, undoubtedly will present serious challenges for conservation. For example, the narrow coastal–subcoastal range of *B. indalo* in Almería province is severely affected by high intensification of greenhouse agriculture (Fig. 15A) and urbanization pressures, probably making of *B. indalo* one of the most threatened species of European Coleoptera.

Despite the noticeable increase of *Berberomeloe* species diversity presented in this paper, there are still large understudied areas, including the eastern Iberian Mediterranean coast, the Iberian north-east (north of the Ebro River), the Guadalquivir river basin, the High Atlas and Atlantic coast of Morocco and the easternmost North African populations from central Algeria to western Tunisia. Previous studies concerning other organisms have shown that marked phylogeographic structure, including old lineages that might represent candidate species, often occur in these regions (Stöck *et al.*, 2008; Recuero *et al.*, 2012; Díaz-Rodriguez *et al.*, 2017; Gonçalves *et al.*, 2015).

Downloaded from https://academic.oup.com/zoolinnean/article-abstract/189/4/1249/5714599 by 81263633 user on 05 August 2020

CONSERVATION CONSIDERATIONS

Several regions in the distribution range of *Berberomeloe* suffer from habitat destruction and alteration, due to excessive urban development (García-París *et al.*, 2006) and degradation driven by human-mediated activities, especially through the replacement of traditional cultivation systems by more extensive and intensive farming. The increase of the use of herbicides and other phytosanitary products on cultivated fields and along road edges, strongly affect insect communities (Nash, 1976; van Swaay & Warren, 1999; Stoate *et al.*, 2001; Stefanescu *et al.*, 2004; Tamayo Muñoz *et al.* 2015; Rodríguez-Flores *et al.*, 2017). These threats are responsible for population declines of *Berberomeloe* in Madrid province (García-París *et al.*, 2006; as *B. majalis*), where *B. comunero* and, more locally, *B. majalis*, occur. These authors reported local extinctions of *B. comunero* around the city of Madrid (Aluche, Hortaleza, Canal, Vicálvaro, Santa Eugenia and Rivas de Jarama). Decline of bees (Apoidea), larvae of which *Berberomeloe* parasitize (e.g. Cros, 1912; Bologna, 1989, 1991; García-París, 1998; García-París & Ruiz, 2008, 2011a), has been suggested as the main factor in the decline of other Meloidae species of the genus *Meloe* Linnaeus, 1758 (e.g. Whitehead, 1991; Ruiz & García-París, 2008; García-París & Ruiz, 2011b). Additional threats have been detected in protected natural areas over the central area of its distribution in Castilla–La Mancha wetlands (Rodríguez-Flores *et al.*, 2016), where large populations of *B. majalis* have still been recorded. A particular threat is the increase in recent years of non-sustainable use of trails and dirt roads by sport practices such as 4×4 and quad vehicles racing. These vehicles are faster than agricultural vehicles, causing different impacts on the coleopteran fauna (Rodríguez-Flores *et al.*, 2016) and particularly on *B. majalis* populations by (1) direct killing of adults and egg clutches, (2) habitat alteration accelerating erosion and (3) direct impact on the wild bee communities (needed to complete the biological cycle of *Berberomeloe*) because they nest on the ground. Likewise, high roadkill rates have been observed on highways (García-París *et al.*, 2006), and it could become a major threat for *Berberomeloe* populations, as has already been reported in other insects (Tamayo Muñoz *et al.*, 2015).

Recent samplings for this study failed to find specimens in large areas of olive tree plantations in western Andalucía (Córdoba and Sevilla provinces), where the authors found *Berberomeloe* to be abundant two decades ago (pers. obs.). Changes in the cultivation procedures for olive trees, including watering and subsequent phytosanitary treatments, might be held responsible for *Berberomeloe* decline. However, across western Iberia, there are well-conserved populations of *Berberomeloe* in an anthropic landscape formation known as 'dehesas' (agrosylvo-pastoral system and cultural landscape mainly from the southern to central Iberian Peninsula, usually composed of *Quercus suber* and/or *Q. rotundifolia* dispersed on herbaceous pastureland; see e.g. Valladares *et al.*, 2004; Roig & San Miguel, 2013) (Fig. 10). These landscape systems are generally managed for livestock farming. Extremadura is the region with the most dehesa systems, with more than a million hectares (e.g. Olea & San Miguel, 2006; Díaz & Pulido, 2009). Conserving this biodiverse landscape system is essential for preserving healthy populations of *B. castuo* in Portugal, Extremadura, western Castilla y León and Huelva.

The other Iberian species, *B. indalo*, *B. payoyo*, *B. insignis* and *B. tenebrosus*, and the North African *B. yebli* and *B. maculifrons* deserve special conservation measures:

Berberomeloe indalo is the most narrowly distributed species in the *B. majalis* species group. Its restricted area of occupancy constitutes a threat factor, particularly because this area is highly affected by intensive agricultural practices, causing loss and degradation of suitable habitats for the species, especially in coastal regions (see: Mota *et al.*, 1996) (Fig. 15A). This province has a surface area of more than 30 000 ha used for horticultural production under greenhouses (Valera *et al.*, 2017) and, located mainly at 'Campo de Dalías', includes an area with intensive greenhouse cultivation of crops (Aznar-Sánchez & Galdeano-Gómez, 2011). These greenhouses occupy mostly lowland areas, which have expanded continuously during the last decades (Aznar-Sánchez *et al.*, 2011). Protected natural areas in the distribution range of *B. indalo* are: Paraje Natural Desierto de Tabernas (11 625 ha), Paraje Natural Sierra Alamilla (8500 ha), Paraje Natural Karst en yesos de Sorbas (2375 ha) and Parque Natural Cabo de Gata-Níjar (49 512 ha) (www.andalucia.org).

The range of *B. payoyo* is confined to a restricted area along the southern Spanish provinces of Cádiz and western Granada, including several extensive protected areas (Parque Natural Los Alcornocales and Parque Natural de la Sierra de Grazalema, among others). Population declines have recently been reported from the province of Cádiz (Cortés-Fossati, 2018b; sub *B. majalis*), mostly attributed to habitat destruction, use of phytosanitary products and changes in landuse. Also, as reported by Cortés-Fossati (2018b), development of new paved roads represents an additional factor that directly (by road kills) or indirectly (by isolation from nearest conspecific subpopulations) affects the suburban populations of *B. payoyo* in Cádiz.

There are no data on demographic trends of any population of the North African species *B. yebli* and *B. maculifrons*. It is highly likely that factors affecting

Downloaded from https://academic.oup.com/zoolinnean/article-abstract/189/4/1249/5714599 by 81263633 user on 05 August 2020

congeneric populations in the Iberian Peninsula would affect both North African endemics. The expansion of monocultures and intensive farming around Fez and adjacent areas could affect the viability of populations of *B. maculifrons*. Similarly, a particular threat for *B. yebli* in the Rif mountains, connected with destruction and fragmentation of habitat (Fig. 15B), comes from aggressive and rapid expansion and intensification of hemp plantations (Labrousse & Romero, 2001), resulting in deforestation (Gatchui *et al.*, 2014) and desiccation of wetlands and aquifers (Velo-Antón *et al.*, 2015). The degradation and loss of suitable habitats due to the increase of urbanization in littoral and subcoastal areas of the eastern Mediterranean coast of Morocco (e.g. regions of Saidia and the mouth of the Moulouya river), and aggressive agriculture development (with indiscriminate use of pesticides and herbicides) in subcoastal plains, constitute important threats for several populations of *B. maculifrons*. In other areas of the range of both species, we have not identified particular threats to the species survival. *Berberomeloe maculifrons* seems to occur frequently and with relatively large populations (e.g. central Middle Atlas, foothills of north-eastern Middle Atlas, Rekkan plateau, pers. obs.). Thus, in most of its range, this species does not seem to show significant conservation problems.

Berberomeloe insignis is listed as 'vulnerable' at a national level (García-París & Ruiz, 2011a) and in the Red Book of invertebrates of Andalucía (García-París & Ruiz, 2008). Within the coastal and subcoastal distribution range of *B. insignis*, there are only two protected natural areas: Parque Natural Cabo de Gata-Níjar (45 663 ha) and Reserva Natural Punta Entinas-Sabinar (1960 ha) (www.andalucia.org). Farming and urban expansion are forcing the isolation of these protected natural areas (García-París & Ruiz, 2008, 2011a). Coastal areas occupied by *B. insignis* are highly vulnerable, because these regions have been severely affected by rapid habitat destruction and degradation through the expansion of intensive farming and urban and touristic developments (Mota *et al.*, 1996; García-París & Ruiz, 2008, 2011a; Ruiz & García-París, 2013). Lack of recent records for many populations along the coastline and its surroundings suggest a drastic population decline and several local extinctions (García-París & Ruiz, 2011a). Inland populations of *B. insignis* are less subject to anthropic pressures (García-París & Ruiz, 2008, 2011a). Within this region, a number of populations are located in protected natural areas, such as the Paraje Natural del Desierto de Tabernas (11 625 ha), Paraje Natural del Karst en Yesos de Sorbas (2375 ha) and Paraje Natural de la Sierra Alhamilla (8500 ha) (www.andalucia.org) or are distributed across submontane regions where urban and touristic pressure is smaller. However, no data on populations trends are available. García-París & Ruiz (2008, 2011a) suggest several conservation measures. A large part of the range of *B. tenebrosus* is protected. The Sierra Nevada lies within different environmental protection programmes as a National Park, Natural Park and Biosphere Reserve (Gómez-Ortiz *et al.*, 2013), which cover an extension of 85 883, 86 432 and 172 238 ha, respectively. In Sierra de Los Filabres, the portion within the province of Granada is protected (Parque Natural Sierra de Baza). There are no data on the demographic trends for any population of *B. tenebrosus*. *Berberomeloe tenebrosus* shares its distribution and habitat with another species of Meloidae endemic to Sierra Nevada, *Mylabris (Micrabris) nevadensis* (Escalera, 1915), considered 'vulnerable' in the Red Books of Spanish Invertebrates (Ruiz & García-París, 2011). Habitat alteration due to the development of winter sport facilities could affect the species at a local scale. Other factors causing degradation of the habitat of *B. tenebrosus* populations (similar to those affecting *M. nevadensis*; see Ruiz & García-París, 2011) would be the following: livestock overgrazing, inadequate forestry practices and construction of new touristic and road infrastructure. Global warming may affect this species by reducing its available habitat, already limited to medium-high elevations.

ACKNOWLEDGEMENTS

We dedicate this work to the memory of Marina Alcobendas, who carried out most of the molecular work included in this work. Thanks for help during field work to N. Percino, G. García, G. Velo, I. Martínez-Solano, P. Mas, M. Esteban, J. Gutiérrez, J. E. Uribe, P. C. Rodríguez, J. Esteban, I. Doadrio, D. Escoriza, E. K. López, J. Aznar, A. Hinckley, D. Herrero, L. Arnaldo, C. Sánchez, J. Lobón, A. Aguado, J. P. Miller, R. García, I. Sánchez, M. Cámara, M. García Rollán, J. París, F. A. Montes, F. J. Pérez López, J. I. López-Colón, M. Pola, P. Vicent, A. Calatayud, I. Esteban, A. Navarro, S. Yubero, M. Cámara del Río, R. Ugarte, and A. Velasco. We specially thank P. Chamorro, who kindly provided the drawing figured in this manuscript. We are grateful for the assistance of M. París (Museo Nacional de Ciencias Naturales of Madrid), O. Merkl (Magyar Természettudományi Múzeum of Budapest), P. Barranco (Universidad de Almería), J. Benzal (Estación Experimental de Zonas Áridas, CSIC, Almería) and A. Mantilleri (Muséum National d'Histoire Naturelle of Paris). Thanks to A. Jorge García, M. Furió and L. Tormo who helped us to obtain the micrographs of the scanning electron microscope, to I. Acevedo for his help with some laboratory procedures, and to P. C. Rodríguez for her help with species delimitation analyses. Thanks to A. François (ECWP,

Downloaded from https://academic.oup.com/zoolinnean/article-abstract/189/4/1249/5714599 by 81263633 user on 05 August 2020

Missour, Morocco) for facilitating the study of the ECWP entomological collection. We thank L. Brooks for making available to us the online pictures of the type specimens of *Meloe majalis* held at the Linnean Society of London. We thank the Instituto de Estudios Ceutíes for its support. The visits of MGP to the Magyar Természettudományi Múzeum of Budapest (HU-TAF) and to the Muséum National d'Histoire Naturelle of Paris (FR-TAF) were supported by the European Union SYNTHESYS Project (http://www.synthesys.info/) 'European Community Research Infrastructure Action' within package FP7 'Capacities'. This work has been funded by the Spanish Government project-grant CGL2015-66571-P (Ministerio de Economía y Empresa-Fondo Europeo de Desarrollo Regional) to MGP. The authors declare that there are no conflicts of interest.

REFERENCES

Abdelilah G, **Taiqui L. 2015.** Modélisation de la distribution spatiale des paramètres bioclimatiques dans la Region Tanger-Tetouan (Rif Occidental). *European Scientific Journal* **11:** 1857–7881.

Avise JC. 2000. *Phylogeography. The history and formation of species*. Cambridge: Harvard University Press.

Avise JC, **Walker D**, **Johns GC. 1998.** Speciation durations and Pleistocene effects on vertebrate phylogeography. *Proceedings of the Royal Society of London B: Biological Sciences* **265:** 1707–1712.

Aznar-Sánchez JA, **Galdeano-Gómez E. 2011.** Territory, cluster and competitiveness of the intensive horticulture in Almería (Spain). *The Open Geography Journal* **4:** 103–114.

Aznar-Sánchez JA, **Galdeano-Gómez E**, **Pérez-Mesa JC. 2011.** Intensive horticulture in Almería (Spain): a counterpoint to current European rural policy strategies. *Journal of Agrarian Change* **11:** 241–261.

Baselga A, **Recuero E**, **Parra-Olea G**, **García-París M. 2011.** Phylogenetic patterns in zopherine beetles are related to ecological niche width and dispersal limitation. *Molecular Ecology* **20:** 5060–5073.

Baudi F. 1878. Europaeae et circummediterraneae faunae heteromerum specierum, quae Comes Dejean in suo catalogo, editio 3^{a}, consignavit, ex ejusden collectione in R. Taurinensi Musaeo asservata, cum auctorum hodierne recepta denominatione collatio. Pars sexta. *Deutsche Entomologische Zeitschrift* **22:** 337–376.

Beauregard H. 1890. *Les insectes vésicants*. París: Félix Alcan.

Benabid A. 1982. *Etudes phytoécologique, biogéographique et dinamique des associations et séries sylvatiques du Rif occidental (Maroc)*. Thèse Doct. ès-Sc. Faculté des Sciences et Techniques St. Jerôme. Université de Droit, d'Economie et des Sciences d'Aix-Marseille, 199.

Benabid A. 1984. Etude phytoécologique des peuplements forestiers et préforestiers du Rif centro-occidental (Maroc). *Travaux de l'Institut Scientifique, Rabat, série Botanique* **34:** 164.

Benabid A. 1985. Les écosystèmes forestiers, préforestiers et presteppiques du Maroc: diversité, répartition biogéographique et problèmes posés par leur aménagement. *Forêt Méditerranéenne* **7:** 53–64.

Benabid A, **Fennane M. 1994.** Connaissances sur la végétation du Maroc: phytogéographie, phytosociologie et séries de végétation. *Lazaroa* **14:** 21–97.

Bickford D, **Lohman DJ**, **Sodhi NS**, **Ng PKL**, **Meier R**, **Winker K**, **Ingram KK**, **Das I. 2007.** Cryptic species as a window on diversity and conservation. *Trends in Ecology and Evolution* **22:** 148–155.

Bologna MA. 1989. *Berberomeloe*, a new west Mediterranean genus of Lyttini for *Meloe majalis* Lineé (Coleoptera, Meloidae). Systematics and bionomics. *Bolletino di Zoologia* **55:** 359–366.

Bologna MA. 1991. *Fauna d´Italia. XXVIII. Coleoptera Meloidae*. Bologna: Edizioni Calderini.

Bologna MA. 2008. Meloidae. In: Löbl I, Smetana A, eds. *Catalogue of Palaearctic Coleoptera. Vol. 5. Tenebrionoidea*. Stenstrup: Apollo Books, 370–412.

Bologna MA, **Pinto JD. 2001.** Phylogenetic studies of Meloidae (Coleoptera), with special emphasis on the evolution of phoresy. *Systematic Entomology* **26:** 33–72.

Bologna MA, **Pinto JD. 2002.** The Old World genera of Meloidae (Coleoptera): a key and synopsis. *Journal of Natural History* **36:** 2013–2102.

Booth-Rea G, **Ranero CR**, **Grevemeyer I. 2018.** The Alboran volcanic-arc modulated the Messinian faunal exchange and salinity crisis. *Scientific Reports* **8:** 13015.

Borchmann F. 1917. Meloidae, Cephaloidae. In: Schenkling E, ed. *Coleopterorum catalogus*. Berlin: W. Junk, 1–208.

Bravo C, **Mas-Peinado P**, **Bautista LM**, **Blanco G**, **Alonso JC**, **García-París M. 2017.** Cantharidin is conserved across phylogeographic lineages and present in both morphs of Iberian *Berberomeloe* blister beetles (Coleoptera, Meloidae). *Zoological Journal of the Linnean Society* **180:** 790–804.

Brito D. 2010. Overcoming the Linnean shortfall: data deficiency and biological survey priorities. *Basic and Applied Ecology* **11:** 709–713.

Brower AV. 1996. A new mimetic species of *Heliconius* (Lepidoptera: Nymphalidae), from south-eastern Colombia, revealed by cladistic analysis of mitochondrial DNA sequences. *Zoological Journal of the Linnean Society* **116:** 317–332.

Brown RM, **Diesmos AC. 2002.** Application of lineage-based species concepts tooceanic island frog populations: the effects of differing taxonomic philosophies on the estimation of Philippine biodiversity. *Silliman Journal* **42:** 133–162.

Brown WL, **Wilson EO. 1956.** Character displacement. *Systematic Zoology* **5:** 49–64.

Brown DM, **Brenneman RA**, **Koepfli KP**, **Pollinger JP**, **Milá B**, **Georgiadis NJ**, **Louis EE Jr**, **Grether GF**, **Jacobs DK**, **Wayne RK. 2007.** Extensive population genetic structure in the giraffe. *BMC Biology* **5:** 57.

Brown JL, **Twomey E**, **Amézquita A**, **Barbosa de Souza M**, **Caldwell JP**, **Lötters S**, **von May R**, **Melo-Sampaio PR**, **Mejía-Vargas D**, **Perez-Peña P**, **Pepper M**, **Poelman EH**, **Sánchez-Rodríguez M**, **Summers K. 2011.** A taxonomic

Downloaded from https://academic.oup.com/zoolinnean/article-abstract/189/4/1249/5714599 by 81263633 user on 05 August 2020

revision of the Neotropical poison frog genus *Ranitomeya* (Amphibia: Dendrobatidae). *Zootaxa* **3083:** 1–120.

Butlin RK, **Smadja CM. 2018.** Coupling, reinforcement, and speciation. *The American Naturalist* **191:** 155–172.

Cardoso A, **Vogler AP. 2015.** DNA taxonomy, phylogeny and Pleistocene diversification of the *Cicindela hybrida* species group (Coleoptera: Cicindelidae). *Molecular Ecology* **14:** 3531–3546.

Carstens BC, **Knowles LL. 2007.** Estimating species phylogeny from gene-tree probabilities despite incomplete lineage sorting: an example from *Melanoplus* grasshoppers. *Systematic Biology* **56:** 400–411.

Charco J. 1999. *El bosque mediterráneo en el norte de África. Biodiversidad y lucha contra la desertificación*. Madrid: Agencia Española de Cooperación Internacional, 370.

Charpentier T. 1818. *Meloë insignis* (p. 258). In: Germar EF. Vermischte Bemerkungen über einige Käferarten. *Magazin der Entomologie* **3:** 228–260.

Cortés-Fossati F. 2018a. Meloidos, 'curitas' y cantaridina: apuntes sobre *Berberomeloe majalis* (Linnaeus, 1758), un coleóptero peculiar. *Sociedad Gaditana de Historia Natural* **6:** 15–20.

Cortés-Fossati F. 2018b. Un primer acercamiento al estado de conservación de las poblaciones de *Berberomeloe majalis* (Linnaeus, 1758) (Coleoptera: Meloidae) en la provincia de Cádiz (España). Observaciones de campo y percepciones del mundo rural sobre el estado de la especie. *Boletín de la Sociedad Entomológica Aragonesa* **62:** 327–331.

Cros A. 1912. Mœurs et évolution du *Meloe majalis* L. *Bulletin de la Société d'Histoire Naturelle de l'Afrique du Nord* **3:** 45–48, 70–72, 93–96, 154–161, 181–190, 209–215.

Cros A. 1913. Mœurs et évolution du *Meloe majalis* L. (suite et fin). Mœurs et évolution du *Meloe majalis* L. *Bulletin de la Société d'Histoire Naturelle de l'Afrique du Nord* **4:** 16–26.

Cros A. 1921. Notes sur les larves primaires des Meloidae avec indication des larves nouvelles (2e série). *Annales de la Société Entomologique de France* **90:** 133–155.

Cros A. 1928. Essai sur la forme contractée (hypnothèque ou pseudonymphe) des larves des Meloidae. *Annales de la Société Entomologique de France* **97:** 27–58.

Darwell CT, **Cook JM. 2017.** Cryptic diversity in a fig wasp community – morphologically differentiated species are sympatric but cryptic species are parapatric. *Molecular Ecology* **26:** 937–950.

Day MC, **Fitton MG. 1978.** Re-curation of the Linnaean Hymenoptera (Insecta), with a reassessment of the taxonomic importance of the collection. *Biological Journal of the Linnean Society* **10:** 181–198.

Dayan T, **Simberloff D. 2005.** Ecological and community wide character displacement: the next generation. *Ecology Letters* **8:** 875–894.

Darriba D, **Taboada GL**, **Doallo R**, **Posada D. 2012.** jModelTest 2: more models, new heuristics and parallel computing. *Nature Methods* **9:** 772.

Díaz M, **Pulido FJ. 2009.** 6310 Dehesas perennifolias de *Quercus* spp. In: VV AA, eds. *Bases ecológicas preliminares para la conservación de los tipos de hábitat de interés comunitario en España*. Madrid: Ministerio de Medio Ambiente, y Medio Rural y Marino, 69.

Díaz-Rodríguez J, **Gehara M**, **Márquez R**, **Vences M**, **Gonçalves H**, **Sequeira F**, **Martínez-Solano I**, **Tejedo M. 2017.** Integration of molecular bioacoustical and morphological data reveals two new cryptic species of *Pelodytes* (Anura, Pelodytidae) from the Iberian Peninsula. *Zootaxa* **4243:** 1–41.

Drummond AJ, **Suchard MA**, **Xie D**, **Rambaut A. 2012.** Bayesian phylogenetics with BEAUti and the BEAST 1.7. *Molecular Biology and Evolution* **29:** 1969–1973.

Escalera MM. 1915. Una especie nueva de *Zonabris* de España. *Boletín de la Real Sociedad Española de Historia Natural* **15:** 493–494.

Escherich K. 1889. Nachträge und Berichtigungen zum Catalogus Coleopterorum von Gemminger und Harold, betreffend die Gattung *Meloë*. *Deutsche Entomologische Zeitschrift* **1889:** 333–335.

Esselstyn JA, **Timm RM**, **Brown RM. 2009.** Do geological or climatic processes drive speciation in dynamic archipelagos? The tempo and mode of diversification in Southeast Asian shrews. *Evolution* **63:** 2595–2610.

Fitze PS, **Gonzalez-Jimena V**, **San-Jose LM**, **San Mauro D**, **Zardoya R. 2012.** A new species of sand racer, *Psammodromus* (Squamata: Lacertidae), from the western Iberian Peninsula. *Zootaxa* **3205:** 41–52.

Folmer O, **Black M**, **Hoeh W**, **Lutz R**, **Vrijenhoek R. 1994.** DNA primers for amplification of mitochondrial cytochrome c oxidase subunit I from diverse metazoan invertebrates. *Molecular Marine Biology and Biotechnology* **3:** 294–299.

Fujisawa T, **Barraclough TG. 2013.** Delimiting species using single-locus data and the Generalized Mixed Yule Coalescent approach: a revised method and evaluation on simulated datasets. *Systematic Biology* **62:** 707–724.

García-París M. 1998. Revisión sistemática del género *Berberomeloe* Bologna, 1988 (Coleoptera, Meloidae) y diagnosis de un endemismo ibérico olvidado. *Graellsia* **54:** 97–109.

García-París M, **Ruiz JL. 2008.** *Berberomeloe insignis* (Charpentier, 1818). In: Barea-Azcón JM, Ballesteros-Duperón E, Moreno D, eds. *Libro rojo de los invertebrados de Andalucía*. Sevilla: Junta de Andalucía, Consejería de Medio Ambiente, 1020–1029.

García-París M, **Ruiz JL. 2011a.** *Berberomeloe insignis* (Charpentier, 1818). In: Verdú JR, Numa C, Galante E, eds. *Atlas y libro rojo de los invertebrados amenazados de España (especies vulnerables)*. Madrid: Dirección General de Medio Natural y Política Forestal, Ministerio de Medio Ambiente, Medio Rural y Marino, 285–294.

García-París M, **Ruiz JL. 2011b.** *Meloe (Lampromeloe) variegatus* Donovan, 1793. In: Verdú JR, Numa C, Galante E, eds. *Atlas y libro rojo de los invertebrados amenazados de España (especies vulnerables)*, **Vol. 1**. Madrid: Dirección General de Medio Natural y Política Forestal, Ministerio de Medio Ambiente, Medio Rural y Marino, 295–302.

García-París M, **Ruiz JL**, **Martínez-Solano I. 1999.** Primeros datos sobre la zona de contacto entre *Berberomeloe*

Downloaded from https://academic.oup.com/zoolinnean/article-abstract/189/4/1249/5714599 by 81263633 user on 05 August 2020

insignis (Charpentier, 1818) y *B. majalis* (Linnaeus, 1758) en Almería (Coleoptera, Meloidae). *Graellsia* **55:** 223–224.

García-París M, **Ruiz JL**, **París M. 2003.** Los representantes de la tribu Lyttini (Coleoptera: Meloidae) de la Península Ibérica. *Graellsia* **59:** 69–90.

García-París M, **Trotta-Moreu N**, **Capote L. 2006.** Estado de conocimiento actual y problemas de conservación de los Meloidae (Coleoptera) de la Comunidad de Madrid. *Graellsia* **62:** 333–370.

García-París M, **Ruiz JL**, **Alonso-Zarazaga MA. 2010.** Catálogo sinonímico de los taxones ibero-baleares de la familia Meloidae (Coleoptera). *Graellsia* **66:** 165–212.

García-París M, **Ruiz JL**, **Percino-Daniel N**, **Buckley D. 2016.** Nombres comunes de las cantáridas y aceiteras (Coleoptera: Meloidae) de España: "las circunstancias obligan". *Boletín de la Sociedad Entomológica Aragonesa* **58:** 245–252.

García-Porta J, **Simó-Riudalbas M**, **Robinson M**, **Carranza S. 2017.** Diversification in arid mountains: biogeography and cryptic diversity of *Pristurus rupestris rupestris* in Arabia. *Journal of Biogeography* **44:** 1694–1704.

Gatchui HC, **Smektala G**, **Solano D**, **Taiqui L**, **Ngoment AF. 2014.** Cannabis cultivation and deforestation in the Site of Bio Ecological Interest (SIBE) of Bouhachem, Morocco. *International Journal of Biological and Chemical Sciences* **8:** 1179–1191.

Gernhard T. 2008. Yule processs. *Journal of Theoretical Biology* **253:** 769–778.

Gonçalves H, **Maia-Carvalho B**, **Sousa-Neves T**, **García-París M**, **Sequeira F**, **Ferrand N**, **Martínez-Solano I. 2015.** Multilocus phylogeography of the common midwife toad, *Alytes obstetricans* (Anura, Alytidae): contrasting patterns of lineage diversification and genetic structure in the Iberian refugium. *Molecular Phylogenetics and Evolution* **93:** 363–379.

Glez-Peña D, **Gómez-Blanco D**, **Reboiro-Jato M**, **Fdez-Riverola F**, **Posada D. 2010.** ALTER: program-oriented format conversion of DNA and protein alignments. *Nucleic Acids Research* **38:** W14–W18.

Gómez A, **Lunt DH. 2007.** Refugia within refugia: patterns of phylogeographic concordance in the Iberian Peninsula. In: Weiss S, Ferranz N, eds. *Phylogeography of southern European refugia*. Dordrecht: Springer, 155–188.

Gómez-Ortiz A, **Oliva M**, **Salvà-Catarineu M**, **Salvador-Franch F. 2013.** The environmental protection of landscapes in the high semi-arid Mediterranean mountain of Sierra Nevada National Park (Spain): historical evolution and future perspectives. *Applied Geography* **42:** 227–239.

González-Megías A, **Gómez JM**, **Sánchez-Piñero F. 2004.** Effects of ungulates on epigeal arthropods in Sierra Nevada National Park (southeast Spain). *Biodiversity and Conservation* **13:** 733–752.

Górriz Muñoz RJ. 1878. Sin título [Observaciones sobre *Meloe majalis*]. *Actas de la Sociedad Española de Historia Natural* **7:** 71–73.

Górriz Muñoz RJ. 1882. *Ensayo para la monografía de los coleópteros melóidos indígenas con aplicación a las ciencias médicas*. Zaragoza: Imprenta y librería de J. Sanz.

Gutiérrez-Rodríguez J, **Barbosa AM**, **Martínez-Solano I. 2017.** Integrative inference of population history in the Ibero-Maghrebian endemic *Pleurodeles waltl* (Salamandridae). *Molecular Phylogenetics and Evolution* **112:** 122–137.

Hewitt GM. 1996. Some genetic consequences of ice ages, and their role in divergence and speciation. *Biological Journal of the Linnean Society* **58:** 247–276.

Hewitt GM. 1999. Post-glacial re-colonization of European biota. *Biological Journal of the Linnean Society* **68:** 87–112.

Hewitt GM. 2000. The genetic legacy of the ice ages. *Nature* **405:** 907–913.

Hewitt GM. 2004. Genetic consequences of climatic changes in the Quaternary. *Philosophical Transactions of the Royal Society B* **359:** 183–195.

Ibáñez C, **García-Mudarra JL**, **Ruedi M**, **Stadelmann B**, **Juste J. 2006.** The Iberian contribution to cryptic diversity in European bats. *Acta Chiropterologica* **8:** 277–297.

ICZN. **1999.** *International code of Zoological nomenclature, 4th edn*. London: International Trust for Zoological Nomenclature, c/o The Natural History Museum, xxix + 306.

ICZN. **2003.** Declaration 44. Amendment of article 74.7.3. *Bulletin of Zoological Nomenclature* **60:** 263.

Johnson NK, **Cicero C. 2004.** New mitochondrial DNA data affirm the importance of Pleistocene speciation in North American birds. *Evolution* **58:** 1122–1130.

Kaliontzopoulou A, **Pinho C**, **Harris DJ**, **Carretero MA. 2011.** When cryptic diversity blurs the picture: a cautionary tale from Iberian and North African *Podarcis* wall lizards. *Biological Journal of the Linnean Society* **103:** 779–800.

Kapli P, **Lutteropp S**, **Zhang J**, **Kobert K**, **Pavlidis P**, **Stamatakis A**, **Flouri T. 2017.** Multi-rate Poisson tree processes for single-locus species delimitation under maximum likelihood and Markov chain Monte Carlo. *Bioinformatics* **33:** 1630–1638.

Katoh K, **Toh H. 2008.** Recent developments in the MAFFT multiple sequence alignment program. *Briefings in Bioinformatics* **9:** 286–298.

Klicka J, **Zink RM. 1997.** The importance of recent ice ages in speciation: a failed paradigm. *Science* **277:** 1666–1669.

Kress WJ, **García-Robledo C**, **Uriarte M**, **Erickson DL. 2015.** DNA barcodes for ecology, evolution, and conservation. *Trends in Ecology & Evolution* **30:** 25–35.

Labrousse A, **Romero L. 2001.** *Rapport sur la situation du cannabis dans le Rif marocain*. Paris: Observatoire français des drogues et toxicomanies, OFDT.

Le Houerou HN. 1989. Classification écoclimatique des zones arides (s.l.) de l'Afrique du Nord. *Ecologia Mediterranea* **15:** 95–144.

Linnaeus C. 1758. *Systema naturae per regna tria naturae, secundum classes, ordines, genera, species, cum characteribus, differentiis, synonymis, locis*, *10th edn*. **Vol. 1**. Stockholm: L. Salvius, 824.

Lucas P. 1847. *Exploration scientifique de l'Algérie pendant les années 1840, 1841, 1842, publiée par ordre du Gouvernement et avec le concours d'une Commission Académique. Sciences physiques. Zoologie. Vol. II. Historie naturelle des animaux articulés. Cinquième classe insectes. Premier ordre. Les coléoptères*. Paris: Imprimerie Nationale, 361–448.

Downloaded from https://academic.oup.com/zoolinnean/article-abstract/189/4/1249/5714599 by 81263633 user on 05 August 2020

Machordom A, **Araujo R**, **Erpenbeck D**, **Ramos MA. 2003.** Phylogeography and conservation genetics of endangered European Margaritiferidae (Bivalvia: Unionoidea). *Biological Journal of the Linnean Society* **78:** 235–252.

MacSwain JW. 1956. A classification of the first instar larvae of the Meloidae (Coleoptera). *University of California Publications in Entomology* **12:** 1–182.

Maddison WP, **Maddison DR. 2016.** *Mesquite: a modular system for evolutionary analysis. Version 3.04*. Available at: http://www.mesquiteproject.org.

Martin RA, **Pfennig DW. 2011.** Evaluating the targets of selection during character displacement. *Evolution: International Journal of Organic Evolution* **65:** 2946–2958.

Martínez-García P, **Comas M**, **Soto JI**, **Lonergan L**, **Watts AB. 2013.** Strike-slip tectonics and basin inversion in the western Mediterranean: the Post-Messinian evolution of the Alboran Sea. *Basin Research* **25:** 361–387.

Mas-Peinado P, **Buckley D**, **Ruiz JL**, **García-París M**, **2018.** Recurrent diversification patterns and taxonomic complexity in morphologically conservative ancient lineages of *Pimelia* (Coleoptera: Tenebrionidae). *Systematic Entomology* **43:** 522–548.

Merrill RM, **Wallbank RWR**, **Bull V**, **Salazar PCA**, **Mallet J**, **Stevens M**, **Jiggins CD. 2012.** Disruptive ecological selection on a mating cue. *Proceedings of the Royal Society B: Biological Sciences* **279:** 4907–13.

Molero Mesa J, **Pérez-Raya F**, **Valle Tendero F. 1992.** Vegetación. In: Molero Mesa J, Pérez-Raya F, Valle Tendero F, eds. *Parque Natural de Sierra Nevada*. Madrid: Rueda, 89–135.

Moritz C, **Pratt RC**, **Bank S**, **Bourke G**, **Bragg JG**, **Doughty P**, **Keogh JS**, **Laver RJ**, **Potter S**, **Teasdale LC**, **Tedeschi LG**, **Oliver PM. 2017.** Cryptic lineage diversity, body size divergence and sympatry in a species complex of Australian lizards (*Gehyra*). *Evolution* **72:** 54–66.

Mota JF, **Peñas J**, **Castro H**, **Cabello J**, **Guirado JS. 1996.** Agricultural development vs biodiversity conservation: the Mediterranean semi-arid vegetation in El Ejido (Almería, south-eastern Spain). *Biodiversity & Conservation* **5:** 1597–1617.

Mota JF, **Cabello J**, **Cueto M**, **Gómez-Mercado F**, **Jiménez E**, **Peñas J. 1997.** *Datos sobre la vegetación del sureste de Almería. (Desierto de Tabernas, Karst en Yesos de Sorbas y Cabo de Gata)*. Almería: Universidad de Almería, 130.

Murphy JC, **Jowers MJ**, **Lehtinene RM**, **Charles SP**, **Colli GR**, **Peres AK Jr**, **Hendry CR**, **Pyron RA. 2016.** Cryptic, sympatric diversity in tegu lizards of the *Tupinambis teguixin* group (Squamata, Sauria, Teiidae) and the description of three new species. *PLoS One* **11:** e0158542.

Nash D. 1976. Some interesting Coleoptera from northeast Essex, England. *The Entomologist's Record and Journal of Variation* **88:** 39–43.

Olea L, **San Miguel A. 2006.** The Spanish dehesa. A Mediterranean silvopastoral system linking production and nature conservation. *Grassland Science in Europe* **11:** 3–13.

Olivier AG. 1797. *Encyclopédie méthodique, ou par ordre de matières; par une société de gens de lettres, de savans et d'artistes; précédé d'un vocabulaire universel servant de table pour tout l'ouvrage, ornée des portraits de Mm. Diderot et d'Alembert, premiers éditeurs de l'Encyclopédie. Histoire naturelle. Insectes. Tome septième*. Paris: Panckoucke, 369–827.

Oliver PM, **Adams M**, **Lee MS**, **Hutchinson MN**, **Doughty P. 2009.** Cryptic diversity in vertebrates: molecular data double estimates of species diversity in a radiation of Australian lizards (*Diplodactylus*, Gekkota). *Proceedings of the Royal Society of London B: Biological Sciences* **276:** 2001–2007.

Ortuño VM, **Arribas O. 2018.** A revision of the *Cymindis ehlersi* complex (Coleoptera: Carabidae: Lebiinae) with description of a new species and ecological notes. *Zoologischer Anzeiger* **276:** 1–14.

Padial JM, **Miralles A**, **De la Riva I**, **Vences M. 2010.** The integrative future of taxonomy. *Frontiers in Zoology* **7:** 16.

Palumbi SR, **Martin AP**, **Romano S**, **McMillan WO**, **Stice L**, **Grabowski G. 1991.** *The simple fool´s guide to PCR*. Honolulu: Special Publ., Department of Zoology, University of Hawaii.

Papadopoulou A, **Anastasiou I**, **Vogler AP. 2010.** Revisiting the insect mitochondrial molecular clock: the mid-Aegean trench calibration. *Molecular Biology and Evolution* **27:** 1659–1672.

Peñas J, **Cabello J**, **Oyonarte C**, **Mota JF. 1995.** Variación altitudinal y diversidad vegetal en matorrales: Sierra de los Filabres (Almería, España). *Acta Botánica Malacitana* **20:** 133–142.

Percino-Daniel N, **Buckley D**, **García-París M. 2013.** Pharmacological properties of blister beetles (Coleoptera: Meloidae) promoted their integration into the cultural heritage of native rural Spain as inferred by vernacular names diversity, traditions, and mitochondrial DNA. *Journal of Ethnopharmacology* **147:** 570–583.

Pérez-Ponce de León G, **Poulin R. 2016.** Taxonomic distribution of cryptic diversity among metazoans: not so homogeneous after all. *Biology Letters* **12:** 20160371.

Pfennig KS. 2009. Character displacement: ecological and reproductive responses to a common evolutionary problem. *The Quarterly Review of Biology* **84:** 253–276.

Pfennig DW, **Murphy PJ. 2000.** Character displacement in polyphenic tadpoles. *Evolution* **54:** 1738–1749.

Pfenninger M, **Schwenk K. 2007.** Cryptic animal species are homogeneously distributed among taxa and biogeographical regions. *BMC Evolutionary Biology* **7:** 121.

Pons J, **Barraclough TG**, **Gomez-Zurita J**, **Cardoso A**, **Duran DP**, **Hazell S**, **Kamoun S**, **Sumlin WD**, **Vogler AP. 2006.** Sequence based species delimitation for the DNA taxonomy of undescribed insects. *Systematic Biology* **55:** 595–609.

Porco D, **Bedos A**, **Greenslade P**, **Janion C**, **Skarzynski D**, **Stevens MI**, **Jansen van Vuuren B**, **Deharveng L. 2012.** Challenging species delimitation in Collembola: cryptic diversity among common springtails unveiled by DNA barcoding. *Invertebrate Systematics* **26:** 470–477.

Posso-Terranova A, **Andrés J. 2018.** Multivariate species boundaries and conservation of harlequin poison frogs. *Molecular Ecology* **27:** 3432–3451.

Puebla O, **Bermingham E**, **Guichard F**, **Whiteman E. 2007.** Colour pattern as a single trait driving speciation

Downloaded from https://academic.oup.com/zoolinnean/article-abstract/189/4/1249/5714599 by 81263633 user on 05 August 2020

in Hypoplectrus coral reef fishes? *Proceedings of the Royal Society of London B: Biological Sciences* **274:** 1265–1271.

Rand AL. 1948. Glaciation, an isolating factor in speciation. *Evolution* **2:** 314–321.

Recuero E, **García-París M. 2011.** Evolutionary history of *Lissotriton helveticus*: multilocus assessment of ancestral vs. recent colonization of the Iberian Peninsula. *Molecular Phylogenetics and Evolution* **60:** 170–182.

Recuero E, **Canestrelli D**, **Vörös J**, **Szabo JK**, **Poyarkov NK**, **Arntzen JW**, **Crnobrnja-Isailovic J**, **Kidov AA**, **Cogalniceanu D**, **Caputo FP**, **Nascetti G**, **Martinez-Solano I. 2012.** Multilocus species tree analyses resolve the radiation of the widespread *Bufo bufo* species group (Anura, Bufonidae). *Molecular Phylogenetics and Evolution* **62:** 71–86.

Reitter E. 1872. Neue Käferarten von Oran gesammelt von Hans Leder. *Berliner Entomologische Zeitschrift* **16:** 167–186.

Ribera I, **Vogler AP. 2004.** Speciation of Iberian diving beetles in Pleistocene refugia (Coleoptera, Dytiscidae). *Molecular Ecology* **13:** 179–193.

Rivas-Martínez S. 1987. *Memoria del mapa de las series de vegetación de España 1:400.000*. Madrid: ICONA.

Rivas-Martínez S, **Costa M. 1970.** Comunidades gipsícolas del centro de España. *Anales del Instituto Botánico A. J. Cavanilles* **27:** 193–224.

Rivas-Martínez S, **Fernández-González F**, **Sánchez-Mata D**, **Pizarro JM. 1990.** Vegetación de la Sierra de Guadarrama. *Itinera Geobotanica* **4:** 3–132.

Rivas-Martínez S, **Díaz TE**, **Fernández-González F**, **Izco J**, **Loidi J**, **Lousa M**, **Penas A. 2002.** Vascular plant communities of Spain and Portugal. Addenda to the syntaxonomical checklist of 2001. Part I. *Itinera Geobotanica* **15:** 5–432.

Rodríguez-Flores PC, **Gutiérrez-Rodríguez J**, **Aguirre-Ruiz EF**, **García-París M. 2016.** Salt lakes of La Mancha (Central Spain): a hot spot for tiger beetle (Carabidae, Cicindelinae) species diversity. *ZooKeys* **561:** 63–103.

Rodríguez-Flores PC, **Pichaco-García P**, **Pérez-Santiago CA**, **García-París M. 2017.** Observations on the natural history of *Deleproctophylla dusmeti* (Neuroptera: Ascalaphidae) in salt marshes of La Mancha (central Spain). *Heteropterus* **17:** 21–33.

Rodríguez-Flores PC, **Macpherson E**, **Buckley D**, **Machordom A. 2018.** High morphological similarity coupled with high genetic differentiation in new sympatric species of coral-reef squat lobsters (Crustacea: Decapoda: Galatheidae). *Zoological Journal of the Linnean Society* **185:** 984–1017.

Roig S, **San Miguel A. 2013.** ¿Cómo se mide el estado de conservación de la dehesa? In: Olea L, Poblaciones MJ, Rodrigo SM, Santamaría O, eds. *Los pastos: nuevos retos, nuevas oportunidades*. Badajoz: Sociedad Española para el Estudio de los Pastos, 3–23.

Ronquist F, **Teslenko M**, **Van der Mark P**, **Ayres DL**, **Darling A**, **Höhna S**, **Larget B**, **Liu L**, **Suchard MA**, **Huelsenbeck JP. 2012.** MrBayes 3.2: efficient Bayesian phylogenetic inference and model choice across a large model space. *Systematic Biolobiology* **61:** 539–542.

Rosado D, **Rato C**, **Salvi D**, **Harris DJ. 2017.** Evolutionary history of the Morocco lizard-fingered geckos of the *Saurodactylus brosseti* complex. *Evolutionary Biology* **44:** 386–400.

Ruiz JL, **García-París M. 2008.** *Meloe (Eurymeloe) nanus* Lucas, 1849. In: Barea-Azcón JM, Ballesteros-Duperón E, Moreno D, eds. *Libro rojo de los invertebrados de Andalucía*. Sevilla: Junta de Andalucía, Consejería de Medio Ambiente, 1030–1037.

Ruiz JL, **García-París M. 2011.** *Mylabris (Micrabris) nevadensis* (Escalera, 1915). In: Verdú JR, Numa C, Galante E, eds. *Atlas y libro rojo de los invertebrados amenazados de España (Especies Vulnerables)*, **Vol. 1**. Madrid: Dirección General de Medio Natural y Política Forestal, Ministerio de Medio Ambiente, Medio Rural y Marino, 303–308.

Ruiz JL, **García-París M. 2013.** Los meloidos (Coleoptera: Meloidae). In: Ruano F, Tierno de Figueroa M, Tinaut A, eds. *Los insectos de Sierra Nevada. 200 años de historia*, **Vol. 2**. Granada: Asociación Española de Entomología, 24–59.

Rull V. 2015. Pleistocene speciation is not refuge speciation. *Journal of Biogeography* **42:** 602–604.

Salvador de Jesús-Bonilla V, **García-París M**, **Ibarra-Cerdeña CN**, **Zaldívar-Riverón A. 2018.** Geographic patterns of phenotypic diversity in incipient species of North American blister beetles (Coleoptera: Meloidae) are not determined by species niches, but driven by demography along the speciation process. *Invertebrate Systematics* **32:** 672–688.

Sanz de Galdeano C. 1997. *La zona interna bético-rifeña*. Granada: Colección Monográfica Tierras del Sur, Universidad de Granada, 316.

Sebbar A, **Hsaine M**, **Fougrach H**, **Badri W. 2013.** Carte des precipitations annuelles au Maroc (1935/2006). *Actes du 26éme Colloque de l'Association Internationale de Climatologie, Cotonou*: 37–43.

Settanni C, **Di Giulio A**, **Finoia MG**, **Bologna MA. 2009.** Intra- and interspecific analysis of first instar larval morphology in the genus *Berberomeloe* Bologna 1989 (Coleoptera: Meloidae). *Zootaxa* **2089:** 52–64.

Schmitt T. 2007. Molecular biogeography of Europe: Pleistocene cycles and postglacial trends. *Frontiers in Zoology* **4:** 11.

Stefanescu C, **Herrando S**, **Páramo F. 2004.** Butterfly species richness in the north-west Mediterranean Basin: the role of natural and human-induced factors. *Journal of Biogeography* **31:** 905–915.

Stoate C, **Boatman ND**, **Borralho RJ**, **Carvalho CR**, **De Snoo GR**, **Eden P. 2001.** Ecological impacts of arable intensification in Europe. *Journal of Environmental Management* **63:** 337–365.

Stöck M, **Dubey S**, **Klütsch C**, **Litvinchuk SN**, **Scheidt U**, **Perrin N. 2008.** Mitochondrial and nuclear phylogeny of circum-Mediterranean tree frogs from the *Hyla arborea* group. *Molecular Phylogenetics and Evolution* **49:** 1019.

Struck TH, **Feder JL**, **Bendiksby M**, **Birkeland S**, **Cerca J**, **Gusarov VI**, **Kistenich S**, **Larsson KH**, **Liow LH**, **Nowak MD**, **Stedje B**, **Bachmann L**, **Dimitrov D. 2018.** Finding evolutionary processes hidden in cryptic species. *Trends in Ecology and Evolution* **33:** 153–163.

Downloaded from https://academic.oup.com/zoolinnean/article-abstract/189/4/1249/5714599 by 81263633 user on 05 August 2020

Stuart YE, **Losos JB. 2013.** Ecological character displacement: glass half full or half empty? *Trends in Ecology and Evolution* **28:** 402–408.

Taberlet P, **Fumagalli L**, **Wust-Saucy AG**, **Cosson JF. 1998.** Comparative phylogeography and postglacial colonization routes in Europe. *Molecular Ecology* **7:** 453–464.

Tamayo Muñoz P, **Pascual Torres F**, **González Megías A. 2015.** Effects of roads on insects: a review. *Biodiversity and Conservation* **24:** 659–682.

Valera DL, **Belmonte LJ**, **Molina-Aiz FD**, **López A**, **Camacho F. 2017.** The greenhouses of Almería, Spain: Technological analysis and profitability. *Acta Horticulturae* **1170:** 219–226.

Valladares F, **Camarero JJ**, **Pulido F**, **Gil-Pelegrín E. 2004.** El bosque mediterráneo, un sistema humanizado y dinámico. In: Valladares F, ed. *Ecología del bosque mediterráneo en un mundo cambiante*. Madrid: Organismo Autónomo de Parques Nacionales. Ministerio de Medio Ambiente, 13–25.

Valle F. 2003. *Mapa de Series de Vegetación de Andalucía*. Madrid: Rueda S.L., 131.

Valle F, **Navarro FB**, **Jiménez MN. 2004.** *Datos botánicos aplicados a la gestión del medio natural Andaluz I: bioclimatología y biogeografía. Manuales de restauración forestal nº 5.* Sevilla: Consejería de Medio Ambiente, Junta de Andalucía, 353.

Van Swaay CAM, **Warren MS. 1999.** *Red data book of European butterflies (Rhopalocera). Nature and environment*. Strasbourg: Council of Europe Publishing.

Velo-Antón G, **el Marnisi B**, **Fritz U**, **Fahd S. 2015.** Distribution and conservation status of *Emys orbicularis* in Morocco. *Vertebrate Zoology* **65:** 131–134.

Vera JA. 2004. *Geología de España*. Madrid: Sociedad Geológica de España-Instituto Geológico y Minero de España, 890.

Vergés J. Fernàndez M. 2006. Ranges and basins in the Iberian Peninsula: their contribution to the present topography. *Geological Society, London, Memoirs* **32:** 223–234.

Vodă R, **Dapporto L**, **Dincă V**, **Vila R. 2015.** Cryptic matters: overlooked species generate most butterfly beta-diversity. *Ecography* **38:** 405–409.

Waters JM, **Fraser CI**, **Hewitt GM. 2013.** Founder takes all: density-dependent processes structure biodiversity. *Trends in Ecology and Evolution* **28:** 78–85.

Whitehead PF. 1991. The breeding population of *Meloe rugosus* Marsham, 1802 (Coleoptera: Meloidae) at Broadway, Worcestershire, England. *Elytron* **5**: 225–229.

Whitney JL, **Bowen BW**, **Karl SA. 2018.** Flickers of speciation: sympatric colour morphs of the arc-eye hawkfish, *Paracirrhites arcatus*, reveal key elements of divergence with gene flow. *Molecular Ecology* **27:** 1479–1493.

Wiens JJ. 2004. Speciation and ecology revisited: phylogenetic niche conservatism and the origin of species. *Evolution* **58:** 193–197.

Wiley EO. 1978. The evolutionary species concept reconsidered. *Systematic Zoology* **27:** 17–26.

Wiley EO, **Mayden RL. 2000.** A critique from the evolutionary species concept perspective. In: Wheeler QD, Meier R, eds. *Species concepts and phylogenetic theory: a debate*. New York: Columbia University Press.

Zink RM, **Klicka J**, **Barber BR. 2004.** The tempo of avian diversification during the Quaternary. *Philosophical Transactions of the Royal Society, Series B: Biological Sciences* **359:** 215–220.

SUPPORTING INFORMATION

Additional Supporting Information may be found in the online version of this article at the publisher's web-site.

Table S1. Morphometric measurements (in mm) of specimens used in this study.
Figure S1. Results of mPTP Species Delimitation analysis (left) and GMYC Species Delimitation analysis (right), showing proposed delimited species as red clades (black branches when there is only one individual for the species).
Appendix S1. Additional material examined of *Berberomeloe*.

Downloaded from https://academic.oup.com/zoolinnean/article-abstract/189/4/1249/5714599 by 81263633 user on 05 August 2020

View publication stats